Transport of NF-κB in the nervous system

Dissertation
Submitted in partial fulfillment of the requirements for
the degree of doctor of natural sciences
- Dr. rer. nat. -

by Thomas Engelen

2011

Cell Biology
Faculty for Biology
Bielefeld University
Germany

Supervisor: **Prof. Dr. Christian Kaltschmidt**
Cell Biology
Faculty for Biology
Bielefeld University

Declaration

I hereby confirm that I have written this thesis on my own and that the only aids used for composing this dissertation are those stated therein.

Thomas Engelen

Acknowledgment

The research work, which this thesis is based on, was done under the scientific supervision and in the workgroup of

Prof. Dr. Christian Kaltschmidt

I like to thank him very much for the opportunity to work on this interesting topic, the financial support and above all for his willingness for discussion, a lot of practical hints and inspiring ideas. His support and motivation were crucial for the success of this work.

Furthermore I want to thank

Dr. Peter Heimann, "the heart of the lab", whose continuous work keeps the lab running.

Prof. Dr. Liehnhard Schmitz and his PhD student Tobias Wittwer for their support with immunoprecipitation protocols, practical hints and the donation of the myc-IκBε expression construct.

Prof. Dr. Horst Hinssen for his help preparing the tissue extractions.

Mr. Bernhardt Kassens of the *Gausepohl Fleisch GMBH* in Harsewinkel for the supply of porcine brains.

our technical assistant Angela Kralemann-Köhler for her innumerable works during cloning, protein extraction and western blotting.

my colleagues Christin Zander, Yvonne Kasperek and especially Patrick Lüning-schroer for the very good cooperation.

all other members of our lab for the good working atmosphere.

I specially thank Carola Eck from the CeBiTec and Dr. Raimund Hoffrogge from the workgroup *cell culture techniques* at Bielefeld University and their supervisors Prof. K. Niehaus and Prof. T. Noll for the performance of mass spectrometry and their guidance for data analysis.

My greatest thank goes to my wife Ute and my family, whose love was the strongest encouragement at all.

I. Table of contents

II. Abbreviations

°C	degree Celsius
Å	ångström, 0.1 nm
AA	amino acid
AB	antibody
ADP	adenosine diphosphate
ANK	ankyrin repeat domain
AP	adaptor protein (for endocytosis)
APS	ammonium persulfate
Arp1	actin-related protein 1 (dynactin subunit)
asn^{284}	aspartic acid on #284 in poly peptide chain
ATP	adenosine triphosphate
BAFF-R	B-cell activating factor receptor
BAG	B-cell lymphoma 2 - associated athanogene
BDNF	brain derived neurotrophic factor
bp	base pairs
BSA	bovine serum albumin
CamKII	calcium calmodulin-dependent protein kinase II
CCV	clathrin coated vesikels
CD40	cluster of differentiation 40
CDS	coding sequence
cf.	*confer* Lat. compare
CHIP	carboxyl terminus of HSC70 interacting protein
cIAP	cellular inhibitor of apoptosis
cm	centimeter
co IP	co immunoprecipitation
CV	column volume
CYLD	cylindromatosis (tumor supressor)
Da	Dalton, $1{,}66 \cdot 10^{-24}$ g
DABCO	1,4-diazabicyclo[2.2.2]octan
dATP	deoxyriboadenosine triphosphate
DBF	developing brain factor

dCTP	deoxyribocytidine triphosphate
DD	death domain
dGTP	deoxyriboguanosine triphosphate
DMEM	Dulbecco's Modified Eagle Medium
DMSO	dimethyl sulfoxide
DNA	deoxyribonucleic acid
dNTP	deoxyribonucleotide triphosphate
DSG	deoxyspergualin
DSP	dithiobis[succinimidylpropionate]
DTT	1,4-dithiothreitol
dTTP	deoxyribothymidine triphosphate
ECL	enhanced chemo luminescence
EDTA	ethylenediaminetetraacetic acid, sodium salt
e.g.	*exempli gratia* Lat. for example
EGF	epidermal growth factor
ELKS	protein rich in glutamate (E), leucine (L), lysine (K), and serine (S)
ESI (MS)	electrospray ionization
et seqq.	*et sequens* Lat.: a*nd the following*
FCS	fetal calf serum
FPLC	fast protein liquid chromatography
FPred	fluorecent protein red
FRAP	fluorescence recovery after photobleaching
FRET	fluorescence resonance energy transfer
g	gram, gravitational acceleration
GFP	green fluorescent protein
GLT-1	of glutamate transporter 1
GR	glucocorticoid receptor
GTP	guanosine triposphate
h	hour
HC	heavy chain (of dynein or immunoglobulin)
HDGF	hepatoma-derived growth factor
HDGFRP-3	HDGF related protein 3

HEK	human embryoic kidney (cell line)
HOP	HSP organizing protein
HRP	horse radish peroxidase
HSC70	heat shock cognate 70, aliases: HSPA8, HSC71, HSP73
HSP40	heat shock protein 40 kDa (cochaperone)
HSPA8	heat shock 70kD protein 8, aliases: HSC70, HSC71, HSP73
IC	intermediate chain (of dynein)
IFN-γ	interferon γ
Ig	immunglobuline
IKK	IκB Kinase
IL	interleukin
IMM	immunophillin
IP	immunoprecipitation
IκB	Inhibitor of NF-κB
kb	kilo base pairs
kDa	kilodalton
LC	liquid chromatography
LPS	lipopolysaccharides
LT-ß-R	lymphotoxin-ß receptor
LUBAC	linear ubiquitin chain assembly complex
M	molar, mol per liter
mA	milliampere
MALDI (MS)	matrix assisted laser desorption/ionization
mg	milligram
min	minute
mL	milliliter
mM	millimolar
mmu	milli mass units, mmu = mDa (milli Dalton)
mRNA	messenger RNA
MS	mass spectrometry
MW	molecular weight

MyD88	myeloid differentiation primary response gene 88
NEMO	NF-kappa-B essential modulator
NES	nuclear export signal
NF-κB	nuclear factor for κ-light chains in B-cells
NGF	nerve growth factors
NLRS	nuclear localization related signal
NLS	nuclear localization signal
ng	nanogram
nm	nanometer
NPC	nuclear pore complex
p23	small ubiquitous cochaperone of HSP90, 23 kDa
p50	protein 50 kDa, mature NF-κB1
p65	protein 65 kDa, see RelA
P75NTR	neurotrophin receptor, 75 kDa
PAGE	polyacrylamide gel electrophoresis
PCR	polymerase chain reaction
PBS	phosphate buffered saline
PBST	phosphate-buffered saline (with) tween
PDTC	pyrrolidone dithiocarbamate
PEST	protein sequence rich in proline (P), glutamic acid (E), serine (S), and threonine (T)
PKA	protein kinase A
PMSF	phenylmethylsulfonyl fluoride
PNS	peripheral nervous system
PP	polypropylene
PPIase	peptidyl-prolyl cis/trans isomerase
ppm	parts per million
RANK	receptor activator of NF-κB
rct.	reaction
RelA	v-rel reticuloendotheliosis viral oncogene homolog A, see p65
RHD	Rel homology domain
RIP	receptor interacting protein

RNA	ribonucleic acid
rpm	revolutions per minute
RT-PCR	reverse transcription (or real time) polymerase chain reaction
s	second
SDM	site directed mutagenesis
SDS	sodium dodecyl sulfate
siRNA	small interfering RNA
SNP	single nucleotide polymorphism
SODD/BAG4	silencer of death domain
TAB2/3	TAK1 binding protein 2/3
TAD	transcription activation domain
TAK1	TGFß-activated kinase
TEMED	tetramethylethylendiamin
Tet	tetracycline
TFA	trifluoroacetic acid
TGF-ß	tumor growth factor ß
TIR	Toll/interleukin-1 receptor
TLR	Toll like receptor
TNF-R	TNF receptor
TNF-α	tumor necrosis factor α
TOF (MS)	time of flight
TPR	tetratricopeptide repeat
TRADD	TNF-R associated death domain protein
TRAF	TNF receptor associated factor
TRIF	TIR domain containing adaptor-inducing interferon-ß
Tris	tris(hydroxymethyl)-aminomethan (buffer)
U	unit
UBD	ubiquitin binding domain
UV	ultra violet (light)
V	Volt
v.i.	*vide infra* Lat. see below

v.s.	*vide supra* Lat. see above
v/v	volume per volume
w/v	weight per volume
WB	Western blot
WT	wild type
α	anti
Δ	deletion
µg	microgram
µL	microliter
µM	micromolar

1 Introduction

1.1 The NF-κB/Rel family

The Nuclear factor-κB was first characterized by Ranjan Sen and David Baltimore. They observed that a factor from nuclear extracts of B-cells binds to the eleven base pair long sequence (GGGGACTTTCC) of the κ light chain enhancer [194]. Later, it became clear that NF-κB is present in various types of cells. The nuclear factor is not a single protein, but consists of two of five different subunits, which form dimers. Characteristic for these subunits is the Rel homology domain (RHD) named after the homolog oncoprotein v-Rel. This domain contains a DNA binding site as well as an interaction / dimerization region and a nuclear localization signal (NLS) [76]. Furthermore, the subunits divide into two groups: One with a transcription activation domain (TAD) and one without. The proteins RelA (p65), RelB and c-Rel contain a transcription activation domain [23, 33, 183, 189, 191, 192], while NF-κB1 (p50) and NF-κB2 (p52) do not. The subunits NF-κB1 (p50) and NF-κB2 (p52) are translated as precursors named p105 and p100, respectively. These proteins contain c-terminal ankyrin repeats similar to the inhibitors of NF-κB (v.i.) [17]. The mature NF-κB subunits are produced by proteolytic cleavage in the proteasome [88, 158]. The composition of the NF-κB dimer is crucial for its function. So the most common heterodimer p50 / p65 works as an enhancer [189] while the homodimers p50 / p50 and p52 / p52 are repressors of transcription lacking the TAD and competing for DNA binding [118]. The inhibitory mechanism is not yet understood. The composition of NF-κB is tissue specific. The p50 / p65 heterodimer is ubiquitous, but NF-κB2, Rel-B, and c-Rel are expressed specifically in lymphoid cells and tissues [30]. All Rel/NF- κB proteins, except RelB, have approximately 25 amino acids N-terminal to the NLS a potential protein kinase A (PKA) phosphorylation site [160] . In case of p65, it is well know that a phosphorylation on this site increases its actitivy [226].

1.2 Inhibitors of NF-κB

In unstimulated cells the NF-κB dimer is retained in the cytoplasm in an inactive state in reason of its association with proteins called inhibitors of NF-κB (IκB) [15].

Today eight inhibitors of NF-κB are characterized: p100, p105, IκB-α, IκB-β, IκB-γ, IκB-ε, Bcl-3, IκBζ and IκB-R. The most common members of the IκB family are IκB-α and IκB-β with a molecular weights of 37 and 43 kDa. They do not only specifically and reversibly inhibit DNA-binding by NF-κB, but also actively dissociate DNA-bound NF-κB in vitro [15, 224]. The cloning of this molecules revealed that they contain repeated sequences of 30–33 amino acids. These were first discovered in the SW16 protein of *Saccharomyces cerevisiae* and named SW16/ankyrin repeats [30, 85]. As described above, the p50 and p52 precursors p105 and p100 also contain ankyrin repeats in their c-terminal regions and are capable of inhibiting NF-κB activity [150, 179]. The c-terminal fragment of p105 is identical to IκBγ generated by alternative splicing in lymphocytes and has inhibitory qualities [99]. The p100 fragment is named IκBδ [187]. The next member of the IκB family IkB-ε stands out by its specificity compared to IκB-α and IκB-β. It apparently only binds to c-Rel, RelA, or their respective homodimers [215]. Additionally it is, similar to the other two, very important for the nuclear import and export of NF-κB/Rel proteins [132]. The other members also have individual qualities: So IκBζ seems to predominantly act in the nucleus [220], IκBR interacts with p50 / p65 heterodimers, but not with p65 homodimers [177], and the inhibitory nuclear protein Bcl-3 can form complexes with p50 and p52 homodimers which are transcriptional activators instead of repressors [28, 70, 73].

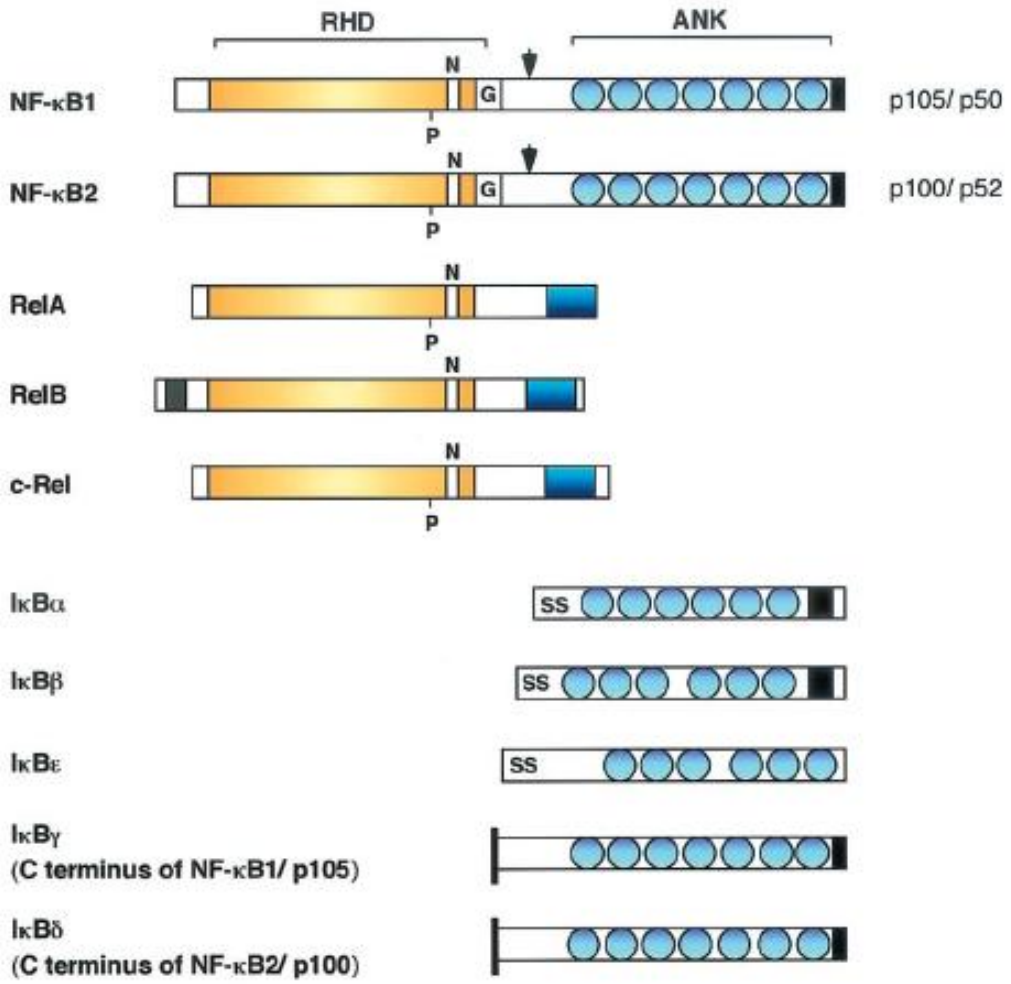

Figure 1.1: Members of the Rel/NF-κB and IκB families of proteins

J. Caamaño and C. A. Hunter, Clinical Microbiology Reviews, July 2002, p. 414–429 [35].

Schematic view of Rel/NF-κB proteins. The arrows indicate the proteolytic cleavage sites of p105 and p100 which produce p50 and p52, respectively. Black boxes indicate the PEST domains, shaded boxes on Bcl-3 indicate trans-activation domains, and gray boxes on RelB indicate leucine zipper domains. Abbreviations: RHD, Rel homology domain; ANK, ankyrin repeat; P, PKA phosphorylation motif, N, nuclear localization site; G, glycine rich region; SS, signal-induced phosphorylation sites.

1.3 Activation of NF-κB via TNF-α

The best known pathway for NF-κB activation is the response to TNF-α. TNF receptors are expressed on a broad variety of cells. Neurons and glia also express TNF receptors [32]. The most important of these receptors for NF-κB activation seems to be p55/TNF-R1 [125]. Mice lacking the TNF-R1 in reason of a genetic defect show traumatic brain injury with reduced NF-κB activation [32]. The so-called canonical pathway of NF-κB activation [27, 190] starts with the TNF-α binding to the trimerized TNF-R1 and the release of the silencer of death domains (SODD/BAG4). This silencer evidently blocks the pathway [104] and it has been speculated that this goes along with the recruitment of the heat shock cognate 70 kDa (HSC70), a member of the heat shock protein family. BAG4 is known to interact and modulate the chaperone activity of HSC70 [31, 198]. The free trimeric death domains (DD) of TNF-R1 can afterward function as an assembly platform for intracellular interactors which subsequently recruits the adapter protein TNF-R associated death domain protein (TRADD), TRAF2/5 and RIP1 [56, 93, 204]. Although RIP1 has a kinase activity, this is not important for the signal transduction [207]. Instead, it is being polyubiquitinated by the TNF-R associated ubiquitin ligases cIAP1 and cIAP2 [22]. This chain does not lead to proteasomal degradation, but serves as interaction platform for TGFß-activated kinase binding protein 2 and 3 (TAB2, TAB3). TAB2 and TAB3 recruit the TGFß-activated kinase (TAK) and enables an interaction with the ubiquitin binding domain (UBD) of the NF-kappa-B essential modulator NEMO [117]. Furthermore, cIAP1 and cIAP2 ubiquitinate themselves and other components of the complex. This enables the association of the so-called linear ubiquitin chain assembly complex (LUBAC) which stabilizes the signaling complex by additional ubiquitin mediated interactions [22]. The protein NEMO is also known as the γ-subunit of the inhibitor of κ B kinase (IKK) complex. By bringing NEMO and TAK closely together, TAK can phophorylate and activate the IKK subunit β at serines 177 and 181 [53]. The IKK complex is targeted to IκBα by its subunit ELKS [63]. The catalytic IKK subunits α and β phosphorylate IκBα at serin 32 and 36 so that it can subsequently be ubiquitinated and degraded [6, 58]. The free NF-κB e.g. p50 / p65 can now be transported into the nucleus and enhance transcription (v.i.).

The importance of ubiquitination for NF-κB signaling / complex multimerization is also shown by deubiquitinating enzymes such as CYLD which can target NEMO and deactivate the IKK complex [127, 208]. Another protein which possesses a deubiquitination and ubiquitination activity is A20 which targets RIP [89]. The SCF (Skp-1/Cul/F box)-type multisubunit E3 ubiquitin ligase holoenzyme, responsible for IκB poly-ubiquitination [222], can also be inhibitied by pyrrolidone dithiocarbamate (PDTC) to prevent NF-κB activation [86].

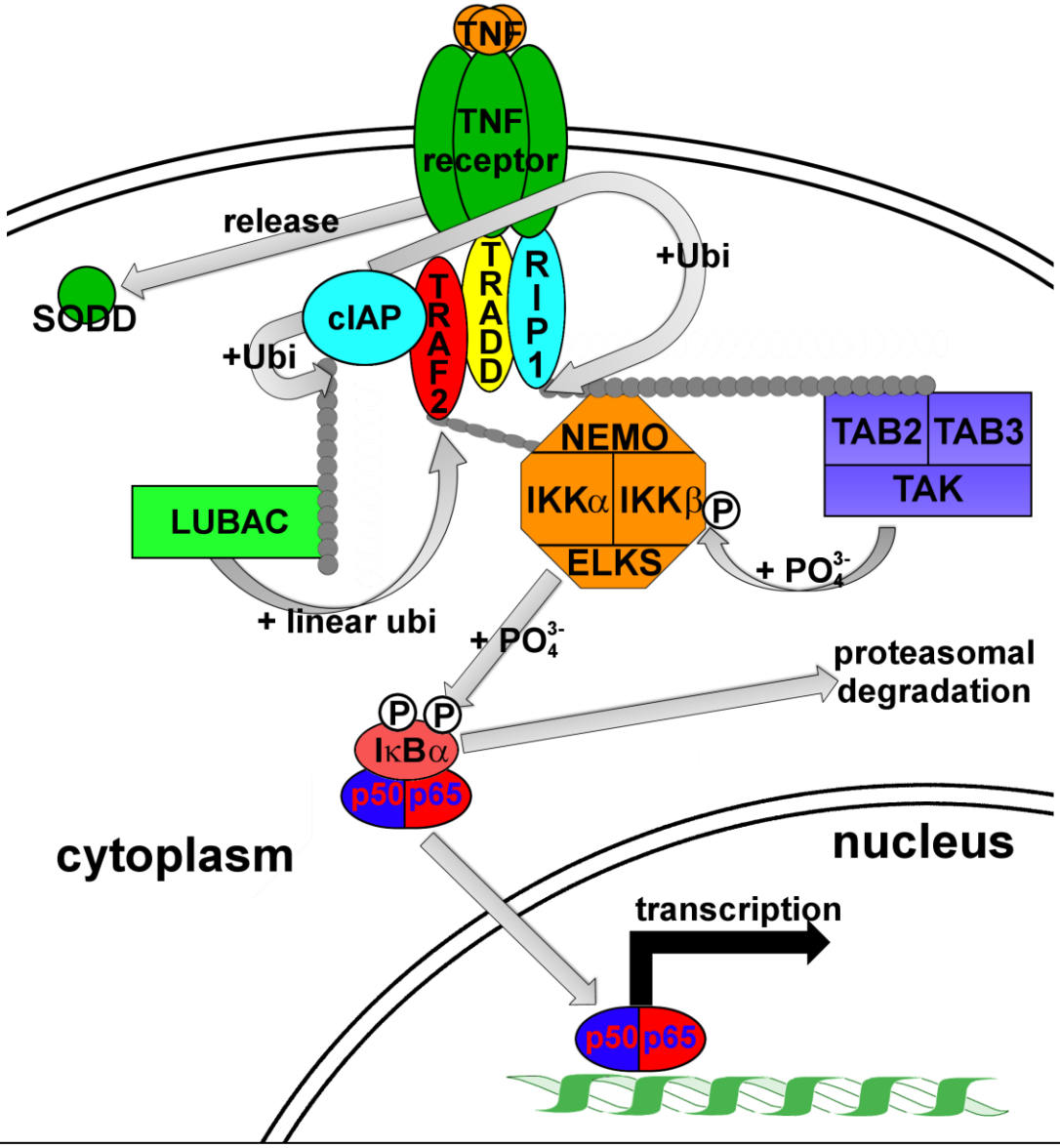

Figure 1.2: Canonical pathway of NF-κB activation by (TNF).

The activation of the TNF receptor by ligand binding releases SODD and enables the binding of TRADD, TRAF2 and RIP1. The TRAF2 associated ubiquitin ligase cIAP ubiquitinates RIP1 and itself. The ubiquitination on RIP1 enables the loose association of the IKK complex via NEMO and the TAK complex via TAB1/2. The ubiquitination on cIAP recruits LUBAC which stabilizes the complex by linear ubiquitin links. This proximity leads to the phosphorylation of IKKb by TAK and the IKK complex can phosphorylate IkBa, recruited by ELKS, and designate it for degradation. The NLS of the NF-kB dimer p50 / p65 is released and NF-kB is transported to the nucleus where it can promote the transcription of its targed genes.

+Ubi=ubiquitination; +PO_4^{3-} =phosphorylation.

1.4 Activation of NF-κB by other stimuli

Besides TNF-α there is a broad variety of other stimuli which induce NF-κB activation. This could be for example TNF, LPS, IL-1, NGF or glutamate. These and many other stimuli are finally integrated by the IκB kinase complex and culminate in NF-κB activation [166]. For example TLRs, as the LPS receptor, are known to use two different pathways: The first using a protein called myeloid differentiation primary response gene 88 (MyD88) and the second depending on the protein TIR domain containing adaptor-inducing interferon-ß (TRIF) [120]. The LPS responding receptors TLR2 and TLR4 recruit MyD88. This protein binds to a members of the IL-1 receptor-associated kinase (IRAK) family, which interacts with TRAF6. TRAF6 binds TAB2, TAB3 and TAK1 and the latter phosphorylates and activates the IKK-complex [3]. The interactions between TRAF6, TAB2, TAB3 and IKK are also ubiquitin dependent [44, 117].

The signal transduction via TLR3 and TLR4 is TRIF dependent. It is very similar to the TNF pathway, in which the proteins TRADD and TRAF2/5 are replaced by TRIF and TRAF6, which also bind RIP1 in order to mediate NF-κB activation. As described above, TLR4 uses both adaptors, MyD88 and TRIF, whereas TLR3 is the only TLR that does not use the MyD88 dependent pathway [120, 219].

1.5 Activation of NF-κB by the non-canonical pathway

The characteristic of the non canonical pathway is the independence from IKKß and NEMO and the dependence on IKKα [51, 195].The non-canonical pathway is used in response to ligand binding to the TNF superfamily receptors CD40, RANK, LT-ß-R and BAFFR [45, 46, 52]. It is rather important in B cells than in neurons and the predominantly activated NF-κB dimer is the p52:RelB heterodimer. The ligand binding to LT-ß-R and BAFFR induces the phosphorylation of IKKα by the NF-κB inducing kinase (NIK) [136, 137, 178, 211]. IKKα itself phosphorylates p100 [218], which is associated with RelB. Phosphorylated p100 is recognized and ubiquitinated $SCF_{ß\text{-}TrCP}$ ubiquitin E3 ligase-complex [7]. The ubiquitination marks the inhibitor for processing into the mature subunit p52 by the proteasome [88]. The resulting RelB:p52-complexes can translocate to the nucleus and activate NF-κB target genes.

1.6 Nuclear import / shuttling

The free nuclear localization signals of NF-κB dimers is folded into a random coil formation, which is able to bind importin. The NLS of p50 and p65 for example are recognized by importin α3 and α4 [67]. While importin α4 predominatly recognizes the p50 / p65 heterodimer, importin α3 also imports p50 homodimers [67] and decreases the constitutional NF-κB activity in this way. The IκB proteins regulate the nuclear import by masking the nuclear localizations signal and inducing an alpha helical conformation [96]. Herein, the inhibitors show a great specificity: while IκB-α only interacts with the NLS of p65 only, IκB-β interacts with both the NLS of p50 and p65 [140]. The alpha helical conformation cannot be recognized by the nuclear import receptor importin alpha [102].

Besides p65, IκBα also contains a NLS which is also masked by interaction with Rel proteins [96, 102, 185]. On the one hand, this enables free IκBα to translocate to the nucleus and dissociate p50 / p65 heterodimers from DNA [224] and on the other hand, it prevents the nuclear import of the trimer. NF-κB is not only imported into the nucleus, but also exported. Therefore p65 [75, 95, 206] and IκBα [75, 95, 107, 139, 206] contain a nuclear export signal (NES), too. This enables the shutteling of NF-κB subunits and is most important to silence the signal pathway besides promoter-specific degradation of p65 via nuclear proteasomes [184].

1.7 NF-κB in neurons

Central functions of the nervous system are information transmission, processing and storage. Most important for these tissues are two cell types: neurons and glia. While neurons receive, transmit and store information, the glia are known as neuronal glue (*greek glia = glue*). They maintain homeostasis and isolate the neurons. Neurons communicate via electric and chemical signals with each other. The place where the electric signal is converted to a chemical and transferred to a neighbour cell is the synapse, consisting of a presynaptic (sending) cell and a postsynaptic (receiving) cell. Usually, the presynaptic site is the terminal of an axon and the postsynaptic site the terminus of a dendrite. Both are extension of neurons, but axons are mostly longer an better isolated and dendtrites are more branched. In many recent

publications, learning and memory is connected with the so-called synaptic plasticity [182]. The synaptic plasticity describes the efficiency of chemical signal transduction by a synapse. This is manly affected by the number of released neurotransmitter and the number of specific receptors.

The participation of NF-κB in synaptic transmission is supported by several studies detecting NF-κB in synapses [112, 145, 146]. A second indication for this hypothesis, is the fact that a positive correlation between p65 mRNA level and synaptic transmission activity was shown [4]. This could be part of a feed forward mechanism. In Drosophila melanogaster, the NF-κB homolog Dorsal colocalizes with the IκB homolog Cactus in high levels in postsynaptic sites of glutamatergic neuromuscular junctions [38]. This substantiates the assumption that NF-κB is used as a retrograde messenger to the nucleus. The transport of NF-κB in living neurons could be observed using a GFP-tagged p65 after glutamate stimulation [146, 213]. Although less is known about the pathway of NF-κB activation in cell of the nervous system, it is probable that there is also a Ca^{2+} dependent one because the CAM kinase II is reported to activate NF-κB [135, 146]. In two different models, this relation is used to create a local p65 knock out in mouse forebrain neurons. Both mouse lines show a severe learning deficit. [71, 146].

Additionally, NF-κB is an important regulator between neurodegeneration and apoptosis or neuroprotective processes including calcium buffering, generation of novel synapses, anti-apoptotic gene expression, caspase inhibition, balancing of reactive oxygen intermediates, etc. [68, 111, 142, 221].

The most frequent heterodimer in the nervous system is p50 / p65 that is either constitutively active or forms a complex with the inhibitory subunit IκB-α [16, 79, 109, 112, 113, 114, 115, 175]. Furthermore, there are κB-binding proteins such as brain-specific transcription factor (BETA), specifically detected in grey matter extracts [124], developing brain factors (DBFs), which were reported to be highly enriched in developing cortex [40], and neuronal κB binding factor (NKBF) with different target sequence requirements [157]. These binding factors do not exclusively bind to specific genes, but there seems to exist a complex system of binding sites, which binds more or less specific one of the transcription factors and act together with other binding sites.

1.8 NF-κB activating or repressing stimuli in neurons

TNF-α triggers in a broad variety of cell types related to the nervous system, such as neuroblastoma, neurons [18, 110], neuroblastoma [61], astrocytes [199], and microglia [133]. It is also reported that TNF-α is able to repress NF-κB activity in neurons under certain circumstances [110], e.g. under oxidative stress [77]. Besides TNF, there is a broad variety of stimuli, which affect NF-κB activity in the nervous system. Many of them are better known for their function in the immune system, like interleukins or inflammation mediators. So interleukin-1 is known to induce NF-κB in neurons and glia cell [78, 166], interleukin-6 in neurons of the peripheral nervous system (PNS) [152], while interleukin-10 reduces the NF-κB activity in astrocytes [170], neurons [14] and microglia [64]. The repression of NF-κB activity in astrocytes can also be triggered by interleukin-4 [170]. The inflammation mediator IFN-γ, which activates T-cells in immune system, can induce NF-κB in microglia in combination with beta-amyloid, which is involved in alzheimers disease and neuronal signal transduction [26]. In addition, exogene stimuli which affect the immune system can influence the NF-κB dependent expression in the nervous system. For example, LPS operates as an NF-κB activator in microglia [19] and astrocytes [169], whereas aspirin (acetylsalicylic acid) represses NF-κB dependent expression in neurons [78].

Besides these inflammatory molecules, the cells of the nervous system also respond to a lot of growth factors by NF-κB activation or repression. The epidermal growth factor (EGF) for example initiates the expression of glutamate transporter 1 (GLT-1) in astrocytes via transcription factor NF-κB [225]. The nerve growth factors (NGF) triggers NF-κB activation in neurons [101], NGF Schwann cells [39] and oligodendrocytes [223], while the brain derived neurotrophic factor (BDNF) activates it in microglia [163] and neurons [34].

Furthermore, neurotransmitter like glutamate [79] and the related kainate [113] are known to signal via induction of NF-κB in neurons and glucocorticoid hormones reduce NF-κB dependent expression in neurons [29]. This vast number of stimuli emphasizes the importance role of NF-κB in the nervous system.

1.9 Neuronal transport of NF-κB

In most cell types, transcription factors are able to reach their targets by diffusion, in contrast to neurons, which neurites could extent far from the cell body. In fact, some motor neurons in the human spine could reach a length of more than one meter. For these distances, an effective kind of active transport system is needed [92]. For intracellular transport, cells have a system of actin filaments and microtubules. [119]. The transport on actin filaments is mediated by the motor protein myosin [130]. The microtubules employ two different motor protein families: The kinesins and dyneins. While transport on microtubules is related to long distances, actin transport is responsible for short. That means that the cargo is often transferred from one type of motor protein to another [94]. Kinesin and dynein are moving in opposite direction according to the polarity of the microtubules. Kinesins typically show positive end-directed movement and dynein drives to the negative ends. In most cells, microtubules are oriented with their negative ends near the nucleus and their positive ends toward the cell periphery [80]. This is also reported for axons in neurons. However, dendrites show this regulation of polarity only near the growth cone, but not in their main length [12]. As described above, the NF-kB p50 / p65 heterodimer binds to importin. This does not only enable the translocation through the nuclear pore complex (NPC), but also delivers associated proteins to the nuclear membrane along microtubules via dynein [37,81, 82]. In addition, the retrograde transport of NF-κB is dependent on an intact NLS [146, 213]. The dynein dependence of NF-κB transport was shown by impeding the transport by overexpression of dynamitin, a subunit of the dynein/dynactin motorcomplex [153]. Dynactin is an accessory multi protein complex of dynein. It increases the processivity of dynein by the interaction of its large subunit p150Glued to the microtubules and dynein. The dynamitin subunits connect p150Glued to the cargo-binding domain. This contains a short polymer of eight subunits of the actin-related protein Arp1, which is pivotal for vesicles binding and other associated polypeptides. The overexpression disturbs the formation of the functional complex. An in vitro complex of p50 and p65 and dynein could also be detected and disrupted by dynamitin [148, 153]. The transport of p50 and p65 on microtubules is neuron specific. Microtubule perturbating drugs like vincristin have no effect on non neuronal NF-κB transport [154]. Nevertheless, there

is little knowledge about interactors in the NF-κB transport. Are there regulators specific for NF-κB transport besides the regulation of NF-κB activation? How is this specificity generated? What does the transport complex look like? Does dynein directly bind importin and importin to NF-κB? To find new NF-κB interactors, a pull down experiment with subsequent mass spectrometry analysis is performed in this thesis.

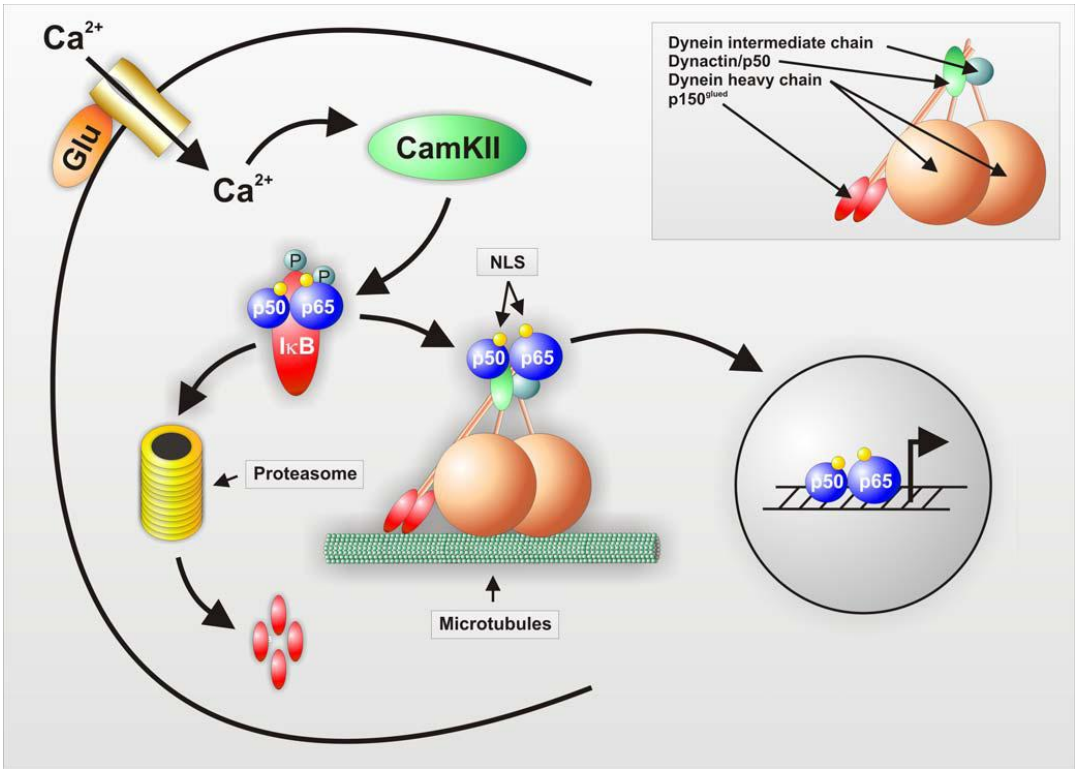

Figure 1.3: NF-κB activation in the synapse

Mikenberg, I.; Widera, D.; Kaus, A.; Kaltschmidt, B.; Kaltschmidt, C. PLoS ONE, 2(7):e589 [153].

Schematic presentation for the NF-κB activation in the synapse and its dynein-mediated microtubule dependent retrograde transport to the nucleus. Neurons stimulated by glutamate activate NF- κB by different signaling pathways (e.g. by CaMKII). IκB is phosphorylated and subsequently degraded in the proteasome. The NLSs of the of NF-κB dimer are unmasked and may bind importin. The complex is transported retrogradely towards the nucleus via an association with the motor protein dynein/dynactin, where it activates NF-kB target genes.

2 Objective of the study

The neuronal NF-κB transport complex is not yet fully characterized. Besides the finding that components like dynein, dynactin, and importin participate in it, a lot of questions related to its properties are still unanswered. Particularly, the connection of NF-κB to the motor protein is not completely discovered. We assume that unknown mediators in an interaction chain between the motor protein (dynein) and the cargo (NF-κB) are necessary for their association, responsible for the generation of specificity, and targets for regulation. These new interactors are to be found by a mass spectrometric analysis of NF-κB complexes, acquired by co-precipitation with the NF-κB subunit p65/RelA from neuronal extracts. The interaction of these components will be verified and tested for its biologic relevance. This data will help to improve our models for neuronal NF-κB transport and may discover new targets for the regulation of neuron specific NF-κB signaling.

3 Material and methods

3.1 Computer software

Biotools	Bruker Daltonics
Blast 2.2.13	NCBI
Codon Usage Analyzer 2.0	Morris Maduro
Excel 2007	Microsoft GmbH
GIMP 2.6.10	Spencer Kimball, Peter Mattis and the GIMP-developer team
KEGG	Kanehisa Laboratories
Mac OS 9.1	Apple Computer, Inc.
Mascot	Matrix sciences
MS Office 2007	Microsoft GmbH
NCBI blast	National Center for Biotechnology Information
Oligo Calc	Northwestern University
Primer3	Withhead Institute for Biomedical Research
Swissprot	Swiss institute of bioinformatics
Vector NTI	Invitrogen
Windows 7	Microsoft GmbH
Windows XP	Microsoft GmbH
ZEN	Zeiss

3.2 Material

3.2.1 Antibiotics

Name	Target organism	Stock conc.	Effective conc. (for selection)
Ampicillin	bacteria	100 mg/mL	50-100 µg/mL
Chlorampenicol	bacteria	35 mg/mL	15 µg/mL
G418	eukaryotes	100 mg/mL	800 µg/mL (HEK293)
Kanamycin	bacteria	50 mg/mL	50 µg/mL
Penicillin / Streptomycin	bacteria	10000 U/mL	100 U/mL
Puromycin	eukaryotes	10 mg/mL	10 µg/mL
Streptomycin	bacteria	10 mg/mL	100 µg/mL
Zeocin	eukaryotes, bacteria	100 mg/mL	800 µg/mL (HEK293), 25 µg/mL

3.2.2 Antibodies

Name	Species, type	Specificity	Supplier	for	Buffer conditions	Dilution
111-035-144	goat, IgG H&L HRP	rabbit	Jackson IRL	WB	PBST	1:4000
C3956	rabbit, polyclonal	myc tag	SIGMA	WB, IP	WB blocking sol., see IP	1:4000 (WB), 1 µg/mL (IP)
F1804 (M2)	mouse, IgG1	Flag tag	SIGMA	IP	see IP	1 µg/mL
F7425	rabbit, polyclonal	Flag tag	SIGMA	WB	1% BSA in PBST	1:2000
MOPC21	mouse, IgG1	none	SIGMA	IP	see IP	2-30 µg/rct.
Sc-371 (C21)	rabbit, polyclonal IgG	IκBα	Santa Cruz	WB	1% BSA in PBST	1:200
sc-8008	mouse, IgG1	p65	Santa Cruz	IP	see IP	2-30 µg/rct.

3.2.3 Bacteria strains

Strain	Genotype
BL21 DE3 pLysS	E. coli B F– dcm ompT hsdS(rB– mB–) gal λ(DE3)[pLysS Camr]
DH5α	fhuA2 Δ(argF-lacZ)U169 phoA glnV44 Φ80 Δ(lacZ)M15 gyrA96 recA1 relA1 endA1 thi-1 hsdR17
HB101	F–, *thi*-1, *hsd*S20 (r_B^-, m_B^-), *sup*E44, *rec*A13, *ara*-14, *leu*B6, *pro*A2, *lac*Y1, *gal*K2, *rps*L20 (str^r), *xyl*-5, *mtl*-1
TOP10	F- *mcr*A Δ(*mrr-hsd*RMS-*mcr*BC) φ80*lac*ZΔM15 Δ*lac*X74 *rec*A1 *ara*D139 Δ(*araleu*)7697 *gal*U *gal*K *rps*L (StrR) *end*A1 *nup*G
XL1 blue	recA1 endA1 gyrA96 thi-1 hsdR17 supE44 relA1 lac [F' proAB lacIqZΔM15 Tn10 (TetR)]

3.2.4 Buffers, media, solutions

All solutions are prepared in water if not described differently. The pH-value is adjusted at room temperature with NaOH or HCl if not described differently.

ATP-Stock solution	500 mM ATP PBS
$CaCl_2$ Solution for chemo competent bacteria	50 mM $CaCl_2$
DMEM complete	DMEM basal medium 10% FCS 2 mM glutamine 2 mM pyruvate Penicillin 100 U/mL Streptomycin 100 µg/mL

dNTPs	10 mM dATP, dCTP, dGTP, dTTP each
ECL Solution A	0.1 M TrisCl pH 8.6 0.025% luminol store at 4°C
ECL Solution B	0.11% p-coumaric acid in DMSO, store dark
Embedding resin	Moviol 50 mg/mL DABCO
Fixation solution for microscopy	4% paraformaldehyde in PBS
Gel extraction solution for MS I (flexibilizer extraction solution)	TFA 0.1% /acetonitrile 60%
Gel extraction solution for MS II	acetonitrile 50%/H_2O 50%
Gel extraction solution for MS III	acetonitrile 50% / NH_4HCO_3 50 mM
Gel extraction solution for MS IV	acetonitrile 50% / NH_4HCO_3 10 mM
Gel extraction solution for MS V (trypsinization buffer)	NH_4HCO_3 10 mM
Glycerol solution for bacteria stocks	65 % (v/v) Glycerin 0.1 $MgSO_4$ 0.025 M Tris Cl, pH 8,0
GST basic cleaning solution I	100 mM Tris-base 0.5 M NaCl pH 8.5
GST basic cleaning solution II	100 mM sodium acetate 0,5 M NaCl pH to 4.5
GST elution buffer	50 mM Tris base 10 mM glutathione 0.1 Triton X-100 pH 8.0 prepare fresh, store at 4°C
GST Rigorous cleaning I	6 M guanidine hydrochloride
GST Rigorous cleaning II	70% ethanol in H_2O

LB agar	LB medium supplemented with
	1.5% agar
LB medium	0.5% yeast extract
	1.0% bacto tryptone
	0.05-1.0% NaCl
	(LB-Lennox 0.5% NaCl)
	Sterilized by autoclav method
Lysis buffer (for brain extracts)	150 mM NaCl
	50 mM HEPES pH 7,6
	2 mM EGTA
	0.5 % Trition X-100
	1 mM PMSF
Lysis buffer (for IP after cross link)	50 mM TrisCl, pH 7,5
	150 mM NaCl
	1% NP-40 (v/v), pH 7,5
Lysis buffer (for IP before cross link)	50 mM HEPES, pH 7,5
	150 mM NaCl
	1% NP-40 (v/v), pH 7,5
PBS	137 mM NaCl
	2.7 mM KCl
	9.6 mM Na_2HPO_4
	2.4 mMKH_2PO_4, pH 7,4
PBST	PBS; 0.05 % (w/v) Tween 20
Permeabilizing solution	0.25% Triton X-100 in PBS
SDS-PAGE running buffer 10x	3% Tris base
	14.4% glycine
	0.5% SDS
SDS loading buffer 4x	0.2 M Tris-Cl pH 6.8
	8 % SDS
	100 mM DTT
	16 % glycerol
	0.01 % Bromphenol blue
	15 mM EDTA

SOC medium 1 L	2% tryptone
	0.5% yeast extract
	0.05% NaCl
	2.5 mM KCl
	20 mM glucose
	pH 7.0, sterilized by autoclav method
TAE-Puffer	40 mM Tris-Acetic acid
	10 mM NaOAc
	1mM Na-EDTA
	pH 7.8
Transfer buffer I	25 mM Tris
(for semi dry blot)	40 mM aminohexanoic acid
	20 % methanol
Transfer buffer II	30 mM Tris
(for semi dry blot)	20 % methanol
Transfer buffer III	300 mM Tris
(for semi dry blot)	20 % methanol
Tyrode's buffer	119 mM NaCl
	4.5 mM KCl
	2 mM $CaCl_2$
	0.5 mM $MgCl_2$
	25 mM Glucose
	0.01 mM Glycine
	10 mM Hepes (pH7.33)
WB blocking solution	5% skimmed milk powder
	in PBS
WB washing solution	0.5% skimmed milk powder
	in PBST

3.2.5 Cell lines

HEK293FT

The HEK293 cell line is a permanent line established from primary human embryonic kidney cells transformed with sheared human adenovirus type 5 DNA [84, 128]. The E1A adenovirus gene is expressed in these cells and participates in the transactivation of some viral promoters, allowing these cells to produce very high levels of protein. The HEK293F cell line is a subclone of HEK293 that was originally obtained from Robert Horlick at Pharmacopeia. This subclone captivates by its fast growth rate and reduced serum requirements. The HEK293FT cell line was produced by transfection of HEK293F with the pCMV-SPORT6TAg.neo plasmid [100]. This plasmid carries the SV40 large T antigen gene controlled by the human cytomegalovirus (CMV) promoter, which is constitutive and promotes high expression levels. The cell line is Gentamycin resistant and a very suitable host for lentiviral production [164]. The expression of the neomycin resistance gene in HEK293FT cells is controlled by the SV40 enhancer/promoter.

3.2.6 Chemicals

If not noted otherwise, all chemicals were either purchased by Sigma, Roche, Fluka or Merck in p.A. Quality. Special chemicals are enlisted here:

10x Taq Puffer #201205	Qiagen
Acrylamide (30%)/bisacrylamide (8%) solution	Roth
Agarose	Roth
APS (ammoniumpersulfate)	Roth
ATP	SIGMA
Coomassie brilliant blue G-250	PIERCE
DABCO	Hoechst
DMEM Medium	PAA
DMSO	MERCK
DNA loading dye (6x)	Fermentas
DRAQ5	Alexis

DSP	Thermo scientific
Ethanol	VWR International
Ethidiumbromide	SIGMA
Gene Ruler DNA Ladder Mix	Fermentas
Glutathione (reduced)	Roth
Luminol (A46859)	SIGMA
Moviol	Hoechst
Phusion buffer HF F-518	Finnzymes
PMSF	SERVA Feinbiochemica
Polyethylenimine	SERVA Feinbiochemica
Ponceau Red	SIGMA
Propidiumiodide	SIGMA
Protein A sepharose beads 50% slurry (P3476)	SIGMA
Protein A/G plus agarose beads	Santa Cruz Biotech
Protein ladder #0671	Fermentas
TEMED (tetramethylethylenediamine)	Roth
Tween20	Applichem

3.2.7 Consumables

µ-Slide 8 wells	ibidi
Cell culture flasks	TPP
Centrifuge tubes	TPP
Cover slips, glass slides	Roth
GSTrap Fast Flow	Amersham Biosciences
Molecular sieve 0.3 nm	MERCK
Pipette tips	Diagonal
Reaction tubes 1,5 mL	Diagonal
Sterile filters	Sarstedt

3.2.8 Devices

Autoclave	A5	WEBECO
Cell culture hood	Hera Safe	Heraeus instruments
Centrifuges	MIKRO 200	Hettich
	MIKRO 22R	Hettich
	RC2-B	Sorvall
	4K15C	Sigma centrifuges
Distillation apparatus	Destamat	Heraeus instruments
Electroph. chamber (DNA)		Mech. Workshop Bielefeld Univ.
Electroph. Sys. (Protein)	45-1010 Class II	PeqLab
Fluorescence microscope	LSM 5 Exiciter Obs. Z1	Zeiss
FPLC	LCC 500	Pharmacia Biotech
FPLC fraction collector	RediFrac	Pharmacia Biotech
FPLC printer	REC 102	Pharmacia Biotech
Hood for microbiology	LaminAir HB2472	Heraeus instruments
Incubator (for bacteria)		Memmert
Incubator (for cell culture)	FunctionLine	Heraeus instruments
Luminometer	Lumat LB 9506	Berthold
Magnetic stirrer	IKA-COMBIMAG REO	Janke & Kunkel
Microscope	CK2	Olympus
Neubauer count. chamber		Roth
PCR- machine	PCR Express	HYBAID
PCR-machine	Master Cycler Gradient	Eppendorf
pH-Meter	MP220	Mettler Toledo
Photometer	Biophotometer	Eppendorf
Power supply	DC Power 5004	Nishizawa
Power supply	E0300-0.1	Delta Elektronika
Power supply	Microcomp Electroph.	Renner GMBH
Pure water treatment plant		Millipore
Roller	low profile roller	Stovall Lifescience inc.
Rotor for 1.5 mL tubes	C28	Labinco
Scales	1409 MP	Sartorius

Scales	FA210-4iCE	Faust
Shaker (37°C, bacteria)	3033	GFL
Shaker	SM25	Bachofer
Sonifier	PG.744	MSE
Thermomixer	5436	Eppendorf
Trans illuminator	Transilluminator 4000	Stratagene
Ultra sonic water bath	Sonorex longlife	Bandelin electronic
Vortex	VORTEX GENIE	BENDER&HOBEIN
Water bath	C10	HAAKE

3.2.9 Enzymes

Antarctic phosphatase	NEB
Phusion high fidelxity DNA Pol	Finnzymes
Restriction endo nucleases	NEB, Fermentas
Taq polymerase	A. Kralemann Köhler, BioV, Bielefeld Univ.
Trypsine (Seq. grade modified)	Promega

3.2.10 Oligo nucleotides

The melting temperatures of all primers are calculated using the basic, the salt adjusted and the nearest neighbor method by the software Oligo Calc. All sequencing primers are optimized for an annealing temperature at 55-60°C.

Primers for PCR-cloning:

Nr.	Name	Target	Sequence (5'-3')
Z032	3-Primer_ Mitte	p65 for SDM	TCT GCC GGG AAG ATG AGG GGG AAC AG
Z033	5-Primer_ Upstream	pENTR/SD/D-TOPO for SDM	CTG GCA CGA CAG GTT TCC CGA CTG G
Z034	3-Primer_ Downstream	p65 in pENTR/SD /D-TOPO for SDM	GAT CAG CTC CAA GGG TGG GCG CGC CGA

Nr.	Name	Target	Sequence (5'-3')
Z035	5-Primer_ Mitte	p65 for SDM	CCC CCT CAT CTT CCC GGC AGA GCC AGC
Z370	p65gexfw	p65 ORF A into pGEX-5X-1	TTG GAT CCC CGA CGA ACT GTT CCC CCT CAT CTT CC
Z371	p65gexrv	p65 ORF Ω into pGEX-5X-1	AAC TCG AGT CTA GAT TAG GAG CTG ATC TGA CTC AG
Z382	pGEXIkBf	IκBα ORF A into pGEX-5X-1	TTG GAT CCC CTT CCA GGC GGC CGA GCG C
Z383	pGEXIkBr	IκBα ORF Ω into pGEX-5X-1	AAT CTA GAC TAT AAC GTC AGA CGC TGG CCT CCA AAC
Z567	HSP90DW	HSP90 ORF Ω into pcDNA3.1(+)	AT CTA GAT TAG TCT ACT TCT TCC ATG CGT GAT GTG TC
Z569	HSPA8DW	HSC70 ORF Ω into pcDNA3.1(+)	AAT CTA GAT TAA TCA ACC TCT TCA ATG GTG GGC CC
Z608	HSP90UP	HSP90 ORF A into pcDNA3.1(+)	TGG ATC CCC ATG CCT GAG GAA ACC CAG ACC CAA G
Z609	HSPA8UP	HSC70 ORF A into pcDNA3.1(+)	TGG ATC CCC ATG TCC AAG GGA CCT GCA GTT GGT ATT
Z772	HSPA8GFP5	BamHI-HSC70 ORF A into pcDNA3.1(+)GFP	GAG CTC GGA TCC ACC ATG TCC AAG GGA CCT GCA GTT GGT ATT
Z773	HSPA8GFP3	HSC70-NotI ORF Ω into pcDNA3.1(+)GFP	CAC CAT GCG GCC GCC ATC AAC CTC TTC AAT GGT GGG CCC TGA G

ORF A: open reading frame start, ORF Ω: open reading frame terminus, SDM: site directed mutagenesis

Sequencing primers

Nr.	Name	Target	Sequence (5'-3')
Z015	P65_5-PrimerII	p65 part 2/3	AAC ACT GCC GAG CTC AAG AT
Z016	P65_5-PrimerIII	p65 part 3/3	AGC CAT GGT ATC AGC TCT GG
Z044	5PrimerI	Pezz18 upstream to MCS	GCT GCG CAA CAC GAT GAA G
Z045	3PrimerIV	P65 part 1/3	CTG GTC CCG TGA AAT ACA CC
Z416	pGEX-5X-5f	pGEX-5X-1 upstream to MCS	ATA CAT GGA CCC AAT GTG CC
Z417	IkBaSeqII	IκBα part 2/2	GTG ATC CTG AGC TCC GAG AC
Z626	HSPA8seq1fw	HSPA8 part 2/3	TGG TCA CAG TGC CAG CTT AC
Z627	HSPA8seq2rv	HSPA8 part 1/3	CAG CAG CAG TTG GCT CAT TA
Z628	HSPA8seq3fw	HSPA8 part 3/3	TTG CTG CTC TTG GAT GTC AC
Z629	HSP90seq1fw	HSP90 part 2/4	CTA TGA TTG GCC AGT TCG GT
Z630	HSP90seq2rv	HSP90 part 1/4	CTG AGG ACT CCC AAG CGT AC
Z631	HSP90seq3fw	HSP90 part 3/4	GAC TGG GAA GAT CAC TTG GC
Z632	HSP90seq4fw	HSP90 part 4/4	AAC TCA GCC TTT GTG GAA CG

The part describes the partition of the insert, which is covered by sequencing result using the indicated primer. The first part contains the start of insert's ORF.

3.2.11 Protease inhibitors

Name	Effective Conc.	Stock conc.	Supplier
aprotinine	10 µg/mL	10 mg/mL	Roth
leupetine	10 µg/mL	5 mg/mL	Roth
NaF	10 mM NaF	500 mM in 9:1 acetic acid/methanol	Roth
pepstatine	1 µg/mL	1 mg/mL	Roth
PMSF	1 mM	100 mM in ethanol	Roth

3.2.12 Reagent kits

DNA Extraction PC500	Macherey-Nagel
Dual-Luciferase Assay System	Promega
In vitro translation kit	Promega
NucleoSpin Extract II	Macherey-Nagel
Protein quantification kit (Rotiquant)	Roth

3.3 Molecular biologic methods

3.3.1 Agarose gel electrophoresis

Depending on the size of the DNA fragments to separate the gel pore size is regulated by the fraction of agarose between 0.8% (w/v) – 1.5% (w/v). The amount of agarose is heated in an appropriate volume of TAE-Buffer to the boiling point. After cooling down to ca. 60°C, 0.5 µg/mL ethidium bromide are added and the evaporated water is supplemented. The gel is casted and after polymerization, the DNA samples are applied with 6x DNA loading dye. A maximum of 100 ng DNA is loaded per millimeter gel width. The separation takes place within an electric field strength of 5 V/cm (Voltage / electrode distance) for ~1 h. The gel is placed on a transilluminator and photographed by a standard digital camera.

3.3.2 PCR cloning

To insert target sequences in the desired expression vectors, all target sequences have to carry an appropriate restriction side and they have to carry a Kozak sequence and ATG (leading peptide) or must be in frame (C-terminal fusion). These features can be added to target sequences by PCR. Therefore, a primer is designed that carries the needed sequence in its overhang. For cloning purpose, a high fidelity proof reading polymerase from Finnzymes is used. After PCR, the product is purified by NucleoSpin Extract II. The DNA strand with the newly appended restriction sites can now be digested. The used reaction composition and PCR machine program are described below.

PCR-Mix (50 µL):

10 µL	5x Phusion buffer HF (high fidelity)
1.0 µL	dNTPs
0.5 µL	Phusion high fidelity polymerase (2 U/µL)
3 µL	5'-Primer (10 pmol/ µL)
3 µL	3'-Primer (10 pmol/ µL)
31.5 µL	distilled water
1 µL	Template (0.1 to 10 pg plasmid template)

Table 3.1: Program for PCR Cloning

Step	Temperature [°C]	Duration [sec]	Cycle number
Initial denaturing	94	30	-
Denaturing	94	30	30
Primer annealing	variable, 60 (standard)	20	
Elongation	72	30 per kb	
Finale elongation	72	300	-
Storage	10	∞	-

3.3.3 Colony PCR

The colony PCR is used to identify clones carrying the desired insert after transformation. Before starting the colony PCR it is controlled if the plate with the insert of interest shows significantly more colonies than a plate with bacteria transformed with the empty vector. When the ratio is adequate a number of clones is picked with a sterile toothpick and transferred into a 1.5 mL reaction tube with 50 µL water. The bacterial material is vigorously mixed with the water by scraping the inner walls of the tube. Afterwards the toothpick is used to inoculate 5 mL LB-medium supplemented with an appropriate selective agent. The bacteria water mix is boiled for 5 min in a thermomixer. Afterwards, it is used as template for the colony PCR. With at least one insert specific primer, it is possible to identify the clones with the desired insert.

PCR-Mix (50 µL):

5 µL	10x Taq buffer (Qiagen, #201205)
0.2 µL	MgCl 25 mM
0.5 µL	dNTPs
0.5 µL	Taq polymerase (1,25 U/µL)
1 µL	5'-Primer (10 pmol/ µL)
1 µL	3'-Primer (10 pmol/ µL)
26.8 µL	distilled water
15 µL	Template (boiled bacteria)

Table 3.2: Program for Colony PCR

Step	Temperature [°C]	Duration [sec]	Cycle number
Initial denaturing	94	30	-
Denaturing	94	30	30
Primer annealing	60	20	
Elongation	72	60 per kb	
Finale elongation	72	420	-
Storage	10	∞	-

3.3.4 DNA construct sequencing

The sequencings of the DNA constructs is performed by the sequencing core facility of the CeBiTec at Bielefeld University. For each reaction, 3 µg DNA (250 ng/µL) and 10 µL 10 mM sequencing primer are sent to the institute.

3.3.5 Dephosphorylation of cleaved vector DNA

To prevent a religation of a cleaved vector backbone in a subsequent ligation reaction, the vector DNA is dephosphorylated after digestion. Therefore, an excess of five units of Antarctic phosphatase are added per µg DNA to the sample directly after restriction. It is incubated for 30 min at 37°C and Afterwards heat inactivated for 5 min at 65°C.

3.3.6 Digestion of plasmid DNA by restriction endonucleases

0.1 to 1.0 µg of plasmid DNA are incubated with one unit of the appropriate endonucleases for 60 min. The buffer conditions and incubation temperature is chosen as recommended by the supplier (Fermentas, NEB). All enzymes are heat inactivated by incubation for 15 min at 65°C if no higher temperature is recommended by the supplier.

3.3.7 Ligation of DNA fragments

As preparation for the ligation, both fragments, the insert and the dephosphorylated vector are separated by agarose gel electrophoresis. The desired bands a cut from the gel with a clean scalpel and extracted with the kit Nucleospin Extract II (Macherey-Nagel) as it is recommended by the supplier. A small fraction of the purified DNA samples is loaded on an agarose gel again and the DNA concentration is estimated by comparison with the DNA ladder bands. For the Ligation 10-40 ng vector DNA, the fourfold equimolar amount of the insert, two units ligase and 10x ligase buffer are combined in 20 µL sample volume. The ligation mixture is incubated for 2 h at room

temperature or at 16°C over night. The whole reaction can directly be used for transformation.

3.3.8 Production of chemo competent E. coli

200 mL LB-Medium are inoculated with a 5 mL over night culture of the desired bacteria strain and cultivated at 37°C and shaking with 250 rpm. The bacteria are cultivated till they reach an OD_{600} of 0.4 - 0.6. Then the culture is transferred to 50 mL centrifuge tubes and chilled on ice for 5 min and Afterwards centrifuged for 7 min at 1600 g. The supernatant is discarded and the pellet resuspended in 10 mL per tube of ice cold $CaCl_2$ solution. The samples are centrifuged again at 1100 g for 5 min. The supernatant is discarded and the pellet resuspended in 2 mL of ice cold $CaCl_2$ solution. The suspension is aliquoted in 100 µL fractions and stored at -70°C.

3.3.9 Transformation of chemo competent E. coli

One aliquot of chemo competent E. coli is thawed on ice per transformation reaction (~10 min). Depending on whether a retransformation or a transformation of a ligation reaction should be performed, either 0.1-1 ng or the whole ligation reaction is used. This DNA is added to the bacteria in a maximum volume of 20 µL. The mixture is incubated for 30 min on ice. After this incubation, a heat shock at 42°C is applied. The duration depends on the bacteria strain and varies between 30 sec and 2 min. After the heat shock, the sample is cooled on ice for 2 min before 1 mL of prewarmed LB or 300 µL prewarmed SOC medium is added and the bacteria are cultivated for 1 hour at 37°C. Afterwards the bacteria are plated on LB agar supplemented with an appropriate selective antibiotic.

3.3.10 Establishing of glycerol stocks

1 mL of fresh, saturated bacteria culture is mixed with 1 mL glycerol solution and frozen at minus 70°C. For use of the stock, a small ice fragment is scraped off by an inoculation loop. The stock may not thaw.

Alternative:
0.85 mL fresh, saturated bacteria culture are mixed with 0.15 mL Glycerin (100%) and frozen at -70°C.

3.4 Protein biochemical methods

3.4.1 Colloidale Coomassie staining

Colloidal Coomassie staining is 20 to 100fold more sensitive than "normal" Coomassie staining and does not interfere with mass spectrometry measurements like classic silver staining. It can detect protein traces down to 5 ng. For the preparation of a colloidal Coomassie staining, the order of mixing the components is important. 10% ammoniumsulfate are dissolved in half of the final water volume, then 10 % phosphoric acid are added. The solution is mixed and filled up to 80% of the final volume with water. 0.12% Coomassie brilliant blue G-250 are added and the solutions is stirred until no large particles are visible any longer. Directly before use, the mixture is filled up to 100% with methanol.
For colloidal staining, the SDS gels need to be washed twice for ten minutes in distilled water to remove the SDS, which otherwise increases the background. Afterwards the gel is placed in the methanol containing staining solution until it reaches the desired intensity or for saturation over night. The contrast can be enlarged by washing in distilled water.

3.4.2 ECL

All western blots are developed by enhanced chemo luminescence. In this technique, the horseradish peroxidase labeled secondary antibody catalyzes the conversion of the enhanced chemo luminescent substrate into a sensitized reagent in the vicinity of the molecule of interest. This produces on further oxidation by hydrogen peroxide, a triplet (excited) carbonyl which emits light when it decays to the singlet carbonyl. Therefore, the 50 mM Tris-Cl buffer (pH 7.35) washed blotting membranE is placed between two transparent plastic sheets. Per membrane (ca. 7 x 9 $cm^{2)}$, 1 mL ECL solution A, 100 µL ECL solution B and 0.3 µL30% H_2O_2 are mixed, added to the membrane, covered with the plastic sheet, and dispersed to a thin layer. The chemo luminescence is measured immediately by a special photo camera.

3.4.3 Purification of GST fusion proteins from E. coli

A single colony of E. coli DH5α or BL21 DE3 pLys, transformed with the gene of interest in the GST expression vector pGEX-5X-1, is used for inoculation of a 5 mL over night culture in selective medium (LB-Medium with 100 µg/mL Ampicillin). This is used as starter for a 400 mL culture on the next morning. The bacteria are incubated at 37°C and 250 rpm until the OD_{600} reaches a value of 0.4 to 0.6. This takes between 3 and 5 hours. At this point, the culture is divided in halves and the protein production is induced in one culture by the addition of 1 mM isopropy-beta-thio galactopyranoside (IPTG). The incubation is prolonged for 3 hours. Afterwards the bacteria are separated by centrifugation at 4500 to 6000 g for 5 min. The supernatant is discarded and all remaining liquid is drawn from the pellet by a pipette. If necessary, the pellet may be shock frozen in liquid nitrogen and stored at -80°C. For lysis, the pellet is resuspended in 10 mL ice cold PBS and sonicated four times for 30 sec. The lysate is cleared by centrifugation for 15 min at 12000 g and 4°C. The cleared lysate can directly be loaded onto the column. For the affinity purification, an FPLC device in combination with an 1 mL Amersham GSTrap Fast Flow column is used. The protein efflux is monitored by a UV spectrometer with printer. The flow rate is 1 mL/min. The column is equilibrated with 4 CV (4 mL) PBS. One to ten mL sample are applied. The column is washed until the UV absorption of the flow through is stable and near to the baseline, but at least with

10 mL PBS. The elution is performed with elution buffer (50 mM Tris, 10 mM glutathione, 0.1% Triton X-100 pH 8.0). This buffer is used until the UV absorption of the flow through is stable, but at least 5 mL. In order to clean it, the column is washed with 5 CV PBS, 5 CV of basic cleaning I buffer (100 mM Tris-HCl, 0.5 M NaCl, pH 8.5), then with 5 CV of basic cleaning II buffer (100 mM sodium acteate, 0.5 M NaCl, pH 4.5) and 5 CV PBS. If the column is clogged with precipitated, denatured proteins, the solutions rigorous cleaning I (6 M guanidine hydrochloride) and II (70% ethanol in H_20) are used. Each of them with 5 CV alternating with PBS. The column can be stored in 20% Ethanol in PBS for long time.

3.4.4 Immunoprecipitation for mass spectrometry

For each immunoprecipitation, 20 mg of brain extract protein are needed. This protein solution is cross linked by the addition of 0.5 mg/mL DSP (dithiobissuccini-midylpropionate) solution in dry DMSO (final concentration 0.5 mg/mL, suitable stem conc. 10 mg/mL) and incubation on ice for 30 min. The cross linking is stopped by Tris buffer pH 8.0 at the final concentration of 25 mM which exhaust the remaining DSP. The cross linked protein is then mixed with 50 µL protein G sepharose 4B fast flow (SIGMA) and the desired amount of anti p65/RelA antibody (sc-8008, Santa Cruz Biot.) or antibody for the isotype control (mouse monoclonal IgG1, MOPC 21, SIGMA). The immunoprecipitates are spun head over tail for 2 hours at 4°C. After the formation of the immunoprecipitates the samples are washed three times. Each washing step consists of a centrifugation for 1 min at 3000 g and the addition of 1 ml lysis buffer (brain extract protocol). After the last washing step, the IPs are centrifuged and the pellet is eluted in 30 µL 1 SDS sample buffer by heating at 60°C for 5 min. The supernatant is used for SDS gel electrophoresis and mass spectrometry analysis.

3.4.5 Immunoprecipitation for western blotting

HEK293FT cells are transfected with Lipofectamine2000™ in a 10 cm plate scale for each immunoprecipitation reaction (see transfection methods). The following expression constructs are used: pcDNA3.1(+)c-myc-HSPA8, pcDNA3.1(+)c-myc-HSPA8mut, pcDNA3.1(+)c-myc-HSP90, pcDNA3.1(+)Pin1, pEF-FLAGpGKpuro p65WT, pEF-FLAGpGKpuro p50 and pCMV c-myc-Iκε. In case of a co transfection, equimolar ratios of these constructs are used. The cells are harvested 36 hours after the transfection. For this purpose they are washed with PBS, resuspended in 1 mL of lysis buffer (50 mM HEPES, 150 mM NaCl, 1% NP-40 (v/v), pH 7,5) and protease inhibitors (1 mM PMSF; 10 µg/mL leupetine, 10 µg/mL aprotinine, 1 µg/mL pepstatine and 10 mM NaF). Subsequently, they are transferred to a 1mL reaction tube and lysed by incubation on ice for 20 min, interrupted by three 30 sec sonication steps. The debris are separated by centrifugation for 10 min at 14000 g and 4°C. The supernatant is used for the IP and the expression test. For the expression test, 50 µL sample are mixed with 12,5 µL 5xSDS sample buffer and loaded on a SDS-PAGE. For the IP, 30 µL 50% protein A sepharose beads are washed once with 1 mL PBS. The beads, 900 µL supernatant, and 1,5 µL (final conc. 1.0 µg/mL) rabbit ANTI-c-Myc (C3956 SIGMA) are incubated spinning head over tail for 2 h at 4°C or 37°C. If indicated, 300 µL axon enriched pig brain extract (3.3 mg protein) and for crosslinking 50 µL DSP (in DMSO, final conc. ~0.5 mg/mL) are added for incubation. After this, the remaining crosslinker is exhausted by the addition of 25 µL 1 M TrisCl pH8.0 (final conc. 25 mM) and by incubation for 15 minutes at 4°C. The beads are centrifuged at 12000 g for 1 min and washed with 1 mL lysis buffer containing 50 mM Tris instead of HEPES. After five washing steps with this lysis buffer and one with PBS, the beads are eluted with 90 µL 1xSDS-sample buffer and ready to load on SDS-PAGE and western blotting. The western blotting is performed using the following antibodies: rabbit polyclonal Anti-Flag 1:4000 (F7425, SIGMA), rabbit polyclonal Anti-c-Myc 1:2000 (C3956 SIGMA), and goat anti-rabbit IgG H+L HRP 1:4000 (111-035-144, Jackson Immuno Research Laboratories).

In the experiments where the Flag tag is used for capturing, the IP is done with Anti Flag M2 (F1804, SIGMA) and protein A/G plus agarose beads (Santa Cruz Biotechnology).

3.4.6 Luciferase assay

The Luciferase assay serves as a tool for the quantification of a promoter activity. It uses two reporter genes, which are co transfected in the cells of interest. Both genes encode luciferases. The firefly luciferase is controlled by the promoter of interest, the other one, the Renilla luciferase, by a constitutive promoter. 36 hours after the transfection, the expression of the luciferases correlates to the activity of their promoters. The two luciferase activities are measured subsequently via the fluorescence provoked by two different substrates. The assay is performed with "Dual-Luciferase® Reporter Assay System" kit from Promega in a 24well scale. Therefore $2x10^5$ cells are seeded per well. The cells are transfected due to the Turbofect® protocol (v.i.). They are transfected with 800 ng of total DNA: 200 ng of the NFκB Firefly Luciferase construct Enh-TK-luciferase designed by Bachelerie et al. [13], 100 ng of the Renilla Luciferase construct pGL4.74[*hRluc*/TK] Vector supplied by Promega and 500 ng of others (see results). The cells are harvested after 36 hours by adding 100 µL passive lysis buffer provided by Promega and rocking for 15 min at room temperature. This crude lysate is diluted 1:20 and stored on ice. Subsequently, both fluorescence values are measured according to the Promega protocol. The constitutive Renilla luciferase activity is used for the normalization of variations in the sample volume, cell viability etc. So each value is a ratio of firefly luciferase / Renilla luciferase.

3.4.7 Mass spectrometry

The MALDI TOF MS analysis was performed by Carola Eck in the CeBiTec at Bielefeld University (supervisor Prof. K. Niehaus) while the LC ESI MS measurements were done by Dr. Raimund Hoffrogge of the "Zellkulturtechnik" workgroup of Prof. T. Noll in the technical faculty at Bielefeld University.

All samples are analyzed by using Mascot. This software compares the experimental data to in silico digested peptide spectra. In silico means that a whole human proteome database is virtually digested with trypsin. Therewith a unique pattern of fragment masses is created for each single protein. Those patterns are compared to the experimental ones. If many fragments of an in silico digested protein are found in a sample, it is more probable that the analyzed sample contains this database protein.

This probability is expressed by a score. The higher the score, the more improbable the detected ions belong to an unknown random protein. It is distinguished between ion scores and protein scores. Ion scores describe the significance of a single peak. A peak is more significant when it can be produced only from a few proteins. If a peak belongs to a common fragment or can be related to many fragments, it is less significant. So it is obvious that large masses are more significant then small ones. The protein scores are based on the combined ion scores.

The MALDI TOF MS Data are compared in a peptide mass fingerprint analysis using a human protein data base from the Kyoto Encyclopedia of Genes and Genomes and no modifications are regarded. The settings for peptide mass tolerance, maximum missed cleavages and peptide charged state are customized for each spectrum. The LS ESI MS/MS data are analyzed by a MS/MS ion search referring to a human protein data base allowing carbamidomethy modifications and oxidations. Peptide mass tolerance is fixed to ±1250 ppm and fragment mass tolerance to ±1250 mmu. Only one missed cleavage is allowed. In both cases, only monoisotopic mass value are regarded.

3.4.8 Preparation gel spots for mass spectrometry analysis

PP-Tubes (1 mL) are treated twice with 500 µL TFA 0.1% /acetonitrile 60% over night to extract flexibilizers. Bands are cut out of the gel with a clean scalpel and put into the pretreated tubes. 250 µL (100 µL for 96 well plate) acetonitrile 50%/H_2O 50% are added to the gel slice and incubated under shaking for 5 minutes at room temperature. The supernatant is removed and 250 µL (100 µL for 96 well plate) acetonitrile 50% / NH_4HCO_3 50 mM are added. After incubation under shaking for 30 minutes at room temperature, the supernatant is removed again. 250 µL (100 µL for 96 well plate) acetonitrile 50% / NH_4HCO_3 10 mM are added to the gel and incubated for 30 minutes at room temperature. The supernatant is removed again and the gel slice dried over night under the flue. 20 µg trypsine (Seq. grade modified, Promega) are diluted in 200 µL of supplied buffer and activated for 15 minutes at 30°C. 1 µL of trypsine solution is mixed with 14 µL NH_4HCO_3 10 mM and added to the dry gel slice. After incubation for 15 minutes at room temperature or 2 hours at 4°C additional 20 µL (10 µL for 96 well plate) NH_4HCO_3 10 mM are added. The

mixture is incubated air tide over night at 37°C and stored at -20°C. For LC ESI MS/MS, potential particulate matter is segregated by centrifugation. The supernatant sample is transferred to a clean septum sealed tube.

3.4.9 SDS polyacrylamide gel electrophoresis

The analytic separation of proteins is performed by SDS polyacrylamide gel electrophoresis in a discontinues buffer system. The components of separating and stacking gel are enlisted in Table 3.3. Therefore, the separating gel is poured first between the glass plates sealed in a casting base of an electrophoresis system from Sigma Aldrich. The stacking gel is protected against evaporation by water saturated isopropyl alcohol during polymerization. After polymerization, the isopropyl alcohol is discarded and the gel is briefly washed with water before pouring of the stacking gel. A Teflon comb is inserted to form the sample bags. Immediately before loading, the sample bags are washed with running buffer and the system is checked for leaks by filling with running buffer and the application of voltage (one 10 x 10 cm^2 mini gel has an electric resistance of ca. 4000Ω). The electrophoresis takes place at 80 V until the dye front leaves the stacking gel. From this time point on, the electrophoresis is continued at 15 mA per gel. As a molecular weight standard, the PageRuler prestained protein ladder #0671 from Fermentas is used (bands at 10, 17, 26, 34, 43, 55, 72, 95, 130 and 170 kDa).

Table 3.3: Composition of separating and stacking gels

	Separating gel			Stacking gel
	(7.5%)	(10%)	(12%)	(3.75%)
30% (w/v) acrylamide, 0.8% (w/v) bis-acrylamide	4.0 ml	5.33 ml	6.4 ml	500 µl
Tris 3 M pH 8.8	2.0 ml	2.0 ml	2.0 ml	---
Tris 1 M pH 6.8	---	---	---	500 µl
SDS 10%	160 µl	160 µl	160 µl	40 µl
H_2O	9.7 ml	8.4 ml	7.3 ml	1.94 ml
TEMED	13.3 µl	13.3 µl	13.3 µl	3.5 µl
ammoniumpersulfate solution 10%, fresh	133 µl	133 µl	133 µl	35 µl
60% sucrose	---	---	---	980 µl
Total for two 10x10 cm Mini-gels	~ 16 ml	~ 16 ml	~ 16 ml	~ 4 ml

3.4.10 Synaptosomal extracts

40 g of brain tissue are washed in 240 mL ice cold homogenization buffer. Afterwards, the tissue is homogenized in 240 mL fresh ice cold buffer in a potter (9 strokes at 900rpm). 280 µL PMSF solution are added. The homogenized material is centrifuged at 850 g for 10 min. The pellet is discarded. The supernatant is centrifuged again at 11500 g for 15 min. The pellet is resuspended in 240 mL homogenization buffer and centrifuged for 15 min at 14000 g. The pellet is solvated in 10 mL lysis buffer. The protein concentration is measured by a Biuret Reaction (Rotiquant kit). For storage, 10% glycerol are added and the protein solution is shock frozen in liquid nitrogen and stored at -80°C.

3.4.11 Tissue extraction

For the preparation of brain extracts, pig brain tissue is purchased in a slaughterhouse and transported on ice or dry ice for the frozen sample. All further steps are performed at 4°C. 300 g of pig brain tissue (180 g per brain) were sheared in an equivalent amount of lysis buffer in a blender on lowest level. One fraction of the hashed brain is directly used for extract, the other one is filtrated by a sieve, which enriches the more robust axon/myelin containing white tissue in the filter cake. The filter cake is mixed with the two fold amount of lysis buffer. Afterwards both, the whole brain and the filter cake, are sheared by ultraturax. After 30 min incubation, the suspension is cleared by two centrifugation steps from all insoluble contaminants: The first is performed at 15,000 g for 20 min. The supernatant is cleared in a second procedure at 40,000 g for 30 min. The protein concentration in the supernatant is measured by a Biuret Reaction (Rotiquant kit). The protein solution is either mixed with 10% Glycerol and shock frozen in liquid nitrogen or directly used for IP.
Mouse whole brain extracts are produced analog with decreased amounts. Up to 2 mg are used. This is equal to four mouse brains.

3.4.12 Western blot

Semi dry electro blot: The SDS gel is equilibrated in distilled water immediately after the electrophoresis for 10 min. A nitrocellulose membrane, 0.2 µm pore size, and six filter papers are trimmed to the same size as the gel. The nitrocellulose is equilibrated in distilled water, while the filter papers are incubated in the solutions described below. The equilibration is suitable when the nitrocellulose membrane show no more white blotches. The material is placed between the graphite electrodes of the blotting aperture in the following order: Downside (anode, positive pole), two filter papers (25 mM Tris, 40 mM aminohexanoic acid, 20 % methanol), one filter paper (30 mM Tris, 20 % methanol), nitrocellulose membrane, gel, three filter papers (300 mM Tris, 20 % methanol), upside (cathode, negative pole). The aperture is burdened with 2 kg. The transfer takes two hours at a current of 1.6 to 1.8 mM per cm^2. The nitrocellulose membrane is stained reversible by 0.1% Ponceau Red solution.

Western blot: The Ponceau Red stained nitrocellulose membrane is washed in distilled water. Free binding sides are blocked by incubation for one hour at 37°C in 5% skimmed milk powder dissolved in PBS. The nitrocellulose membrane is washed three times for 10 min with washing buffer (0.5% skimmed milk powder and 0.02% Tween 20 in PBS). The first antibody is applied in the appropriate buffer (see antibodies). 4 mL buffer volume are needed for a 9x7 cm^2 blot. The membrane is applied to the inner wall of a round tube upside inside. The incubation takes place over night at 4°C. After the incubation, the membrane is washed again three times for 10 min with washing buffer (v.s.). The secondary antibody is applied in the same way as the first, but it is incubated only for one hour at room temperature. Subsequently, the blot is washed again (v.s.) and equilibrated in 50 mM Tris-Cl Puffer pH 7.35 for 10 min. Afterwards the western blot can be developed by ECL.

3.5 Cell biological methods

3.5.1 Cell culture conditions

All cells are maintained at 37°, 5% CO_2-content and 90% relative humidity.

3.5.2 Cell passage

The adherent growing cell line HEK293FT is cultivated in DMEM complete medium supplemented with 200 µg/mL G418 in order to maintain the plasmid pCMVSPORT6TAg.neo. The medium is changed at least every three days. If the cells are confluent, they are divided by a ratio between 1:10 and 1:20. Therefore, the medium is discarded and the cells are washed with a volume of PBS equal to medium volume. The cells are dissociated by addition of a volume of trypsin/EDTA solution which covers the complete surface of the cell culture dish. The trypsin is incubated one minute at 37°C. After trypsinization, the cells are carefully resuspended in an appropriate volume of medium and seeded.

3.5.3 Thawing and freezing of cells

Thawing: The cells are rapidly warmed in a 37°C water bath. After the melting of the ice, the cell sample is mixed with 9 mL of prewarmed medium in a centrifuge tube. The cells are centrifuged at 210 g for 5 min. The supernatant containing DMSO is discarded and the cells are plated in 10 mL fresh medium.

Freezing: After trypsinization and counting, 1-1,5·10^7 cells are centrifuged for 5 min at 210 g and 4°C and resuspended in 1 mL of cold medium supplemented with 10% (v/v) DMSO. The cells are transferred to a cryo tube, frozen for 1-3 days at 70°C and stored in liquid nitrogen.

3.5.4 Transfection methods

Three different transfection methods are used: Transfection with Lipofectamine 2000™ (Invitrogene) or TurboFect™ (Fermentas), with PEI (polyethylenimine) [147].

Lipofectamine transfection: The vector DNA and the Lipofectamine 2000™ reagent amounts indicated in Table 3.4 are diluted in serum and antibiotic free DMEM Medium, gently mixed and incubated for 5 min at room temperature. After incubation, they are combined and incubated for further 20-30 min to form precipitates. Meanwhile, the HEK293 FT cells are seeded in a density, so that they are 40% confluent in antibiotic free medium. The exact number of cells can be found in Table 3.5. After precipitate formation, the DNA / Lipofectamine 2000™ mixture is added dropwise to the cells. After six hours, the antibiotic free medium must be replaced by Penicillin and Streptomycin containing medium. The cells can be harvested after 24 to maximum 48 hours incubation.

TurboFect™ transfection: The TurboFect™ transfection is quite similar to the work with Lipofectamine 2000™ reagent, but there is no need to use serum and antibiotic free medium. Furthermore, it is not necessary to premix the reagent or change the medium 6 hours after transfection.

PEI transfection: The poly cationic substance polyethylenimine works like TurboFect™. It forms complexes with the DNA, mask the negative charge with its positive amine groups, it is taken up by endocytosis, inhibits lysosomal degeneration of the DNA and enables their nuclear uptake. The effectiveness of PEI transfection

depends strongly on the molecular weight and complexity (branched, unbranched) of PEI. In this work, a crude mixture of PEI is used (Serva, Cat. No.: 33141.04). The indicated amounts of PEI and DNA (Table 3.4) are each mixed in PBS (Table 3.4), incubated for 5 min, combined, and incubated for 20 min at room temperature. Meanwhile, the number of cells for 60% confluency (Table 3.5) is seeded in a plate. After incubation, the DNA/PEI complexes are added dropwise. The medium is mixed by rocking the plate back and forth. A medium change after 6 hours is not necessary, but it increases the viability of the cells. The cells can be harvested after 24 to maximum 48 hours incubation.

Table 3.4: DNA and reagents amounts

Plate type	Medium / buffer	Lipofectamine 2000™		TurfoFect™		PEI (1 µg/µL)	
		DNA	Reagent	DNA	Reagent	DNA	Reagent
24 well	2x50 µL	0.4 µg	0.7 µL	0.8 µg	1,5 µL	-	-
12 well	2x100 µL	0.7 µg	1.2 µL	2 µg	3 µL	3.2 µg	3.6 µL
6 well	2x200 µL	1.7 µg	3.3 µL	4 µg	4 µL	9 µg	10 µL
6 cm Ø	2x500 µL	4 µg	8 µL	6 µg	6 µL	18 µg	20 µL
10 cm Ø	2x500 µL	10 µg	20 µL	8 µg	8 µL	54 µg	60 µL
15 cm Ø	2x500 µL	25 µg	50 µL	-	-	-	-

Table 3.5: Cell densities

Plate type	Area	Cell number for 40% confluency	Cell number for 60% confluency
24 well (one well)	2.0 cm^2	$3.4x10^6$ per plate	$5.1x10^6$ per plate
12 well (one well)	3.8 cm^2	$3.0x10^6$ per plate	$4.5x10^6$ per plate
6 well (one well)	9.6 cm^2	$4.0x10^6$ per plate	$6.0x10^6$ per plate
6 cm Ø	21 cm^2	$1.3x10^6$	$2.0x10^6$
10 cm Ø	57 cm^2	$4.0x10^6$	$6.0x10^6$
15 cm Ø	150 cm^2	$1.0x10^7$	$1.5x10^7$

3.5.5 Determination of cell density

The cell number/density is determined by using a Neubauer counting chamber. Therefore, 10 µL cell suspension are applied between the counting chamber and the cover slip. Four of the large, central quadrates, each containing 25 small quadrates, are counted and the average is calculated. The equation is valid:

(1) cell density = average $x \cdot 10^4$ cells/mL

3.5.6 Nuclear localization assay

A steril coverslip roughened in 80% phosphoric acid is placed in a well of a 6 well plate for each sample. $4x10^6$ HEK293 FT cell are seeded per six well plate and transfected with 4 µg of total DNA per well. The DNA mixture is composed of 1 µg FPred-p65 and, if indicated, 2.8 µg GFP or HSC70-GFP and/or 100 ng IκB expression plasmid complemented with empty expression vector. The expression of IκB here leads to a cytoplasmic localization of p65 by masking the NLS sequence of p65/RelA. For the transfection, the Turbofect® protocoll is used. After 24 hours of expression, the cells are washed with PBS, fixed with 4% paraformaldehyde in PBS, washed again twice in PBS and permeabilized by an incubation with 0.25% Triton X-100 in PBS for five minutes. Then the cells are washed again (v.s.) and they are stained with 10 µM DRAQ5 (Alexis) in PBS for 15 minutes on the coverslip. Afterwards, the cells are washed and embedded in Moviol with 50 mg/mL DABCO (1,4-**D**i**a**za**bic**yclo[2.2.2]**o**ctan). The resin hardens over night. The flourescence is observed in confocal microscopy using the Zeiss Observer with a 40x planar Neofluar oil 1.3 objective (400 fold total magnification). The nuclear fluorescence is recorded via DRAQ5 (Em<max 681 nm / 697 nm intercalated to dsDNA) using a far red filter (551-757 nm), the fluorescence of FPredp65 is recorded using a red filter 547-660 nm and the green fluorescence of HSC70-GFP or GFP is detected between 492-539 nm. The fluorescence pictures are analyzed by the ZEN software. The nucleus, assisted by the DRAQ5 fluorescence, and the whole cell are defined as regions. The mean fluorescence of the red and green channel is detected and used for the calculation of the ratio $F_{nuclear}/F_{cell}$. The relative nuclear localization increases with this quotient.

3.5.7 In vivo nuclear localization assay

HEK293 FT cells are transfected with Turbofect™ and cultivated in camber slides. For the transfection, a mastermix is used for cell seeding. It consists of $1.33x10^6$ cell combined with 3.5 µL Turbofect™ solution and 2.5 µg DNA (50% HSC70-GFP or GFP, 12.5% FPredp65, 5% IκBα and 32.5% pcDNA3.1) in 10 mL medium. 500 µL of this mastermix are seeded per well (~1 cm^2). The cells are cultivated for 24 hours. Afterwards, the medium is replaced by 500 µL 37°C prewarmed Tyrode's buffer [119 mM NaCl, 4.5 mM KCl, 2 mM $CaCl_2$, 0.5 mM $MgCl_2$, 25 mM Glucose, 10 mM Hepes (pH7.33), 0.01 mM Glycine]. The cells are stimulated with 25ng/ml TNF and observed under a confocal microscope. The microscope is placed under a 37°C temperate tent. A planar apochromat 63x 1.4 Oil Objective is used. Only red and green fluorescence is detected. The filter settings are the same as described above.

4 Experimental results

4.1 Description and cloning of expression constructs

For the subsequent described work, a number of expression plasmids is used. In the following, the cloning strategy used to create this constructs will be explained. The GST expression plasmids are created on the base of the commercial pGEX-5X-1 vector. This plasmid promotes the expression of GST without further modifications. The coding sequences (CDS) for IκBα and p65 are amplified from two constructs supplied by Ilja Mikenberg, PhD student of Prof. Dr. C. Kaltschmidt at the University of Witten/Herdecke: pENTR_SD_D-TOPO_IKB-alpha-V5-His and SD_D-TOPO_TAP-p65(WT)-V5-His [153]. IκBα was simply amplified using the primers pGEXIkBf and pGEXIkBr. While pGEXIkBf contains a BamHI site, pGEXIkBr is designed with an XbaI restriction site. These endo nuclease recognition sequences are used for subsequent cleavage and ligation into pGEX-5X-1. The template for p65/RelA contained a point mutation. This was corrected by site-directed mutagenesis using the primer Z032-Z035. The two hybridized products of site directed mutagenesis are amplified by the primers (5'-p65 in pGEX) and (3'-p65 in pGEX). These primers enable the cloning into pGEX-5X-1 similar to IκBα.

For the co-immunoprecipitation, the constructs pEF FLAGpGKpuro B p65 WT (FLAG-p65/RelA), pcDNA3.1(+)c-myc-HSPA8 (c-myc-HSPA8), pcDNA3.1(+)c-myc-HSP90AA1 (c-myc-HSP90) and pCMV c-myc-IκBε (c-myc-IκBε) are used. While the last, pCMV c-myc-IκBε, was a thankful donation from the group of Prof. Dr. M.L. Schmitz of the institute for Biochemistry of the University Gießen, the other three constructs are created by PCR cloning. The original template for construction of the HSPA8 and HSP90 expression plasmids was ordered at geneservice (part of the Source BioScience plc group), see Table 4.1: Template origin of HSPs. The templates are amplified via the primers Z609 and Z569 (for HSPA8) and Z608 and Z567 (for HSP90). The PCR products with a size of 1941 and 2259 bp are ligated into the purchasable vector pezz18 which was digested with the blunt end cutter SmaI. The ligation is verified by a diagnostic digestion and full length (CDS) sequencing (for primer sequences see Material & Methods). From this vector, both coding sequences are transferred to pcDNA3.1(+)c-myc using the BamHI and XbaI restriction sites. The vector pcDNA3.1(+)c-myc was constructed

by the insertion of a poly linker. It consists of two primers that encode the immunogen synthetic peptide corresponding to amino acid residues 410-419 of human c-myc protein (E Q K L I S E E D L) [21, 212]. The coding sequence is gag caa aag ctc att tct gaa gag gac ttg [217]. The two primers are phosphorylated, hybridized and ligated via KpnI and BamHI into the commercially available pcDNA3.1(+) (Invitrogen). The PCR cloning of HSPA8 leads to a point mutation in the coding base 203. Thus the triplet TTT is replaced by TGT, which leads to the expression of Cystein on amino acid 68 instead of Phenylalanine. The mutant is named HSPA8mut. The mutation is repaired by the replacement of the mutated sequence between the restriction sites EcoRI and PpuMI from the original clone HSPA8 in pCMV-Sport 6. Flag-p65/RelA was expressed using the plasmid pEF FLAGpGKpuro B p65 WT. This plasmid was constructed by transferring the BamHI / XbaI excised p65 from pGEX-5X-1 p65 WT into pEF FLAGpGKpuro. This vector is offered in three variants for different reading frames, from which variant B was chosen for this construct.

Table 4.1: Template origin of HSPs constructs

Final construct	Template	Clone ID	MGC	Accession NCBI
pcDNA3.1(+) c-myc-HSPA8	HSPA8 in pCMV-Sport 6	3920744	17984	BC016179
pcDNA3.1(+) c-myc-HSP90AA1	pCR-BluntII TOPO HSP90	40118488	149801	BC121062.2

For fluorescence microscopy, three fluorescent fusion proteins are used: the red FPred-p65, HSPA8-GFP and GFP. The construct FPred-p65 was kindly supplied by Christin Zander, PhD student of Prof. Dr. C. Kaltschmidt at Bielefeld University. The GFP expression plasmid pcDNA3.1(+) GFP was constructed by Patrick Lüningschroer, PhD student of Prof. Dr. C. Kaltschmidt as well.

pcDNA3.18(+) HSPA8-GFP which was created based on pcDNA3.1(+) GFP. HSPA8 was amplified from HSPA8 in pCMV-Sport 6 using the primer Z772 and Z773 by PCR and ligated into pcDNA3.1(+) GFP via BamHI and NotI.
All constructs are verified by diagnostic digestion or colony PCR and by sequencing the CDS.

4.2 Generation of bait protein for immunoprecipitation and co IP

For the identification of new NF-κB (RelA) interaction partners, it is necessary to generate a bait protein, which mimics the interaction qualities of p65/RelA and can be easily purified. This features makes it possible to co purify the bound interaction partners. The most obvious choices are a p65 fusion protein with an affinity tag or an anti p65 antibody, which binds the interactors via its antigen. In both cases, it is desirable to achieve high yields because only a little quantum will bind interaction partners. Therefore, only high amounts of interacting protein allow their identification in mass spectrometry.

4.2.1 Expression and purification of GST fusion proteins

In the first place, new NF-κB interactors should be isolated by a GST pull down. Therefore, the NF-κB subunits p65/RelA and IκB are expressed with the GST tag as N-terminal fusion proteins. This enables the co purification of the subunits and pre incubated interactors via affinity chromatography. The GST tag alone is also expressed to serve as negative control in the pull down experiment. To yield high amounts of GST fusion proteins, it is expressed in bacteria. Before its use in the pull down experiment, it is purified by affinity chromatography and the elution fraction is analyzed in mass spectrometry.

The Glutathion-S-Transferase tag is encoded by the vector pGEX-5X-1 which was expressed in DH5α and BL21 DE3 pLys (data not shown). The expression is good in both strains. The major advantage of BL21 DE3 pLys over DH5α is the fact that the basal expression is much lower. This is important for the expression of toxic

proteins. A disadvantage of BL21 DE3 pLys is that it is harder to transform than other strains. The expression is strong no matter which bacteria strains are used and toxicity is no problem so that all further experiments were done with DH5α. The GST protein in the bacterial extracts is purified by an affinity chromatography using a GSTrap FastFlow column (Amersham) linked to a FPLC system (Pharmacia). The protein efflux can be measured by UV absorption. Figure 4.1: Affinity purification of GST shows the relative UV absorption during the purification of GST. From the collected fraction 3 to 14, a high absorption is monitored produced by the unbound protein. From fraction 15 to 20, the absorption decreases, while all material with no affinity for the glutathione matrix is washed away. Starting to collect sample 21, the running buffer is replaced by the elution buffer containing 10 mM Gluthatione. This leads to an UV elution peak between fractions 24 to 27. The delay of three fractions between buffer change and elution matches to the tube volume of ~3 mL. The high baseline of the elution buffer compared to the PBS used for loading and washing depends on a low content of Triton X-100 in the elution buffer. This optimizes the elution by inhibiting unspecific hydrophobic interactions.

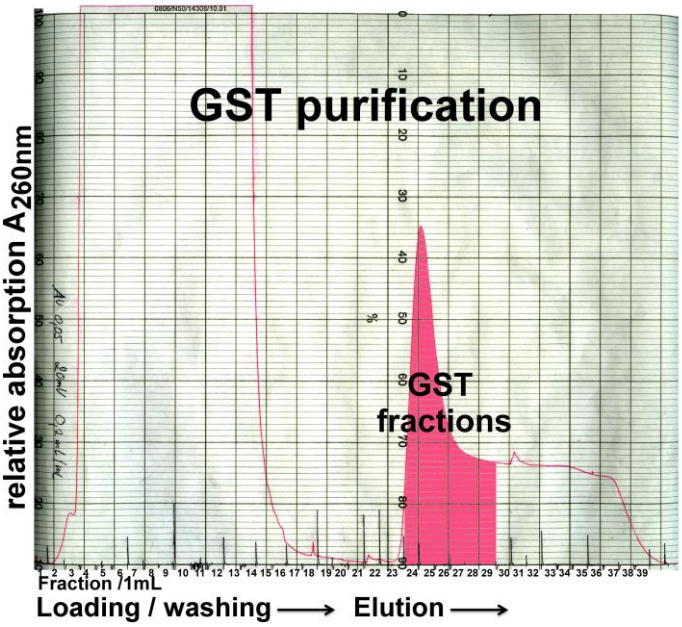

Figure 4.1: Affinity purification of GST

The GST tag encoded by the plasmid pGEX-5X-1 was expressed in DH5α. The bacterial extract was loaded on a GSTrap fast flow column. Equilibration, loading, and washing were performed with GST binding buffer. When the UV absorption was stable, near to the baseline (fraction 21), GST was eluted by a buffer containing Glutathione.

The coomassie stained SDS gel in Figure 4.2: Purified GST in SDS-PAGE indicates the protein content in the different fractions: Extract, flow through, wash and elution. The fractions 24, 25, 26 and 29 show a protein content of a molecular weight slightly bigger than 26 kDa. The band of fraction 25 is the strongest, while 24 and 26 are equally strong and fraction 29 shows only a faint protein trace. GST has a molecular weight of approximately 28 kDa so that it is quite sure that the purification was successful. Nevertheless, the protein from this gel band is analyzed by MS.

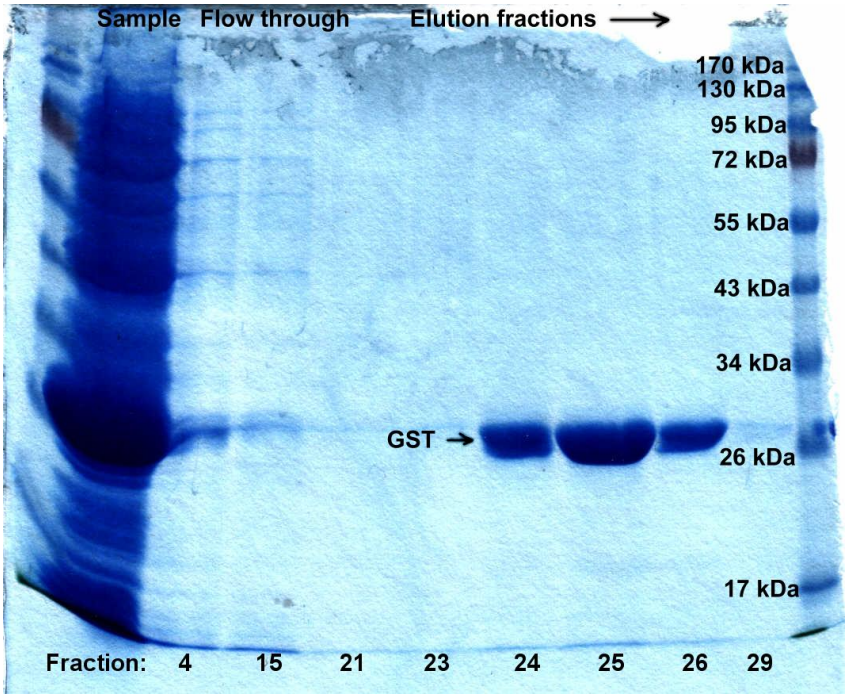

Figure 4.2: Purified GST in SDS-PAGE

The raw extract and the fraction of the affinity purification (see Figure 4.1) of GST was loaded on SDS gel and was coomassie stained. The lanes show the loaded extract, flow through and elution from left to right. The fraction number is indicated below the lane. The buffer change to elution buffer was done after the collection of fraction 21.

In the next two pictures, the purification of the two potential bait proteins for immunoprecipitation is shown. The procedure is analog to the purification of GST. In Figure 4.3, the fractions of the GST- IκBα purification are shown in a coomassie stained SDS gel. The figure shows that the glutathione affine proteins, fractions 28 and later, could be separated from the unbound proteins, fractions 4 to 23. The elution fractions contain proteins of different sizes, mainly 60 kDa and 40 kDa and some proteins smaller than 34 kDa. The largest corresponds to the molecular weight of GST- IκBα which is 62.1 kDa.

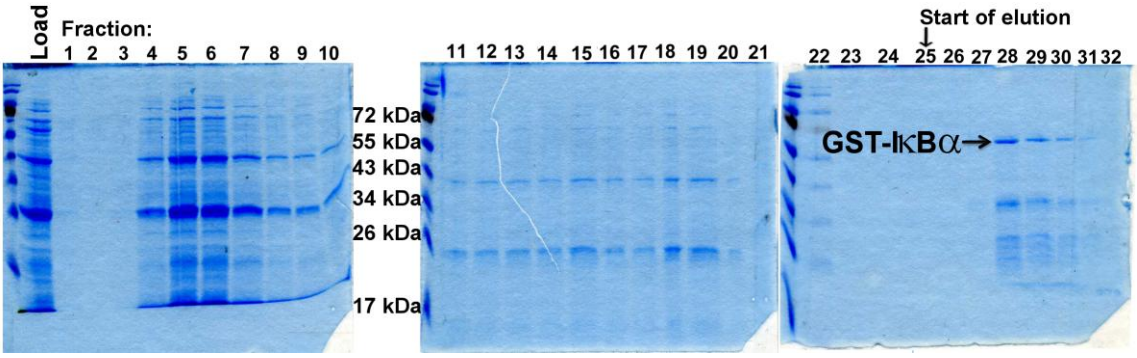

Figure 4.3: Purified GST-IκBα in SDS-PAGE

The IκBα ORF was cloned into the vector pGEX-5X-1 and expressed in DH5α. The bacterial extract was loaded on a GSTrap fast flow column. Equilibration, loading, and washing were performed with GST binding buffer. The chromatography was monitored by UV measurement of the efflux. The elution was started with the collection of fraction 25, as soon as no significant flow through was detectable in UV measurement. The extract and all collected fractions were loaded on SDS gel. The gel was stained with coomassie brilliant blue.

The last of the purified proteins is GST-p65/RelA. This would be most important for the search of interactors. The coomassie stained SDS gel of the collected fraction is displayed in Figure 4.4. In the first row, the raw extract before the chromatography is displayed. Fraction 4 and 30 representatively show the flow through of unbound protein. Fraction 34 is nearly protein free, so the buffer conditions were changed for elution. Two fractions later, the GST affine protein is eluted. Unfortunately, there is

no single protein band, but a complex pattern consistent of four major sizes, namely ~60 ~50, ~33 and ~30 kDa, and several smaller bands. Neither is there a band which matches the size of GST-p65 (86.6 kDa). So it is hard to tell if the visualized proteins are fragments of the desired GST-p65 or something else, but the result of the GST purification with only one band points out that the expressing bacteria do not produce GST affine proteins in relevant amounts. A mass spectrometry analysis should prove that the proteins are fragments of GST-p65.

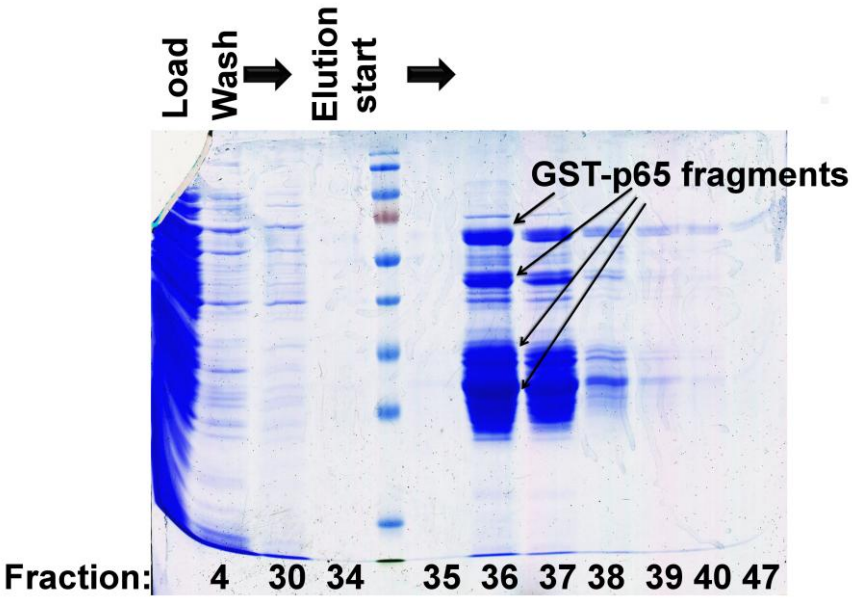

Figure 4.4: Purified GST-p65/RelA in SDS-PAGE

The coding sequence of the p65/RelA gene was inserted into pGEX-5X-1 and expressed in DH5α. The bacterial extract was loaded on a GSTrap fast flow column. Equilibration, loading and washing were performed with GST binding buffer. The chromatography was monitored by UV measurement of the protein efflux. The elution was started with the collection of fraction 34, when no significant flow through was detectable in UV measurement. The extract and chosen fractions were loaded on SDS gel. The fractions 4 and 30 represent flow through and wash while 34 to 40 monitor the elution. The gel was stained with coomassie brilliant blue.

4.2.2 MALDI-MS analysis of fusion proteins

The mass spectrometry was performed as described in material and methods via tryptic digestion, but the analysis for the identification of the expressed and purified proteins was done in two steps. In the first one, the detected ion masses were correlated to theoretical mass fingerprint of the desired protein. Each correlation of an m/z value to a peptide mass was referred to as a match. The biotools software enlists the found matches and calculates the sequence and intensity coverage. In a second step, the spectrum was compared to an E. coli proteome data base by Mascot. The protein with the highest score fits best to the m/z data. This score cannot be related to the biotools analysis of the fusion proteins. For a direct comparison, the found peptide-m/z-matches and the sequence coverage must be used. If the desired transgenic fusion protein is not the purified one, the analyzed protein must be from bacterial origin.

Figure 4.5 shows the mass spectrum of GST and the sequence covered by peptides of identified mass printed in red. It also gives the values for intensity (74.3) and sequence coverage (47.9) in percent. Additionally, the detected peptides masses are distributed over the whole sequence including N- and C-terminus.

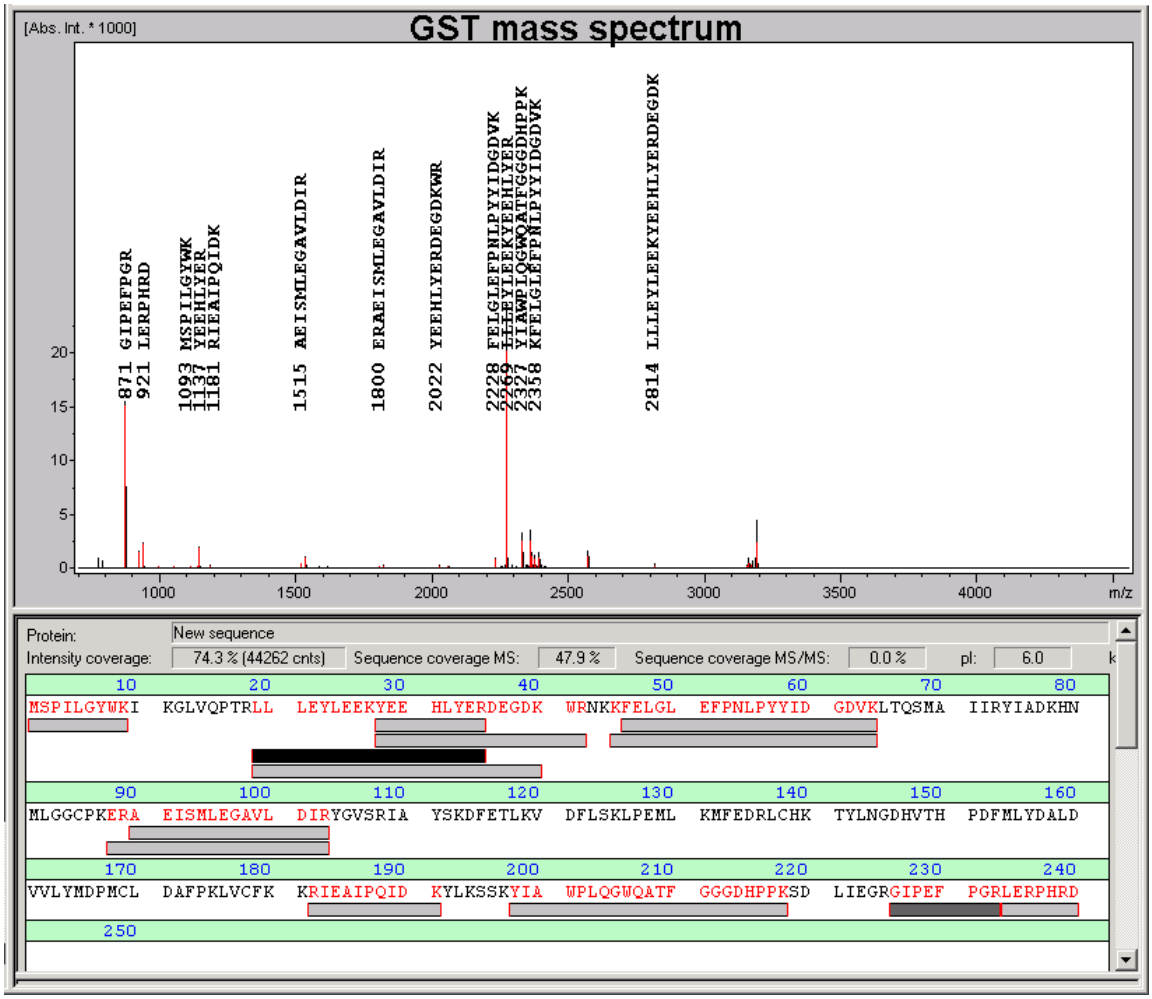

Figure 4.5: MALDI-MS analysis of purified GST

The putative GST band of about 28 kDa in Figure 4.2 was excised from the gel and analyzed in MALDI-MS. The lower window shows the protein sequence of GST. The fragments, which mass/charge (m/z) peaks were detected, were marked with bars and red letter. The dark grey and black bars refer to intense mass peaks. The upper window shows the mass spectrum with the peptide sequences added to the referring m/z peak.

Table 4.2: MALDI-MS results of GST samples shows data of the biotools (single comparison to desired protein) and mascot analysis (comparison to E. coli data base). The two enlisted molecular weight values are not the theoretical molecular weight of GST (28.0 kDa). The apparent molecular weight (first column) describes the size in gel (see Figure 4.2: Purified GST in SDS-PAGE) and the second molecular weight (MS - second column), describes the size of GST up to the last amino acid, which belongs to a detected/matched peptide. This values are equal because the apparent size corresponds to the theoretical size and the C-terminal peptide fragment could be detected by mass spectrometry. The third and fourth column show the sequence and intensity coverage resulting from the comparison of the MS data to the GST sequence with biotools (cf. Figure 4.5). The same comparison leads to the number of peptide matches to mass/charge peaks, which is represented by the number of grey and black bars in the lower window of Figure 4.5. The last three columns indicate the allocation of the MS data to the most probable E. coli protein, including the sequence coverage and number of matches.

So what might be the result of this analysis? The sequence coverage to the E. coli exonulease IV small subunit (61%) is a little bigger than to GST (47.9%), but the bacterial protein is very small, only 8.9 kDa. The sequence has also only one third of the length of GST. This is reflected by the number of peptide to m/z matches of only 3 in case of the E. coli exonuclease subunit to 13 matches aligning to the GST sequence, too. This means that it is probable that the bacterial exonuclease subunit is a random allocation, while the analyzed protein band really contains GST.

Table 4.2: MALDI-MS results of GST samples

Mol weight in kDa		Seq. cov.	Int. cov.	Nr. matches	BDB**		
Apparent	MS*				Protein	Seq. cov.	Nr. matches
~28	28.0	47.9%	74.3%	13	exonuclease VII small subunit	61%	3

*Sequenced to the last AA.

**Bacterial data base search (to exclude fragments belonging to a protein of the bacterial host strain)

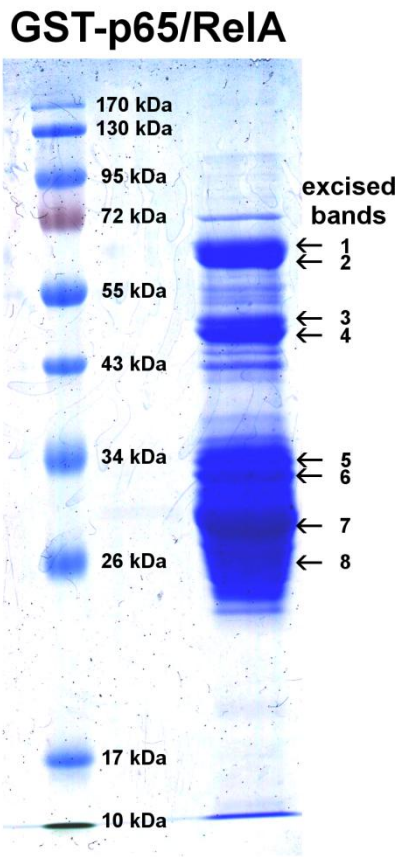

Figure 4.6: GST-p65/RelA spots analyzed by MS

The figure shows the main elution fraction of the affinity purificated GST-p65/RelA (see Figure 4.4, lane 36). The marked bands were excised from the gel and analyzed by MALDI-MS. The result is enlisted in Table 4.3.

From the elution fraction 36 (cf. Figure 4.4) eight samples were analyzed in MS. These samples are indicated in Figure 4.6. The corresponding data is enlisted in Table 4.3: MALDI-MS results of GST-p65/RelA (86.6 kDa) samples. Besides the apparent size in gel and the theoretical size of the protein truncated c-terminal to the last peptide matches in MS, the table also contains the calculated weight of a protein fragment, which is discontinued at the rare codon following on the last detected peptide. Although GST-p65/RelA has a molecular weight of 86.6 kDa, the data suggests that in sample one and two, GST-p65 is found in a truncated form. The sequence coverage (23.7% and 31.1%) and the number of matches (14 and 20) are convincingly high in relation to the length of the protein (778 AA). The comparison to the bacterial data base names two different proteins, the galactose operon repressor and the vitamin B12 dependent methionine synthase. The galactose operon repressor aligned to the first sample data is smaller (343 AA). The sequence coverage is in the same range (26%). The vitamin B12 dependent methionine synthase is probably not the analyzed one because it exhibits a very low sequence coverage 9% and only ten matches although it is much longer than GST-p65 (1227 AA). However the most convincing argument for the identification of GST-p65 is it that in some of the eight analyzed samples the same peptides are found (cf. appendix 1), which means that these spectra contain the same m/z peaks. This is a sign for the presence of the same protein in the samples. Of course this GST-65 must be fragmented due to the apparent size in SDS gel. Evidence for the truncation can also be found in the MS analysis. The smaller the apparent size in gel, the fewer peptides are detected in MS directing from C-terminus. Furthermore, the theoretical molecular

weight of a protein truncated directly C-terminal to the last matched peptide is approximately equal to the apparent size. For example, the first sample was picked from the gel at an apparent size of 60 kDa. In the mass spectrometric analysis of this sample, the last (closest to C-terminus) tryptic peptide of GST-p65, which could be allocated to a m/z peak, spans from AA 506 to 522 (cf. appendix 1). From N-terminus to AA 522, GST-p65 has a theoretical molecular weight of 59.8 kDa. AA 524 is an arginine encoded by a rare codon. The molecular weight of a GST-p65 truncated at this codon would have a Mw of almost exact 60 kDa. These similarities are visible analyzing all different eight bands.

Table 4.3: MALDI-MS results of GST-p65/RelA (86.6 kDa) samples

	Mol weight in kDa						**BDB [4]**			
Nr.	**Apparent**	**MS [1]**	**Rare] codon [2]**	**Seq. cov.**	**Intensity cov.**	**matches [3]**	**Protein**	**Score**	**Seq. cov.**	**Matches [3]**
1	~60	59.8	60.0	23.7%	81.0%	14	galR	60	26%	7
2	~60	59.8	60.0	31.1%	74.3%	20	Methionin synthase (metH)	33	9%	10
3	~50	47.6	50.4	20.1%	89.9%	13	ygeF[5]	33	24%	4
4	~47	47.6	50.4	16.6%	57.7%	11	ycaJ [5]	44	20%	7
5	~33	34.5	35.7	13.4%	49.6%	11	Mannose permease IIab	38	28%	6
6	~32	32.5	35.7	12.0%	58.9%	10	Ycbf [5]	30	27%	4
7	~30	29.5	29.8	16.7%	72.5%	12	Ycbf [5]	37	35%	5
8	~26	25.5	29.8	11.4%	69.3%	10	Ybdm [5]	37	30%	5

[1] Calculated mol. weight of the fragmented protein up to the last in MS detected peptide
[2] Calculated mol. weight of the fragmented protein to the amino acid encoded by a rare triplet next to the last detected peptide
[3] Matches of m/z peak (in MS) to the mass of a tryptic peptide
[4] Bacterial data base search
[5] Hypothetic protein

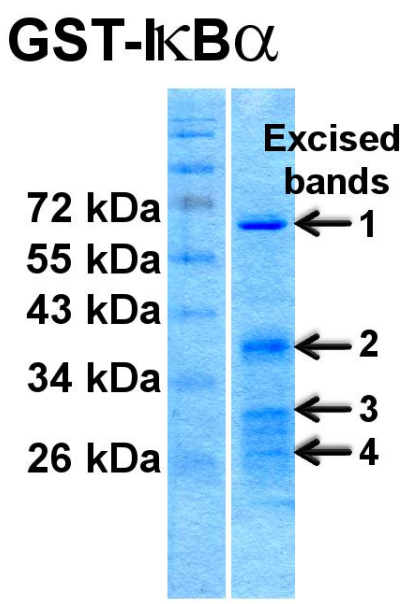

Figure 4.7: GST-IκBα spots analyzed by MS

The figure shows the main elution fraction of the affinity purificated GST- IκBα (see Figure 4.3) lane 28). The marked bands were excised from the gel and analyzed by MALDI-MS. The result is enlisted in Table 4.4.

The elution fraction 28 (cf. Figure 4.3) manifests strong spots at 60 and 40 kDa and some weaker ones. These two and two at ca. 30 and ca. 27 kDa are tested in MS (cf. Figure 4.7). The MS data was analyzed as described above. Sample 2 was delivered no spectrum. The correlation of the data to the desired GST-IκBα was convincing for sample 1. This sample showed a sequence coverage of 19.5% and 10 matches peptides to GST-IκBα compared to a sequence coverage of 19.5% and 7 matches to the best fitting E. coli ABC transporter ATP-binding protein. The apparent MW and the allocation of m/z peaks to peptides distributed over the whole protein sequence allow the conclusion that the protein has full length. Sample 3 and 4 exhibit only a very low sequence coverage, which allows no identification. However, four m/z peaks were detectable in all three samples. This peaks could be allocated to four peptides AA29-27, AA28-35, AA182-191 and AA183-191. This is an indication for degraded GST- IκBα in sample 3 and 4.

Table 4.4: MALDI-MS results of GST- IκBα (62.1 kDa) samples

	Mol weight		Seq. cov.	Intensity cov.	Matches [2]	BDB [3]			
Nr.	**Apparent**	**MS [1]**				**Protein**	**Score**	**Seq. cov.**	**matches**
1	~60 kDa	52.9 kDa	19.5%	38.5%	10	hypothetical ABC transporter ATP-binding protein ybit	27	19%	7
3	~30 kDa	22.5 kDa	5.0%	31.6%	4	purine nucleotide synthesis repressor	25	12%	3
4	~25 kDa	22.5 kDa	5.0%	18.6%	5	4-aminobutyrate aminotrans-ferase	33	10%	4

[1] Calculated mol. weight of the fragmented protein up to the last in MS detected peptide
[2] Matches of m/z peak (in MS) to the mass of a tryptic peptide
[4] Bacterial data base search

4.3 Detection of new p65/RelA interaction partners

New neuronal NF-κB (RelA) interaction partners and potential cargo adaptors should be identified by immunoprecipitation of associated complexes from tissue extracts with an anti p65/RelA antibody. For this purpose, it was necessary produce a neuronal extract, which contains high levels of p65/RelA with a high affinity to the IP antibody and large amount of undegraded proteins. Afterward, the proteins had to be separated and identified. This was done by electrophoresis and mass spectrometry.

4.3.1 Tissue extraction

As a source for neuronal NF-κB interactors, the most convenient choice is mammalian brain tissues. The big advantage of tissues instead of neuronal cell cultures is that it is much easier to yield a high amount of proteins and it is certain that the cells are not degenerated, which often happens to cell lines. The major difficulty in working with tissues is that we work with non human proteins. As we want to investigate the human neuronal transport, the used recombinant proteins have the human sequence. They might not always interact with proteins of other mammals. For the following experiment, three tissue sources are open: mice and pigs. Mice or rats have the advantage that their genome is sequenced and all their proteins are known in sequence if not in function. Also, the phylogenetic relationship between rodents (rodentia) and homo is closer then between even toed ungulates (artiodactyla) and homo. The pig's genome is not fully sequenced yet. This makes it harder to identify protein in mass spectrometry, because the similar, but slightly different human genome must be used after mass spectrometry for the peak allocation.

Before using neuronal protein extracts for immunoprecipitation, different extraction protocols were tested. The protein yield was determined by a biuret test. All samples were checked for degradation by electrophoresis and consecutive coomassie staining. Additionally, the extracts were tested for NF-κB (RelA) with sc-8008. By performing a final ultracentrifugation step, it was ensured that the extracts only contain soluble proteins.

The following coomassie stained gel shows a distinct band pattern. This excludes a high level of degradation. In this connection, the mouse tissue extracts are most distinct, followed by the pig's synaptosomal extract, axonal enriched extracts and at least the pig's whole brain extracts. Additionally, the differences in the pattern show the diversity of sample origin. The signal in western blot is the strongest if axon enriched pig brain is used. RelA is easily detectable in the pig whole brain extracts, too. The signal of pig synaptosomal and mouse brain extracts is poor. The protein concentration indicated in Table 4.5 shows that the high amount of starting material in case of the pig in contrast to the mouse tissues leads to 10 to 20 fold higher final concentrations. The final volume of protein solution of mouse brain extracts are about 10 mL. This volume is also 20 fold larger if using pig material.

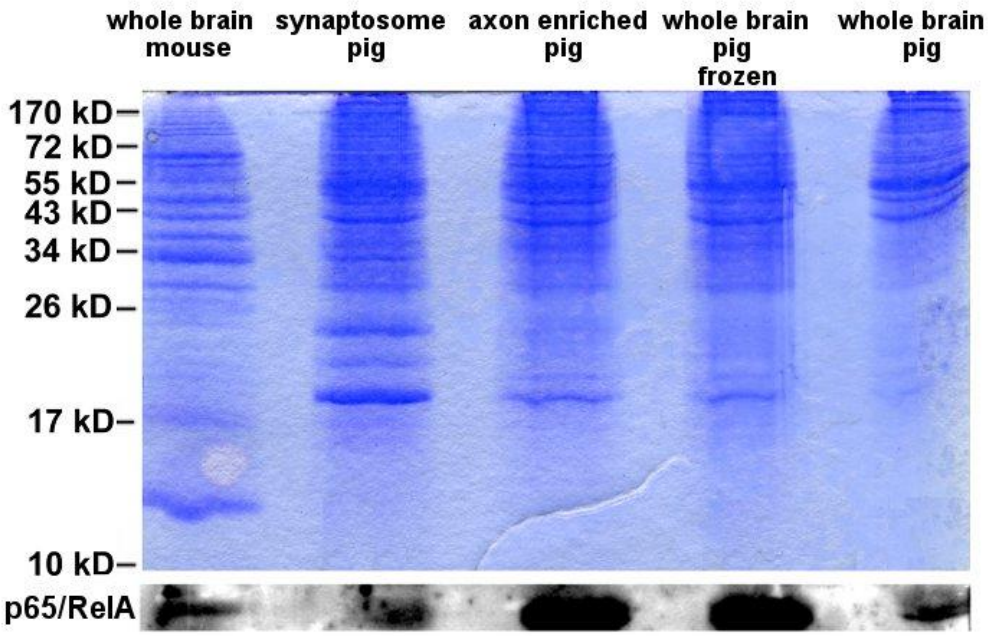

Figure 4.8: Protein extracts in coomassie staining and anti RelA blot

The neuronal extracts were prepared as described and 20 µg of each protein sample were loaded on SDS gels. Two gels were run parallel, one was coomassie stained, the other one was used for a western blot with anti p65/RelA (sc-8008).

Table 4.5: Protein concentration determined by Biuret test

Extraction	Whole brain mouse	Synaptosome pig	Axon enriched pig	Whole brain pig frozen	Whole brain pig
Concentration	0.8 mg/mL	14 mg/L	11 mg/mL	20 mg/mL	9 mg/mL

4.3.2 MALDI-MS analysis of immunoprecipitates

The experiment for the identification of novel NF-κB interactors is described in Figure 4.9. The porcine brain extracts were used as a source of neuronal proteins from which NF-κB interactors were precipitated and identified. Therefore, the extracts were incubated with an anti p65/RelA antibody (sc-8008) and protein G sepharose beads in presence of the cross linker DSP (dithiobis[succinimidyl-propionate]) (Figure 4.9, step 1). The immunoprecipitates of anti p65/RelA and an

unspecific antibody of the same subclass (MOPC21) for isotype control were separated by a one dimensional SDS-PAGE (step 2). Both lanes of the SDS-gel were cut into 36 slices (step 3). All samples were tryspin digested and analyzed in MALDI-MS. Seven slices were additionally tested in LC-ESI-MS/MS (step 4). Those seven slices were highlighted in red (step 3). The mass spectrometry data was analyzed by Mascot (step 5). Only proteins which were absent in the isotyp control were referred to as a hit (6).

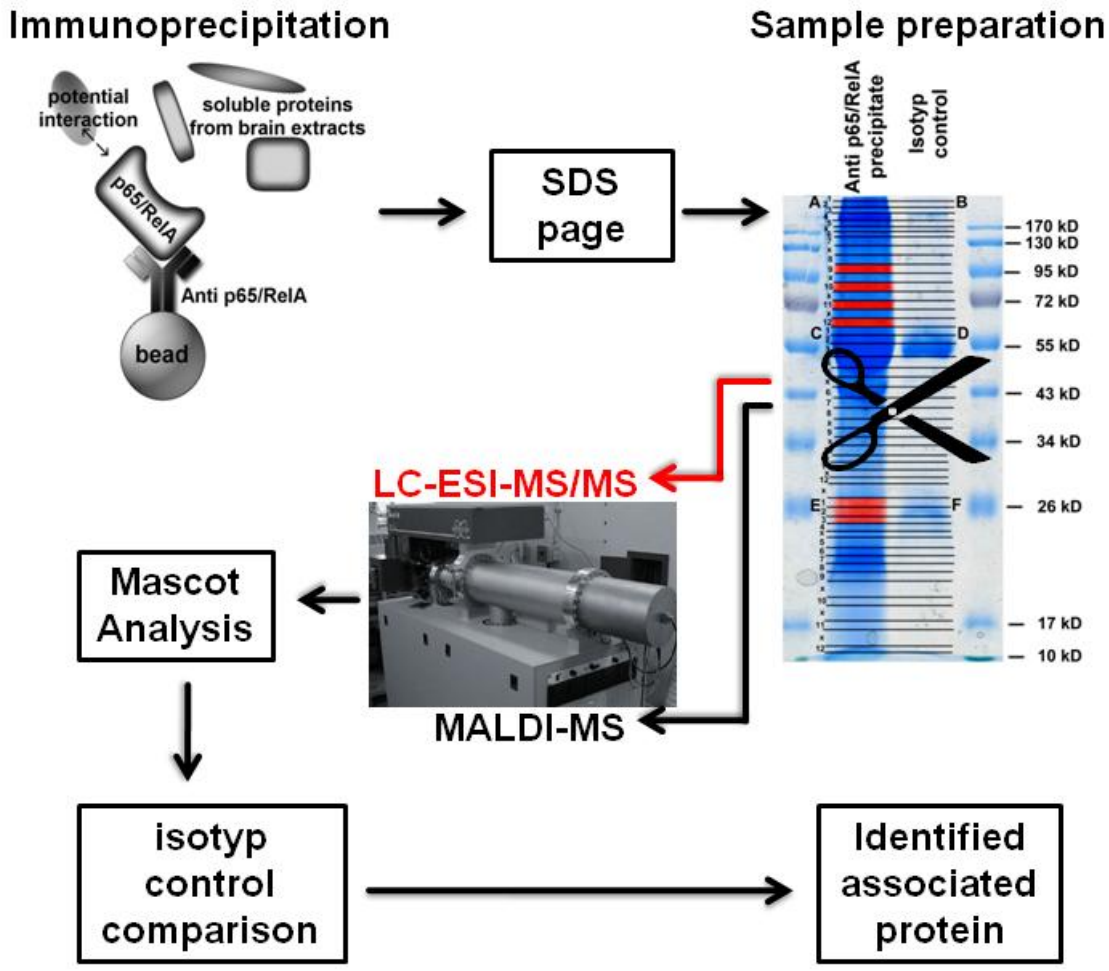

Figure 4.9: Flow chart - identification of p65/RelA interactors

The mascot analysis is a fingerprint analysis using a human protein data base from the Kyoto Encyclopedia of Genes and Genomes (KEGG). No modifications were regarded. The settings for peptide mass tolerance, maximum missed cleavages and peptide charged state were customized for each spectrum. All proteins with a score bigger than 56 are significant $p<0.05$. Additionally, the identified ones had to be of the same size or smaller than the excised band in the SDS-PAGE indicates, because oligomeres were disrupted by the reducing and denaturing properties of the SDS loading buffer. A protein with significant smaller molecular weight than the protein fraction in the gel slices could not be the detected one. The identified peptide might have a larger molecular weight than the gel indicates. This occurred when the analyzed protein was a degraded fragment, but in this study this was not the case. Either the degradation of the extracts was on a very low level or the score of those degraded proteins was too low. The score of identifying a degraded protein fragment is always smaller compared to a full length protein because the number of mass peaks is restricted. An ion derived from the missing part cannot be found.

The following proteins were identified in order of their molecular weight: clathrin, heavy polypeptide (Hc), MW: 191493, score: 144; dynamin 1, MW: 97346, score: 71, heat shock 70kDa protein 8 (HSC70), MW: 70854, score: 101; NEFL; neurofilament, light polypeptide MW: 61739, score 73; tubulin alpha 6 MW: 49863, score 79 (multiple hits); beta 5-tubulin, MW: 49639, score 108; beta actin, MW: 41710, score: 76 (multiple hits); hepatoma-derived growth factor, related protein 3, MW: 22606, score 59 (multiple hits). The given molecular weight is the nominal mass of the unmodified peptide chain. Multiple hits means the protein could be found in more than one sample. These proteins are enlisted in Figure 4.10 next to the gel slice where they are detected.

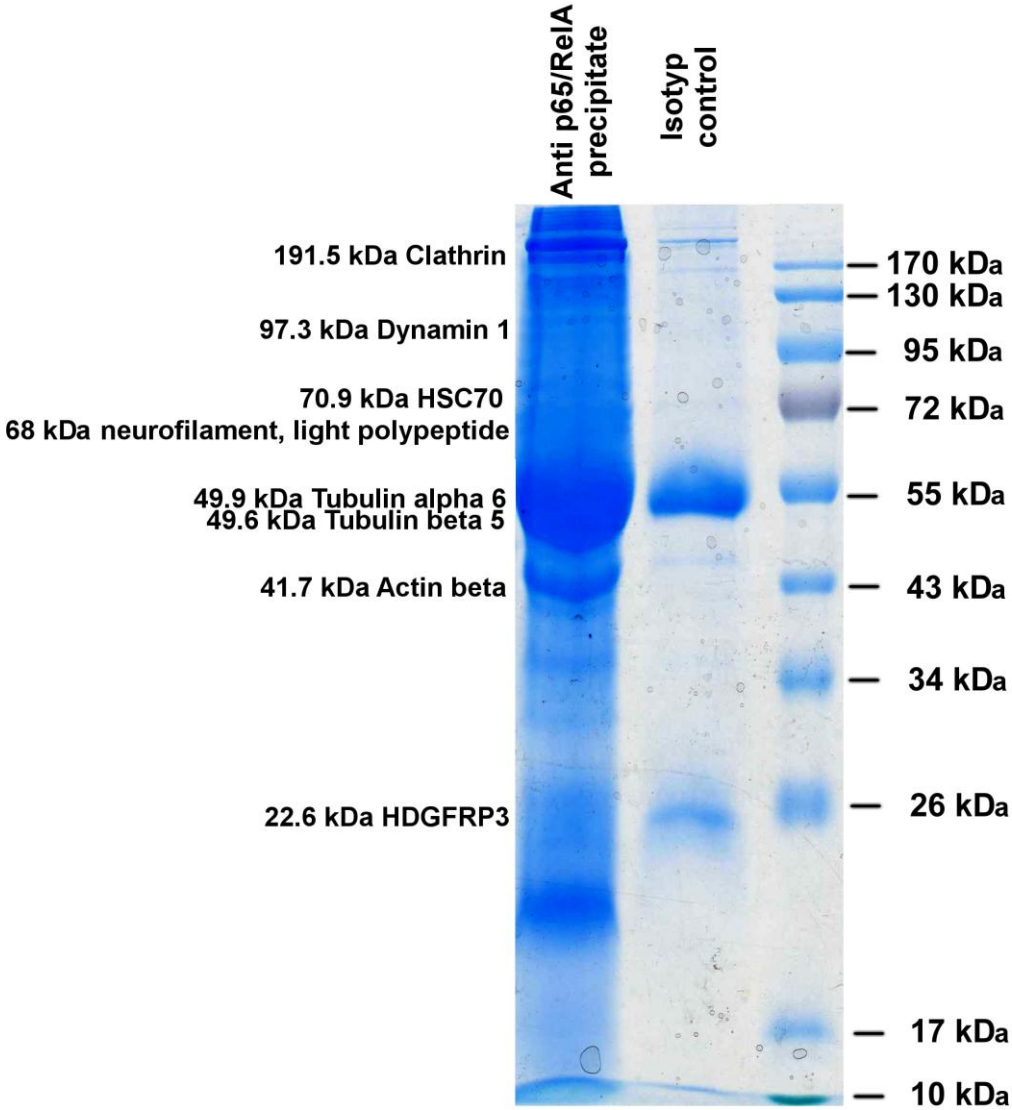

Figure 4.10: Protein hits in MALDI-MS

Porcine brain extract were immunoprecipitated with anti p65/RelA AB on protein G sepharose and complexes stabilized by cross linking with DSP. An IP with the AB MOPC21 served as isotyp control. The IP were separated in a 1D SDS gel. Each lane (p65/RelA precipitate and control) were cut into 36 slices and prepared for MS by trypsin digestion. All 36 slices were analyzed by MALDI-MS. The data was analyzed by Mascot comparing to a KEGG human protein data base. Only proteins with a score >56 ($p<0.05$) were regarded. Only if a protein was absent in the corresponding isotyp control, it was considered as a specific hit. All hits were marked next to the corresponding gel segment.

4.3.3 LC-ESI-MS/MS Analysis of immunoprecipitates

The liquid chromatography electro spray ionization tandem mass spectrometry has two major advantages over matrix assisted laser desorption ionization mass spectrometry. The first one is that the liquid chromatography allows an additional, very restrictive size separation of samples before mass spectrometry analysis. That is quite important because although a gel separation has been performed, there is still a batch of proteins in every slice. The more complex the sample mixture is, the more complex is the spectrum. A complex spectrum makes it difficult to identify proteins because the scores are lower. The second advantage of LC-ESI-MS/MS is that two measurements can be performed. One is carried out after mild ionization of the particles embedded in small droplets of solvent with nearly no fragmentation and a second with fragmented particles. This enables the measurement of masses of the whole tryptic fragments and provides information about characteristic fragmentation. This leads to much higher score values. Seven samples, which contain a mixture of proteins according to the MALDI-MS analysis, are chosen to be tested in LC-ESI-MS/MS (Figure 4.11). These samples in a range of about 95 to 60 kDa and 27 to 24 kDa should also contain the p65/RelA subunit and in the last case, the IgG light chain of the IP antibody.

The LS ESI MS/MS data were analyzed by a MS/MS ion search referring to a human protein data base allowing carbamidomethyl modifications and oxidations. Peptide mass tolerance was fixed to ±1250 ppm and fragment mass tolerance to ±1250 mmu. Only one missed cleavage was allowed. In both cases, only monoisotopic mass value were regarded. The better accuracy of the LC-ESI-MS/MS data allows to set a higher threshold of a sore of 80.

The following protein hits from MALDI-MS could be confirmed by LC-ESI-MS/MS: Dynamin 1, MW: 89521 score: 225; HSPA8, MW: 70854, score 416 (multiple hits); putative uncharacterized neurofilament, light polypeptide, MW: 61392 score: 279 (multiple hits); Tubulin alpha-6, MW: 49791 score: 109. The following new hits were detected: HSP90 alpha (cytosolic), class A member 1, MW: 84607, score: 701; HSP90 alpha (Cytosolic), class B member 1, MW: 83212, score. 521; highly similar to Dihydropyrimidinase-related protein 2, MW: 58126, score 315 (multiple hits); Immunoblobulin light chain (Fragment), MW: 24015, score: 80. Only the three heat shock proteins HSPA8 (HSC70), HSP90AA1 and HSP90AB1 can be related to a unique sequence with the indicated molecular size. In all other cases there a number of transcription variants or related proteins, which could be also the detected one.

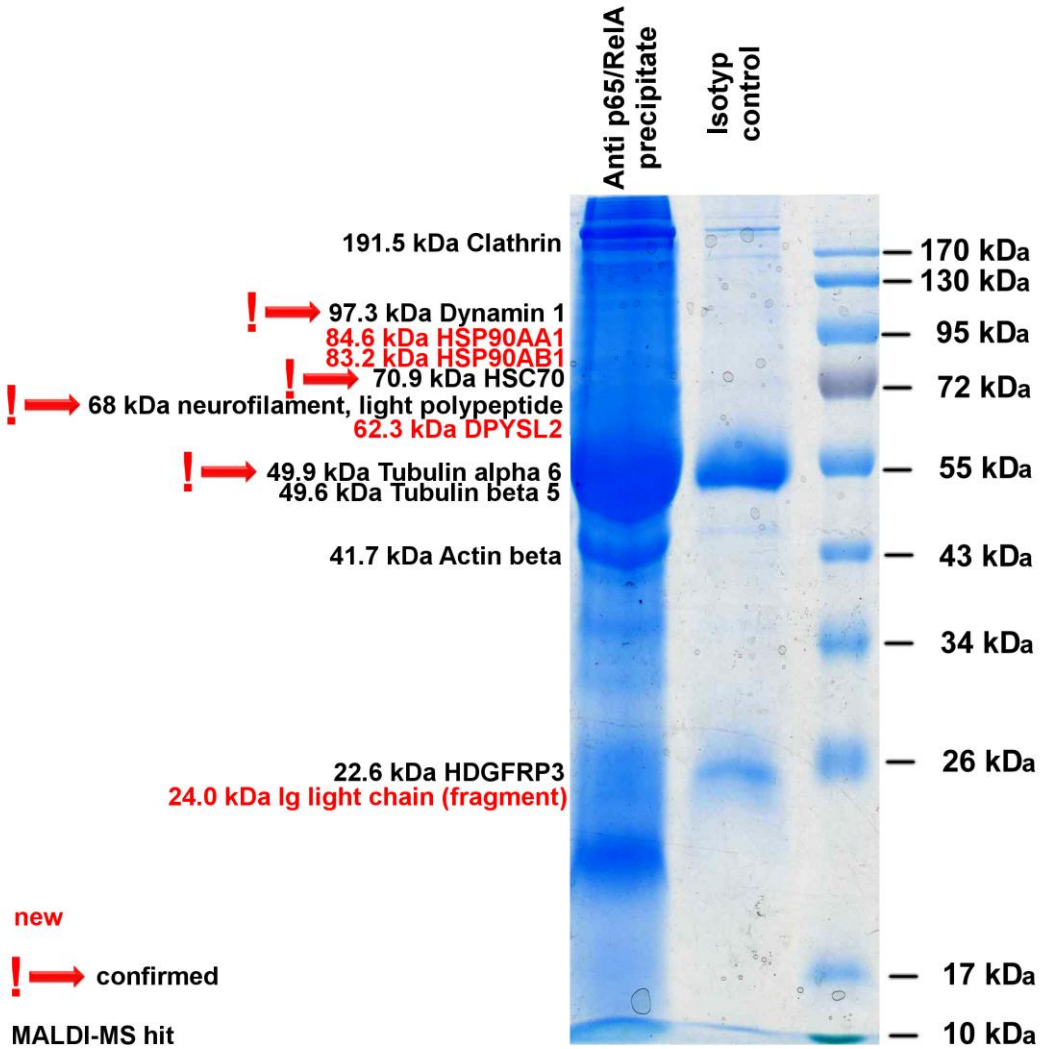

Figure 4.11: Additional protein hits in LC-ESI-MS/MS

Porcine brain extract were immunoprecipitated with anti p65/RelA AB on protein G sepharose and complexes stabilized by cross linking with DSP. An IP with the AB MOPC21 served as isotyp control. The IP were separated in a 1D SDS gel. Each lane (p65/RelA precipitate and control) were cut into 36 slices and prepared for MS by trypsin digestion. All 36 slices were analyzed by MS. Seven samples in range of 95 to 60 and 27 to 24 kDa were additionally analyzed by LC-ESI-MS/MS. This data was analyzed by Mascot comparing to the human protein data base from UniProt. Only proteins with a score >80 were regarded, if those proteins were absent in the corresponding isotyp control. The figure shoes the protein hits next to the corresponding gel segment. The new by LC-ESI-MS/MS detected proteins were marked red and confirmed hits of the former MALDI-MS were labeled by an exclamation mark. The MALDI-MS hits were signed in black letters.

4.4 Verification of NF-κB / HSP interactions by co-immunoprecipitation

Co-immunoprecipitation is used to detect protein-protein interactions. Therefore the first hypothetical interaction partner is coupled via an antibody to a matrix or bead which can be separated by centrifugation/sedimentation. If the second interaction partner is present, it is separated, too. The second protein can be detected for example by western blot afterwards. The co-immunoprecipitation is chosen for verification of the hypothetical interactions, because it is very reliable method in one direction. That means that on the one hand, it easily produces false negative results, but hardly false positive. There are many reasons for false negative results: low signal intensity, not physiological conditions or in the worst case the antibody epitope is blocked by the interaction. False positive results can virtually only appear by unspecific binding, for example between the second interactor and a capturing antibody. This can be excluded by additional controls. That means an interaction detected by Co-IP is surely possible in vivo, but it is also possible that two proteins which interact in vitro do not meet in vivo, so that although they can interact they will not interact. Hence it is necessary to verify if there is a biological function of this interaction.

4.4.1 Setting of immunoprecipitation conditions

The function of an immunoprecipitation assay is strongly affected by some surrounding conditions. First, the presumed interaction partners must be present in sufficient and stable concentration. That means for the following experiments, that a high and stable expression rate is needed. Second, the antibodies need to bind their target specifically and sensitively under the chosen general conditions. At last, the buffer conditions must support the extraction of the proteins and keep them dissolved, but also enable the interaction. For the first purpose, detergents are added to the immunoprecipitation buffer which may inhibit the interaction, particularly if

Figure 4.12: IP proof of principle (scheme)

they are too strong or too highly concentrated. A preceding attempt with common RIPA (**r**adio **i**mmuno**p**recipitation **a**ssay) buffer recipes containing sodium deoxycholate showed no interaction (data not shown). All experiments were performed in the presence of the mild detergent NP40 and small amounts of Triton X-100 (used for the brain extracts).

The following western blotted immunoprecipitates should demonstrate that the chosen conditions were appropriate to detect protein-protein interactions. The Flag tagged NF-κB subunit p65/RelA should co precipitate with its well known interactor IκBα, which is endogenously expressed by the cell line HEK293 FT. The western blot shows the expression controls in the left column. The upper Flag band indicates that the transgenic Flagp65 is expressed. The lower excerpt shows a part of a IκBα band on the right, indicating that also endogenous IκBα is present. The middle column shows the isotype controls produced by performing the IP with an unspecific antibody of the same isotype as the capturing antibody Flag M2. The isotype control is empty, so neither IκBα nor any unknown cross reacting protein binds to mouse IgG1 or the beads. The right column shows a strong Flagp65 and a weak, but clear IκBα signal after immunoprecipitation with anti Flag M2 mouse IgG1. This indicates that Flagp65 is precipitated and IκBα is co purified.

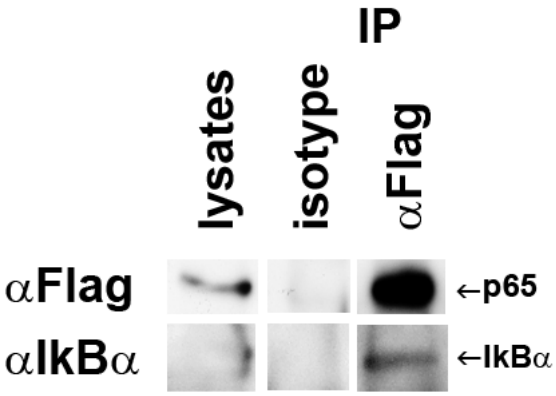

Figure 4.13: IP proof of principle

Three 6 cm plates of HEK293 FT cells were transfected with FLAGp65 according to the Lipofectamin 2000™ protocol. The cell harvest took place after 39 h. The lysate was used for two IPs with anti Flag M2 antibody and isotype control. The precipitate and the crude lysate were checked for Flag epitope (upper panel) and endogenous IκBα (lower panel).

4.4.2 Immunoprecipitation of p65 / HSP complexes without crosslinker

After the establishment of the method, the buffer conditions and protein input were applied to the Co-IP of the proteins of interest p65/RelA, HSC70, and HSP90, which, as heat shock proteins, seem to be quite probable candidates for NF-κB transport. The antibody setting is changed. To avoid the use of lots of different antibodies, which all had to be tested in a western blot, both interaction partners were tagged. The anti myc antibody has proven to be very sensitive and specific. It was used as the capturing antibody for IP. That means the myc-tagged interaction partners were next to the beads and Flagp65 was the second interactor to detect. The first used Flag M2 antibody was replaced by a polyclonal rabbit anti Flag antibody (F7425) in the western blot, which is less specific (irrelevant band below 40 kDa), but more sensitive. As a positive control for an NF-κB interaction, the IκBε subunit was used. The isotype control was replaced by samples transfected with only one interaction partner. This avoids false positive results by hypothetical proteins which might specifically cross react with both antibodies (myc-Flag) or capturing antibody and second interaction partner.

Because HEK293 is a kidney cell line and does probably not express all proteins which are needed for axonal transport on a sufficient level, we added axon enriched brain extracts to mimic axonal conditions. In case that HSC70, HSP90 and p65/RelA are part of a multi protein complex in axonal transport, the extract should provide potential missing complex subunits. The used HSC70 construct carried a mutation in the ATPase domain (Phe68→Cys) as a consequence of a point mutation during the cloning procedure. The effect of this mutation was unknown and will be compared to the wild type later.

The next figure shows top down the detected Flag tagged p65/Rela after IP, the myc tagged first precipitated protein, the Flag tagged protein in untreated lysates and the myc tagged proteins in untreated lysates.

The lowest western blot excerpt in Figure 4.14 shows the expression controls of the myc tagged proteins. The spots in column 2 and 5 indicate the expression of HSC70, 3 and 6 the expression of HSP90 and 3 and 7 the expression of IκBε. Their different heights reflect their molecular masses of ~53 kDa (IκBε), 70 kDa (HSC70) and 90 kDa (HSP90). The next excerpt above shows the expression of Flag tagged p65/RelA in the lysates. A spot indicates Flag-p65 in column 1, 5, 6, and 7. The second part of

the figure top to bottom shows the IP controls: The myc tagged proteins directly captured by the anti myc antibody used for IP. In all samples where a myc tagged protein is expressed, it is precipitated by IP (column 2-7). In this western blot, the Immunglobuline heavy chain (IgG Hc, ~50 kDa) of the capturing antibody is also detectable. The upper excerpt shows that under the chosen conditions an interaction of p65/RelA neither to HSC70 nor to HSP90 was detectable (column 5 and 6). Precipitation of IκBε leads to co-precipitation of Flag65/RelA (column 7). That means the experimental configuration is in principle suitable for the detection of an interaction, but the result "there is no interaction" could also be false negative due to a weak interaction and low signal intensity (v.s.) or using a mutated HSC70.

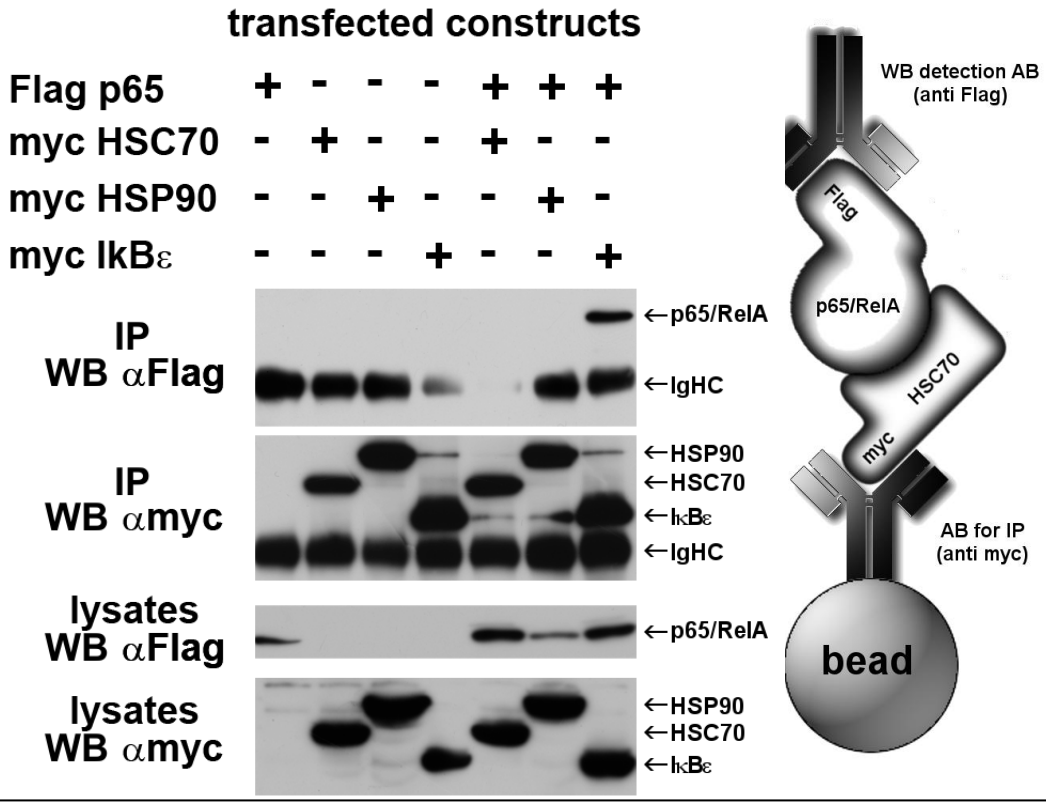

Figure 4.14: p65/RelA and HSP CoIP without crosslinker

For each sample, one 10 cm plate was transfected with the indicated constructs according to the Lipofectamin 2000™ protocol. Cells were harvested after 36 h and lysate supernatant used for IP. Capturing antibody was rabbit anti myc on protein A sepharose beads. The IP was performed in presence of axon enriched brain extracts. The four panels show top down the anti Flag blot after IP, the anti myc blot after IP, the anti Flag blot of the HEK-lysates and anti myc blot of HEK-lysates. p65/RelA combined with IκBε served as positive control.

4.4.3 Cross linked immunoprecipitation of p65 and heat shock protein complexes

To increase the sensitivity of the co-immunoprecipitation, the experiment was repeated in presence of a cross linking reagent: DSP (dithiobis[succinimidylpropionate]). DSP is a homobifunctional N-hydroxysuccinimide ester (NHS-ester) of a molecular weight of 404.42 kDa. This cross linker is thiol-cleavable and forms peptide bonds with primary amines with N-Hydroxysuccinimide (NHS) as leaving group. The spacer arm length is 12 Å. It can cross link any two primary amines (of Lysine or Arginine) with a fixed distance of up to 12 Å. That does not mean that a direct interaction is necessary, but there must be at least a physical association with mediators. The HSC70 Phe68→Cys mutant was still in use.

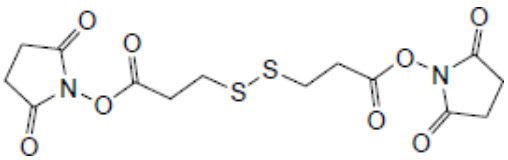

Figure 4.15: Chemical structure of DSP

With the complexes crosslinked by DSP, an interaction between p65/RelA and HSC70 was detectable (see Figure 4.16, column 5, IP αFlag). In all other matters, the result was similar to the previous ones without cross linking.

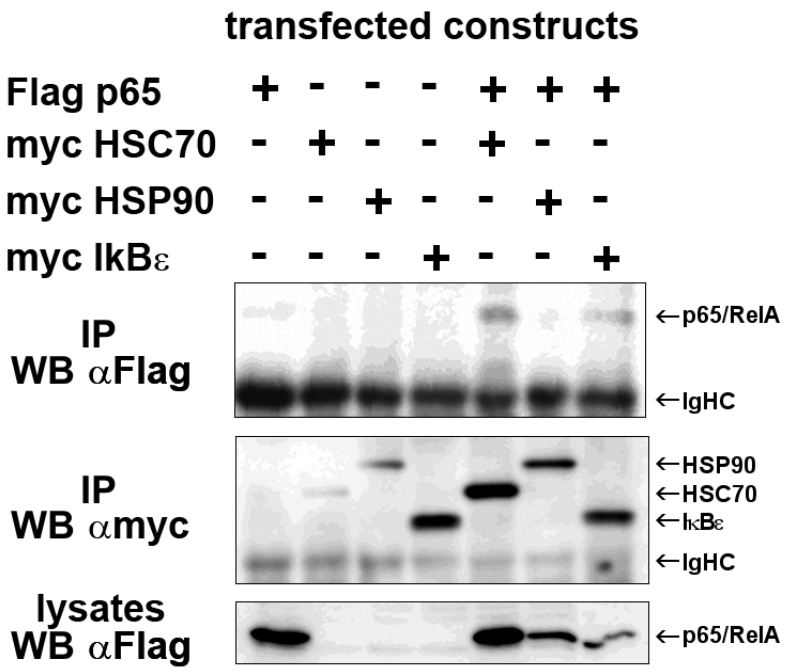

Figure 4.16: p65/RelA and HSP CoIP cross linked

For each sample, one 10 cm plate was transfected with the indicated constructs according to the Lipofectamin 2000™ protocol. Cells were harvested after 36 h and lysate supernatant was used for IP. Capturing antibody was rabbit anti myc on protein A sepharose beads. The IP was performed in presence of axon enriched brain extracts and complexes were cross linked with DSP. The four panels show top down the anti Flag blot after IP, the anti myc blot after IP, the anti Flag blot of the HEK-lysates and anti myc blot of HEK-lysates. p65/RelA combined with IκBε serves as positive control.

4.4.4 Decrease of p65/RelA-interaction by HSC70 mutant

During the cloning of the HSPA8 construct, the random mutant Phe68→Cys was produced. This mutation is located in the ATPase domain [216]. The interaction characteristics of this mutant were compared to the wild type.

The differences are displayed in Figure 4.17. Column 1 and 2 (wild type and mutant) show the negative controls with either Flagp65 or HSC70. Column 3 displays the positive control, the interaction of p65/RelA and IκBε. The fourth column shows the pattern of interest: the p65/RelA and HSC70 association. While the wild type shows an interaction band in the Flag blot, there is none using the mutant at the same degree of intensification.

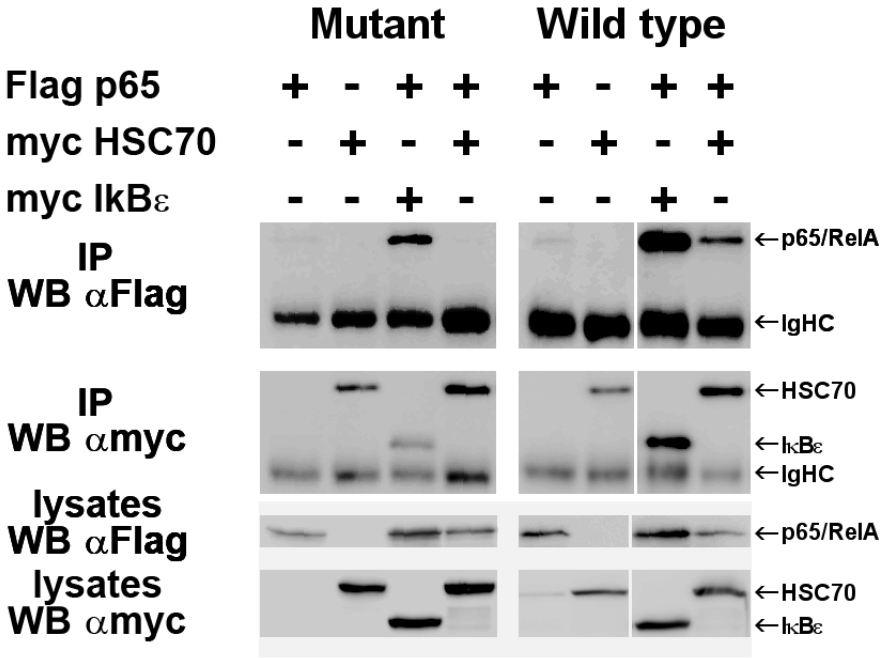

Figure 4.17: Decrease of p65/RelA interaction by HSC70 Phe68→Cys mutant

A 10 cm plate per sample was transfected with the indicated constructs according to the Lipofectamin 2000™ protocol. Cells were harvested after 36 h and lysate supernatant was used for IP. Capturing antibody was rabbit anti myc on protein A sepharose beads. The IP took place in presence of 0.5 mg cross linker and 3.3 mg brain extract per reaction. The panels show top down the anti Flag blot after IP, the anti myc blot after IP and anti Flag blot and anti myc blot of the lysates. p65/RelA combined with IκBε serve as positive control.

4.4.5 Dependence of p65 / HSC70 interaction on neuronal proteins and/or ATP

The next question to answer is, is the interaction of RelA/p65 and HSC70 specific for neurons. A specificity for neurons can be based on the requirement of certain mediators with form a stable multi protein complex together with RelA/p65 and HSC70. These mediators could only be expressed in some cells, e.g. in neurons. In previous tests, there was always added protein extract from porcine brain tissue. This should enable the formation of neuron specific multi protein complexes. The next tests served to check if the addition of the protein extract is necessary or if the interaction takes also place in an unmodified HEK293 cell lysates. Secondly, it was tested if an increased level of ATP influences the interaction. HSC70 exhibits an ATPases activity and can undergo conformational changes like other heat shock protein and multimerize in dependence to the ATP level, which all effects the function of HSC70. In this experiment, the HSC70 wild type was used.

Figure 4.18 shows an interaction p65/RelA with HSC70 only if a cross linker is added (column 5). In this sample, no neuronal protein extract is present. For this reason, the brain extract and the presence of neuronal proteins is not essential for the interaction. The addition of ATP alone does not enable the detection of the uncross linked interaction complex (column 6). The interaction in column 5 seems to be stronger than in former experiments. This could be based on the mutant wild type exchange and must be compared directly.

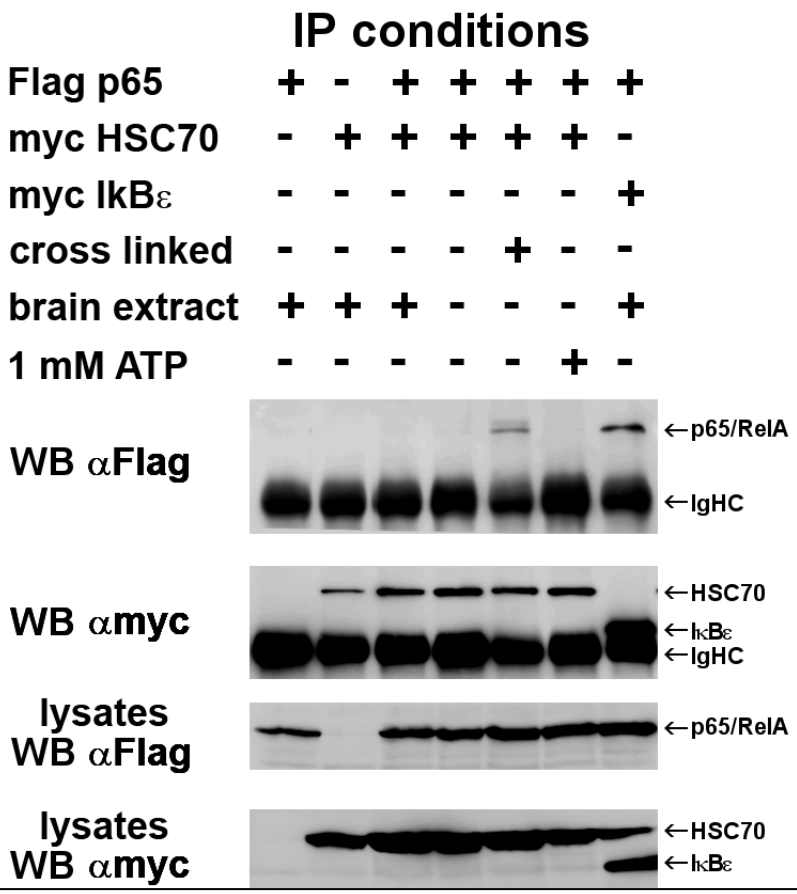

Figure 4.18: Depends p65/RelA - HSC70 interaction on ATP and neuronal proteins? (pretest)

For each sample, one 10 cm plate was transfected with the indicated constructs according to the Lipofectamin 2000™ protocol. Cells were harvested after 36 h and lysate supernatant was used for IP. Capturing antibody was rabbit anti myc AB on protein A sepharose beads. The IP took place in presence of 0.5 mg cross linker, 3.3 mg brain extract and 1 µmol ATP per reaction if indicated in a column. The four panels show top down the anti Flag blot after IP, the anti myc blot after IP, the anti Flag blot of the HEK-lysates and anti myc blot of HEK-lysates. p65/RelA combined with IκBε serves as positive control.

To find out if the addition of neuronal proteins from axon enriched brain extracts stabilizes the interaction complex, this had to be tested based on the cross linked system. In Figure 4.19, the association of p65/RelA and HSC70 is monitored in presence of cross linking reagent and neuronal proteins in relation to only cross linked, to only neuronal protein supplemented and to untreated sample. The first of

these settings shows a definite sign of interaction (Figure 4.19 column 5). The second cross linked sample without neuronal proteins illustrates a faint band (column 6), while both samples without cross linker show none (column7 and 8). The proteins from porcine brain extracts seem to be non essential, but beneficial for the association.

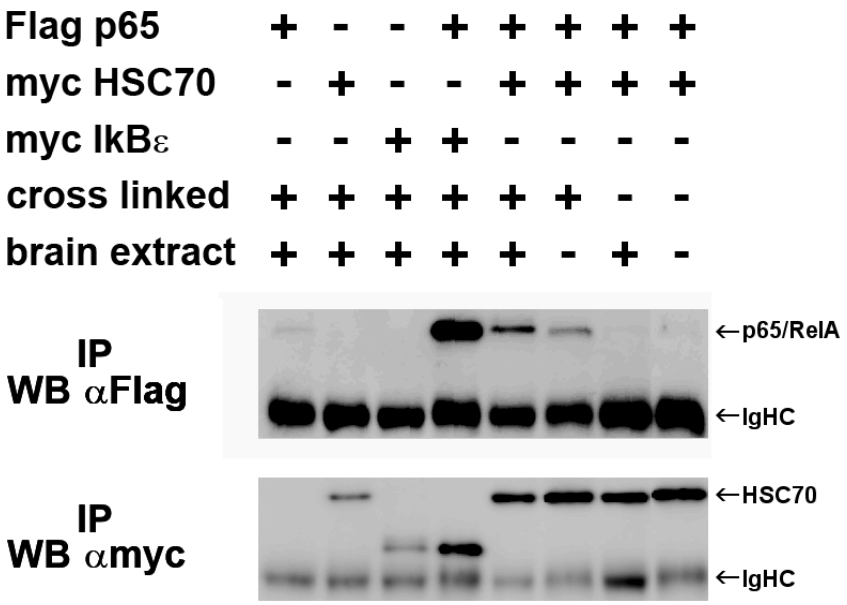

Figure 4.19: Neuronal proteins influence p65/RelA and HSC70 interaction

For each sample, one 10 cm plate was transfected with the indicated constructs according to the Lipofectamin 2000™ protocol. Cells were harvested after 36 h and lysate supernatant was used for IP. Capturing antibody was rabbit anti myc on protein A sepharose beads. The IP took place in presence of 0.5 mg cross linker and 3.3 mg brain extract per reaction if indicated in a column. The two panels show top down the anti Flag blot after IP and the anti myc blot after IP. p65/RelA combined with IκBε serves as positive control.

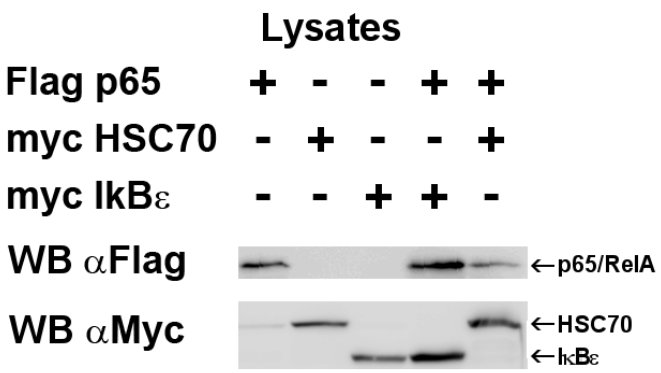

Figure 4.20: Lysate/Expression controls appendant to Figure 4.19.

The upper panel shows the anti Flag blot of the HEK-lysates and the lower one the anti myc blot of HEK-lysates related to the IPs in Figure 4.19.

4.4.6 ATP and temperature dependence of p65/RelA & HSC70 complex formation

To analyze the relevance of ATPases activity of the HSC70 subunit for the interaction, it was observed under increasing ATP concentrations. Parallel the influence of temperature on the interaction was checked, because temperature could be needful for catalytic activity of HSC70 or the kinetic of complex formation.

The upper panel in Figure 4.21 shows the interaction band: The signal of the flag tagged second interactor p65/RelA. All cross linked samples interact. If the IP is performed at 37°C, the cross link is dispensable. ATP does not enable p65/RealA and HSC70 to associate in absence of a crosslinker. There is only a weak correlation between ATP concentration and the signal intensity of co IP. Only the sample incubated with 1 mM additional ATP shows a slightly stronger signal. The 0 µM and 1 mM sample show double bands, while there are single bands at 10 and 100 µM ATP. All controls show the expected signals: the immunoprecipitated first interactor myc-HSC70 (second panel from top) and the expression controls prepared from the lysates (the two smaller panels).

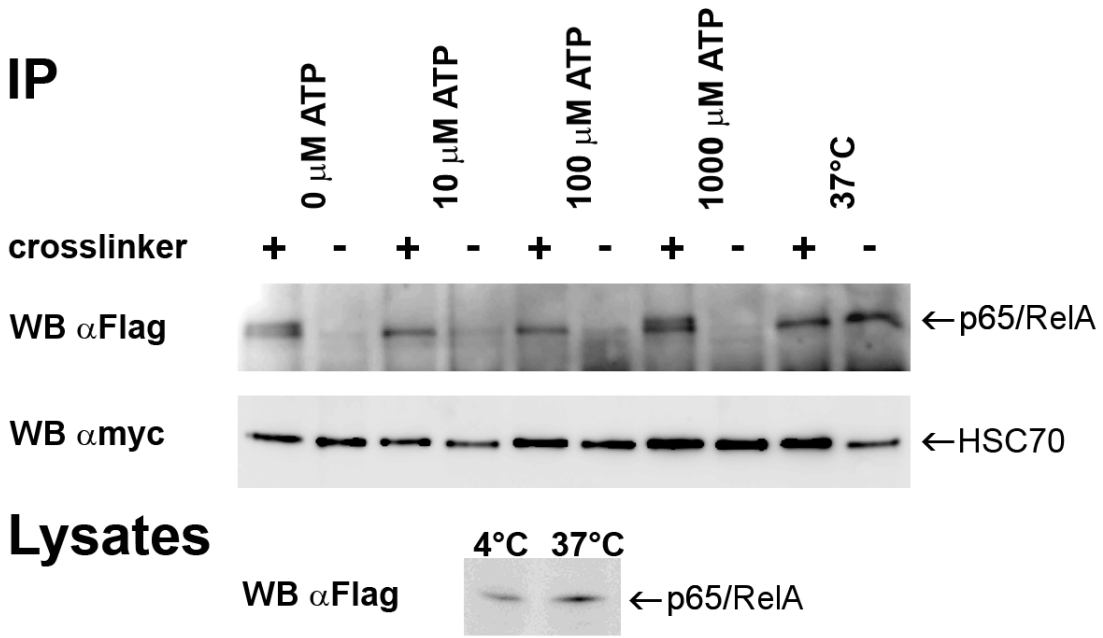

Figure 4.21: ATP and temperature dependence of p65/RelA & HSC70 complex formation

A 10 cm plate per sample was transfected with Flagp65/RelA and myc-HSC70 according to the Lipofectamin 2000™ protocol. Cells were harvested after 36 h and lysate supernatant used for IP. Capturing antibody was rabbit anti myc on protein A sepharose beads. The upper two panels show the western blots after IP, the two lower panels present the WBs of the expression controls/lysates. The samples were incubated for the IP in presence of the indicated ATP concentration and 4°C or without ATP at 37°C. All experiments were performed with and without cross

4.5 Functional test for HSC70 influence on NF-κB activity by luciferase assay

The functional relevance of HSC70 on NF-κB activity was tested with the *Dual-Luciferase® Reporter Assay* of Promega. The used cell line was HEK293 FT. The fluorescence measurement took place 36 hours after transfection with the luciferase reporter genes and the indicated expression constructs. The measured relative fluorescence reflects the NF-κB activity. It was calculated by normalization of the NF-κB dependent firefly luciferase fluorescence value with the constitutive Renilla luciferase fluorescence value.

The assay was tested by overexpression of p65/RelA. Overexpression of p65/RelA with 500 ng of construct enhances the NF-κB activity 63-fold (column 1 & 3, Figure 4.22, P<0.01 Newman-Keul's test), while a fifth of this amount still increases the activity 32-fold (column 1 & 4, Figure 4.22). This is significantly lower, reduced to about half of the activity of the sample group with 100% (500 ng) p65/RelA construct (column 3 & 4, Figure 4.22, P<0.05 Newman-Keul's test). The overexpression of HSC70 alone does not show an effect (column 1 and 2, Figure 4.22).

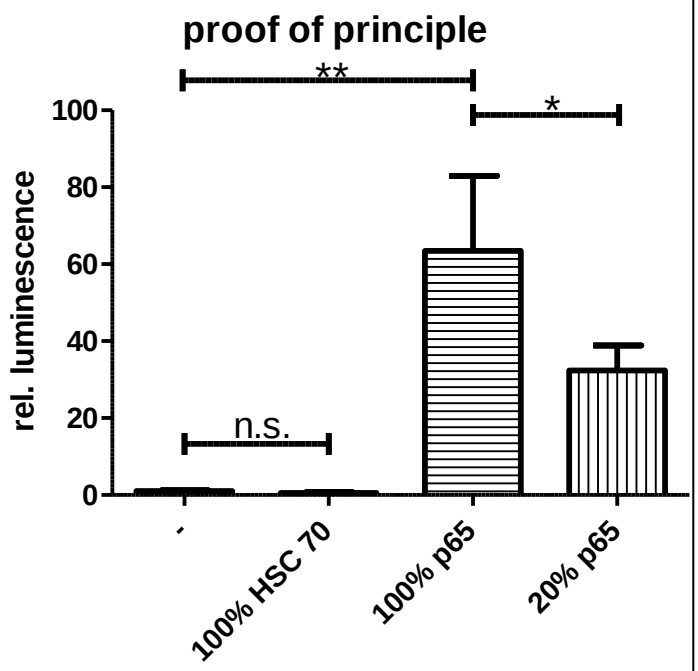

Figure 4.22: Luciferase assay - proof of principle

$2x10^5$ HEK293 FT cells per sample were transfected with the luciferase reporter constructs and additionally with 500 ng vector DNA composed of HSC70 or p65/RelA and complemented with empty expression vector. The NF-κB activity was measured via a luciferase reporter gene assay (n=5).

To test the assumption that there is a positive correlation, maybe a proportional relationship at an appropriate expression range, between HSC70 expression and NF-κB activity, the last was measured at increasing HSC70 levels. This was done in presence of slight overexpression of p65/RelA (100 ng of expression vector) to have an intensified NF-κB activity and increased overall effects. Although the individual errors of each value lead to insignificant differences between the samples with increasing HSC70 expression, the overall slope is significantly larger than zero (Figure 4.23). The correlation coefficient of a linear regression is 0.9215. Based on the slope of the regression line, the NF-κB activity increases by 47 to 156% while the amount of HSC70 expression vector is raised from zero to 400 ng.

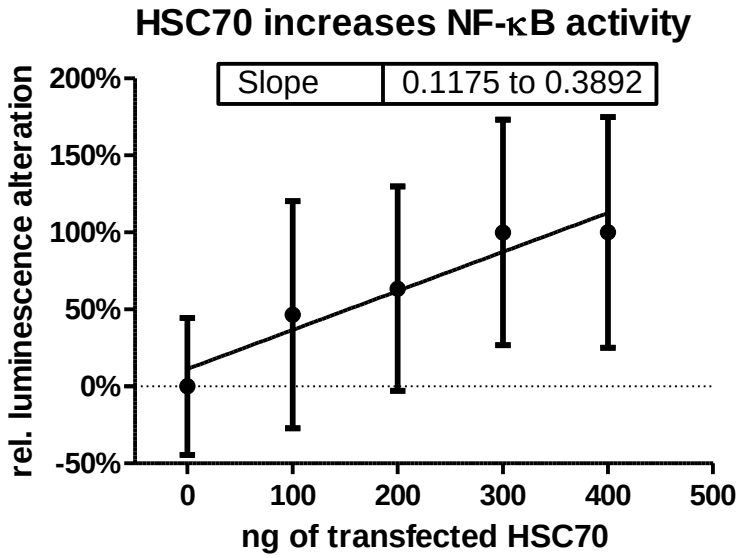

Figure 4.23: HSC70 increases NF-κB activity

$2x10^5$ HEK293 FT cells per sample were transfected with the luciferase reporter constructs and additionally with 100 ng of p65/RelA construct and increasing amounts of HSC70 construct complemented with empty expression vector. The NF-κB activity was measured via a luciferase reporter gene assay (n=5).

In the next presented luciferase assay, larger groups of samples are compared. The first samples were transfected with 50 ng of p65/RelA construct complemented to 500 ng with an empty expression vector. The second sample group was transfected with 50 ng of p65/RelA and 450 ng of HSC70 construct. The last group was transfected like the first, but treated with deoxyspergualin 24 hours before lysis and luciferase measurement.

The HSC70 transfected cells show a significant increase of ca. 32% in NF-κB activity compared to the first control group (column 1 & 2 in Figure 4.24, P<0.001, Tukey's Test). The DSG treatment results in no alteration in NF-κB activity.

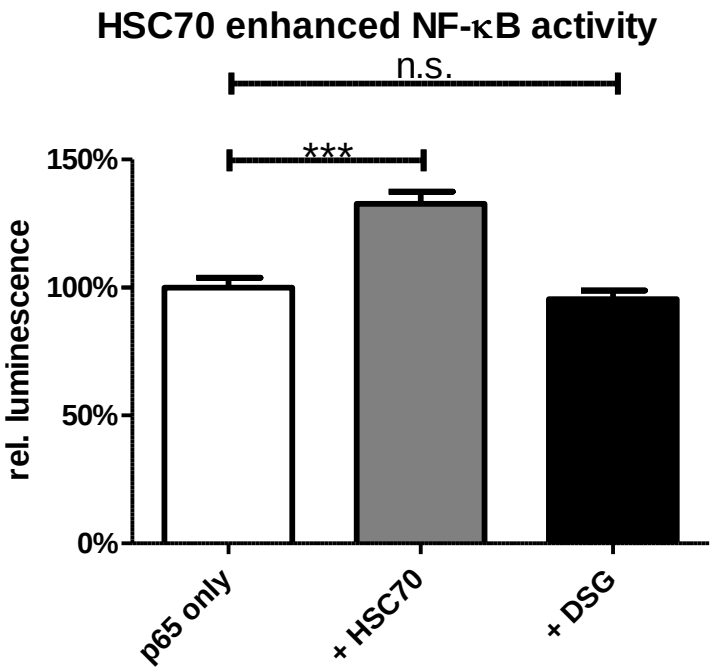

Figure 4.24: HSC70 increases NF-κB activity

$2x10^5$ HEK293 FT per sample were transfected with the luciferase reporter constructs and with 50 ng of p65/RelA construct. Additionally the first and the last sample group were transfected with 450 ng empty expression vector while the second was transfected with 450 ng of HSC70 expression vector. The third sample group was incubated for 24 h in presence of 10 µg/mL deoxyspergualin (DSG). The NF-κB activity was measured via a luciferase reporter gene assay (n=16).

4.6 Nuclear localization assay

The following experiment serves to test if an increased HSC70 expression level effects the nuclear localization of the NF-κB subunit p65/RelA. Therefore HEK293 FT cells were transfected with an FPred-RelA expression construct and partially with a HSC70-GFP or a GFP expression vector. Because the used cell line has a high endogenous expression and a high state of nuclear p65/RelA, an NF-κB inactive state was achieved by co expression of the NF-κB inhibitor IκB. For the assay, the transfected cells were fixed, nuclear stained with DRAQ5, embedded and photographed under a confocal microscope. Only double transfected cells, controlled by the red fluorescence of FPred-p65 and the green fluorescence of either GFP or HSC70-GFP were used for analysis. The nucleus and the whole cell body were defined as regions and their mean fluorescence is detected. The localization of the fluorescent proteins was measured as a ratio of mean fluorescence in nucleus divided by mean fluorescence in the whole cell. Therefore, a high ratio means a strong nuclear localization while a smaller ratio means that most of the fluorescence was cytoplasmic.

The next diagram shows that the co expression of IκB leads to a significant decrease of nuclear p65/RelA as it was expected, no matter if the cells are co transfected with GFP (column 1 & 3, Figure 4.25, $p<0.001$, Newman Keul's test) or HCS70-GFP (column 2 & 4 Figure 4.25, $p<0.001$, Newman Keul's test). The new result is that HSC70 increases the nuclear localization of RelA/p65 in comparison to GFP in the active state without additional IκB (column 1 & 2 Figure 4.25, $p<0.05$, Newman Keul's test). In presence of IκB, HSC70 leads to no significant difference in p65/RelA localization (column 3 & 2 Figure 4.25).

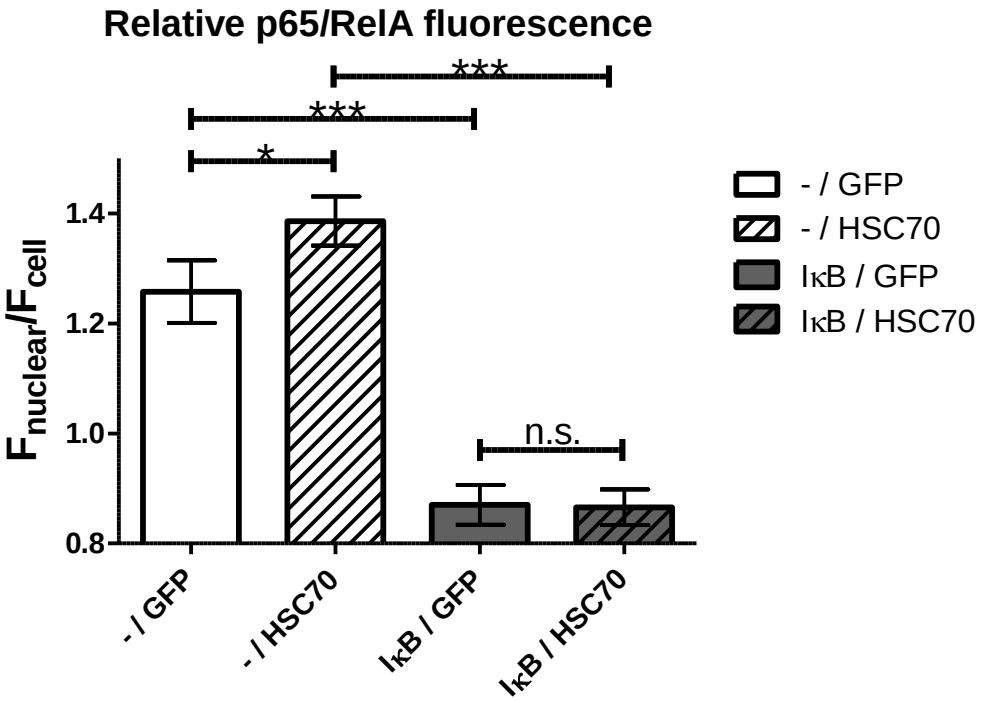

Figure 4.25: Relative p65/RelA fluorescence

$4x10^6$ HEK293 FT cell were seeded in a six well plate and transfected with 4 µg of total DNA per well. The DNA mixture was composed of 1 µg FPred-p65 and, if indicated, of 2.8 µg GFP or HSC70-GFP and/or 100 ng IκB expression plasmid complemented with empty expression vector. After 24 h of expression the cells were fixed, embedded and observed in confocal microscopy. The mean fluorescence of FPred in the nucleus and the whole cell was recorded and the ratio calculated. Sample sizes were: -/GFP n=36, -/HSC n=46, IκB/GFP n=53, IκB/HSC70 n=37.

If HSC70 is important for p65/RelA nuclear transport, it must respond itself to the trigger we used for NF-κB nuclear localization. Parallel to the nuclear / cell ratios of red p65/RelA fluorescence, the ratios of the green fluorophores were determined. The next graph shows that GFP does not significantly responds to IκB overexpression (column 1 & 3 Figure 4.26). It is more or less strongly localized in the nucleus, unlike HSC70-GFP which is severely affected by IκB. Its nuclear level is strongly reduced (column 2 & 4, Figure 4.26, P<0.01, Newman Keul's test).

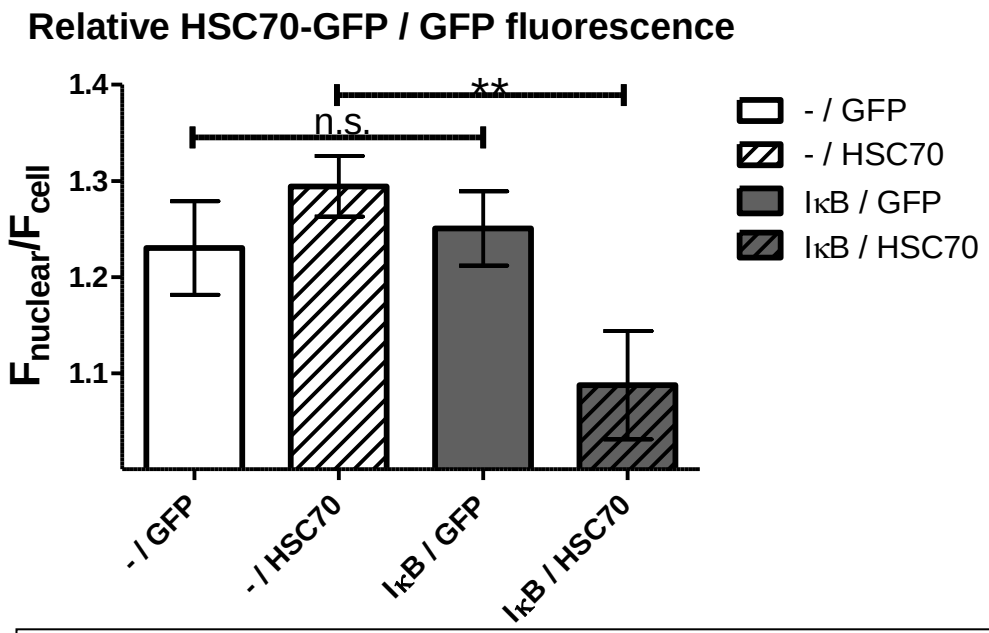

Figure 4.26: Relative HSC70-GFP / GFP fluorescence

$4x10^6$ HEK293 FT cell were seeded in a six well plate and transfected with 4 µg of total DNA per well. The DNA mixture was composed of 1 µg FPred-p65 and if indicated 2.8 µg GFP or HSC70-GFP and/or 100 ng IκB expression plasmid complemented with empty expression vector. After 24 h of expression the cells were fixed, embedded and observed in confocal microscopy. The mean fluorescence of GFP in the nucleus and the whole cell was recorded and the ratio calculated. Sample sizes are -/GFP n=36, -/HSC n=46, IκB/GFP n=53, IκB/HSC70 n=37.

4.7 In vivo nuclear localization assay

In the former assay it was observed that the co-transfection of HSC70 besides auxiliary p65/RelA in unstimulated HEK cells, equipped with a high endogenous NF-κB activity, shows a significantly higher level of nuclear p65/RelA than a transfection without HSC70. This is an indication that HSC70 is involved in NF-κB transport. If this transport / import system is important for NF-κB signaling due to the canonical pathway, this must be proven in a in vivo experiment. In this experiment, the NF-κB signaling was induced by a TNFα stimulus. The nuclear localization of NF-κB was monitored by expression of an FPred-p65/RelA fusion protein as described in the in vitro experiment. We compared cells transfected with HSC70-GFP fusion protein and GFP as control group. The green fluorescence was also used to monitor a potential nuclear co-localization. As the endogenous NF-κB activity of HEK293 FT and their high base level of nuclear NF-κB would have impeded the measurement of a nuclear NF-κB increase, all cells were transfected with IκB in a small copy number. This strongly reduced the basal amount of nuclear p65/RelA. For technical reasons, no zero value was measured. This is possible because it is reported for MEFs that the major effects of the TNFα stimulus take place after 10 to 30 minutes after treatments [197]. This was verified for HEK293FT in a pretest. First, the cells were stimulated with TNFα and afterwards a selected cell or cell group is observed by flourescence microcopy for 40 min at 37°C.

The result of this experiment is presented in two figures and two charts. Figure 4.27 exemplarily shows two cells. One was transfected with GFP, the other one with HSC70 GFP. They are displayed 10 and 40 minutes after TNFα treatment. Both cells were photographed using a red fluorescence filter for FPred and a green one for GFP. The merge image is shown below. Comparing these two cells, no time dependent increase in nuclear p65/RelA is detectable. Furthermore, there is no change in GFP or HSC70-GFP localization, but the nuclear p65/RelA level is conspicuously lower in the HSC70-GFP transfected cells. Additionally, the p65/RelA seems to aggregate by time.

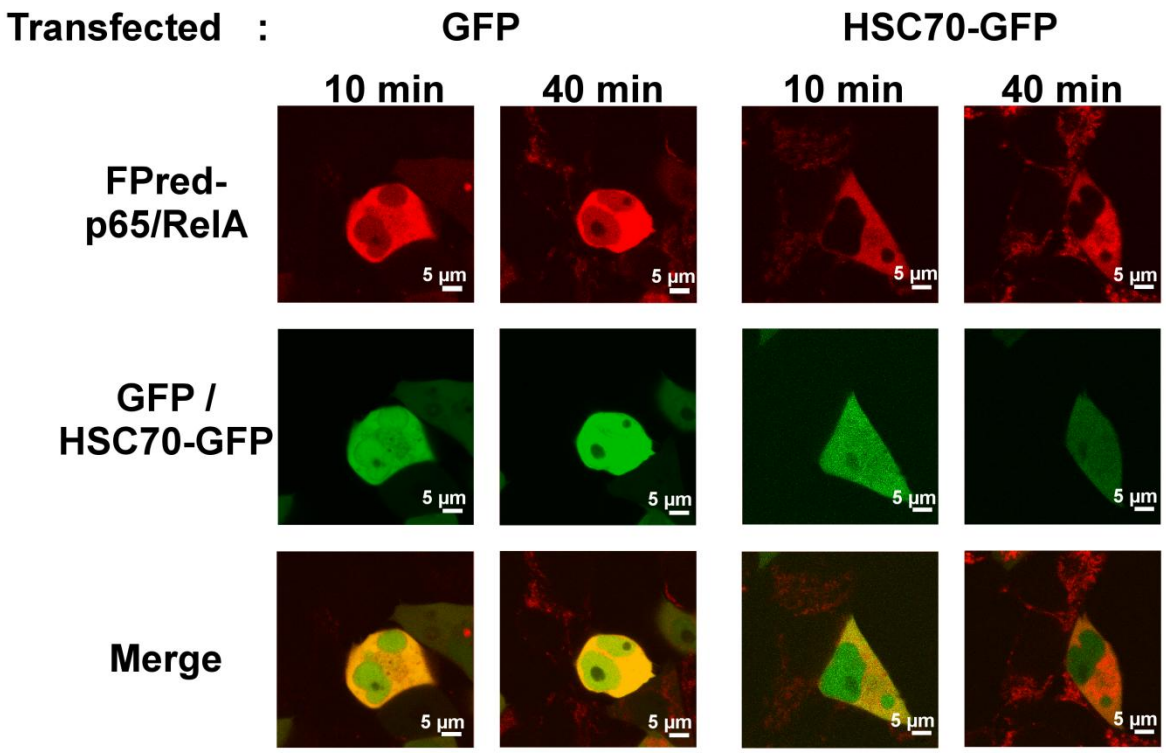

Figure 4.27: In vivo nuclear localization exemplary overview

HEK293 FT cells were transfected with Turbofect™ and HSC70-GFP or GFP, FPredp65 and IκBα. They were cultivated on chamber slides. 24 hours after transfection, the medium was replaced by 37°C prewarmed Tyrode's buffer and the cells were stimulated with 25 ng/ml TNF at time point zero. The fluorescence of FPredp65, HSC70-GFP or GFP was observed under a confocal microscope tempered at 37°C.

Figure 4.28 confirms the observations, that HSC70 transfected cells contain less nuclear p65/RelA. It is also visible that there is no time dependent, clear increase in nuclear p65/RelA, but the aggregation of red fluorophore FPred-p65/RelA increases by time.

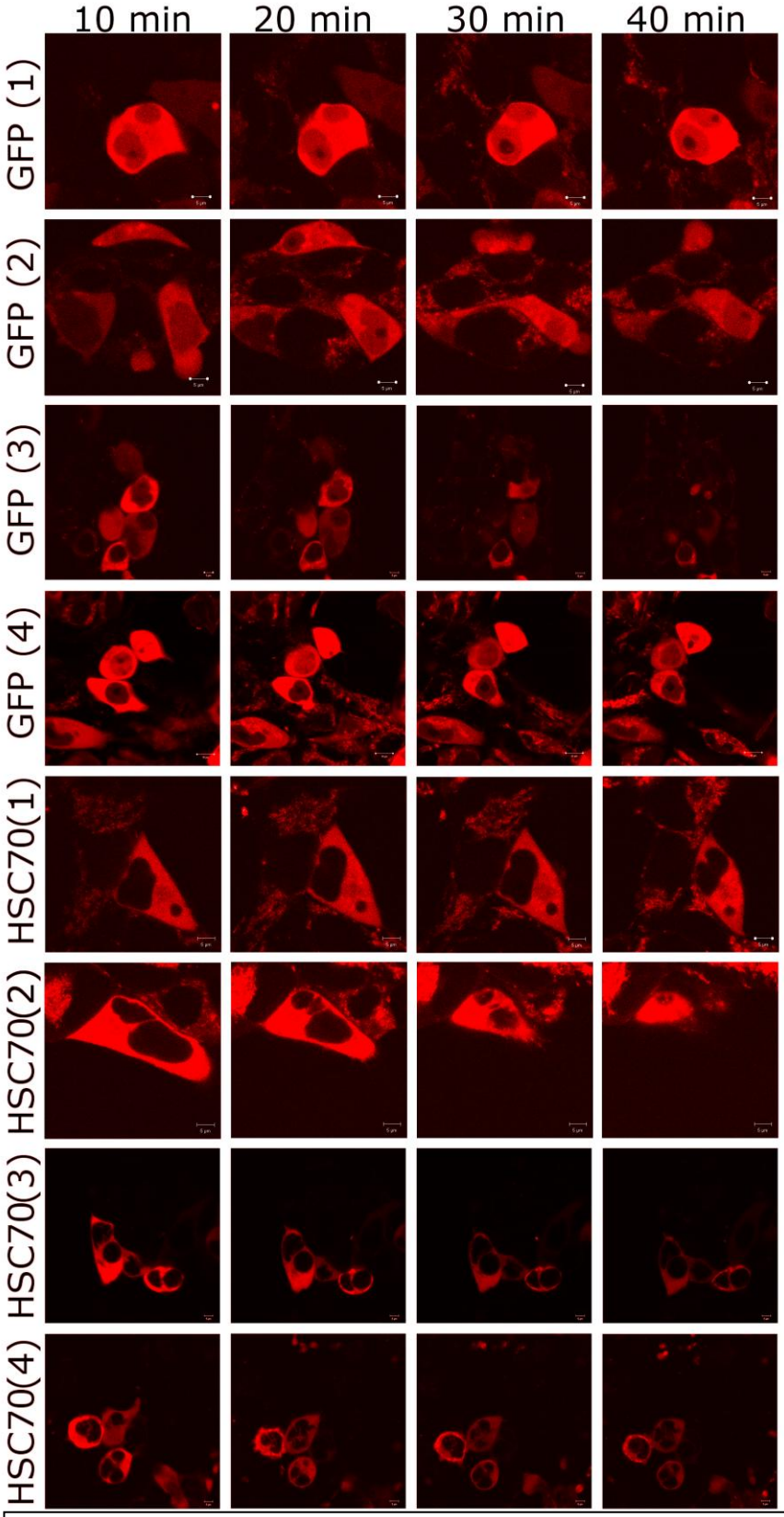

Figure 4.28: In vivo nuclear localization of p65/RelA

HEK293 FT cells are trans-fected with Turbofect™ and HSC70-GFP or GFP, FPredp65 and IκBα. They are cultivated on chamber slides. 24 hours after trans-fection, the medium is replaced by 37°C prewar-med Tyrode's buffer and the cells are stimu-lated with 25 ng/ml TNF. The fluores-cence of FPredp65 is ob-served under a confocal microscope. The microscope is placed under a 37°C tempered tent. This fi-gure shows the fluore-scence of FPred p65/RelA of exemplary cells co-transfected with GFP (upper four rows) and HSC70-GFP (lower four rows).

The statistical evaluation of the fluorescence presented in Figure 4.29 approves the observations from Figure 4.27 and Figure 4.28. There is no significant increase in nuclear localization of p65/RelA by time. However, the nuclei of the HSC70-GFP transfected cells (column 4, Figure 4.29) contain significantly less p65/RelA than the GFP transfected control group after 40 minutes (column 2, $P<0.05$, Newman Keul's test). Figure 4.30 shows no significant variations in HSC70 or GFP distribution, but there seems to be a trend to a higher nuclear localization with enduring exposure to the test conditions.

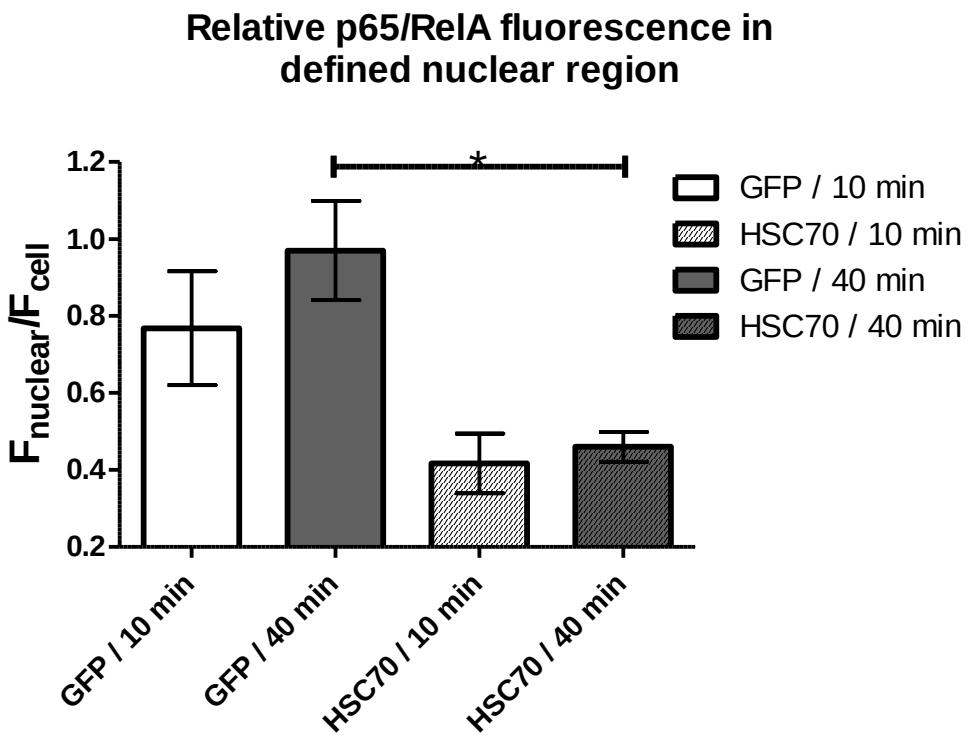

Figure 4.29: Statistic of the in vivo nuclear localization of FPred-p65/RelA

HEK293 FT cells were transfected with Turbofect™ and HSC70-GFP or GFP, FPredp65 and IκBα. They were cultivated on chamber slides. 24 hours after transfection, the medium was replaced by 37°C prewarmed Tyrode's buffer and the cells were stimulated with 25 ng/ml TNF. The fluorescence of FPredp65 was observed under a confocal microscope. The microscope was placed under a 37°C tempered tent. The mean Fluorescence of FPredp65 was recorded in the nuclear region and the whole cell. The Fluorescence ratio of these ROIs was used for data analysis. Sample sizes are GFP/10 min n=10, - GFP/40 min n=10, HSC/10 min n=6, HSC/40 min n=6.

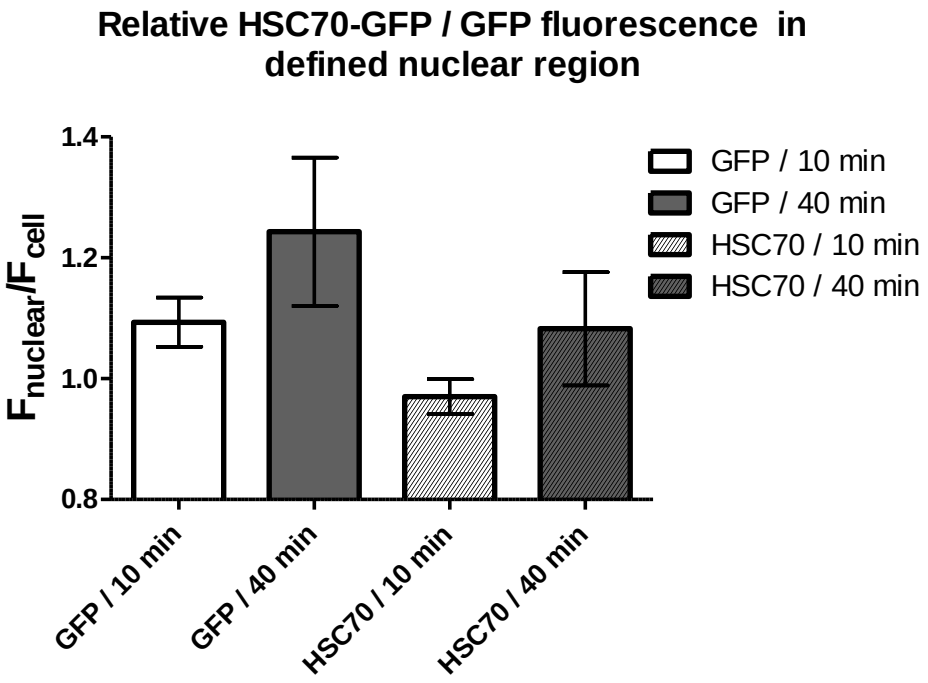

Figure 4.30: Statistic of the in vivo nuclear localization of HSC70-GFP

HEK293 FT cells were transfected with Turbofect™ and HSC70-GFP or GFP, FPredp65 and IκBα. They were cultivated on chamber slides. 24 hours after transfection, the medium was replaced by 37°C prewarmed Tyrode's buffer and the cells were stimulated with 25 ng/ml TNF. The fluorescence of FPredp65 was observed under a confocal microscope. The microscope was placed under a 37°C tempered tent. The mean Fluorescence of GFP or HSC70-GFP was recorded in the nuclear region and the whole cell. The Fluorescence ratio of these ROIs was used for data analysis. Sample sizes are GFP/10 min n=10, - GFP/40 min n=10, HSC/10 min n=6, HSC/40 min n=6.

5 Discussion

5.1 Expression of p65/RelA in E. coli is inefficient in reason of differential codon usage

The p65/RelA sequence of the fusion protein GST-p65 was encoded by a human cDNA. The codon usage of this sequence is different to E. coli. This means that the bacteria may have only a few tRNA to read out some codons and to translate them to an amino acid, because this specific AA is usually encoded by another triplet in E. coli. A rare codon may lead to a spontaneous stop of the translation. The GST-p65 fusion protein was only expressed in c-terminal truncated forms. This truncation correlates with the appearance of rare codons in E. coli. These rare codons are used in less than 1% of all occasions to encode an amino acid by its specific codons. So it is probable that the truncated forms with about 60, 50 and 35 kDa are created by translation stops evoked by rare codons. This difficulties could be dealt with by using E. coli strains supplemented with additional tRNA genes like BL21-CodonPlus-RIL and BL21-CodonPlus(DE3)-RIL, but the number of additional tRNA is limited. The mentioned strains have increased tRNA levels for the arginine codons AGA and AGG, the isoleucine codon AUA, and the leucine codon CUA, but not for the arginine codon CGG [201]. Another possibility to express GST-p65 is the codon optimization of the coding sequence, but because of the successful immunoprecipitation with an antibody against p65/RelA, the sc-8008 from santa cruz, the expression of GST-tagged p65/RelA was not pursued any longer. With GST and GST-IκBα on hand, there are useful tools for the search of IκBα interactors.

5.2 A protocol for the search for p65/RelA interactors from porcine tissues has been established

p65/RelA interactor were purified by co-immunoprecipitation for brain extracts and identified by mass spectrometry after SDS gel separation. The protein input used for immunoprecipitation and mass spectrometric analysis was altogether soluble, ensured by ultracentrifugation. This is important to avoid false positive results by insoluble proteins which may be co-purified during the immunoprecipitation. Any

protein identified by mass spectrometry should have a direct or indirect interaction to the NF-κB subunit RelA. But while false positives could be decreased by extract preparation, isotype controls or by the increase of the score, there will always be false negatives or interactors which could not be detected. This is a result of the limited sensitivity of the method. The signal strength of the mass/charge peaks in the mass spectrum and therefore the probability of a valid protein identification depends on numerous parameters. These are among others the strength of interaction, the individuality of the tryptic fragment pattern, the concentration of the interactor and the complexity of the analyzed sample. The strength of interaction was improved by the use of the cross linking agent DSP. The fragment pattern after digestion with trypsin is protein specific and could not be optimized.

The complexity of the sample is determined by the pre mass spectrometry separation, like the performed gel electrophoresis. For further reduction of the complexity, two different methods are recommended: Two dimensional electrophoresis (isoelectric focusing and SDS-PAGE) instead of simple one dimensional SDS-PAGE or an additional sensitive size exclusive chromatography. Due to the about tenfold increase in sample requirement using 2D gel electrophoresis compared to the 1D electrophoresis, for an equivalent intensity after coomassie staining, the second way was chosen. Besides the MALDI-MS, a combined liquid chromatography ESI-MS/MS was performed. This allows a very precise size exclusive separation of proteins even with similar molecular weight. This enables for example the detection of HSP90AA1 beneath dynamin 1. The less complex samples lead to more simple spectra and higher scores. The threshold for protein scores was increased from 56 to 80 using liquid chromatography. This increases the overall reliability of results from the improved mass spectrometry method.

To guarantee a concentration of interactors as high as possible, porcine brain tissue extract was used as a source for neuronal NF-κB interactors. This source delivered a much higher protein yield, concentration, and as well as total mass than the mouse tissues (cf. Table 4.5). Using porcine extract, it was possible to use the same protein input for IP as suggested by Ilja Mikenberg [153] in a high concentration. The four different protocols tested for the extraction of pig brain tissues only lead only to small differences in concentration and total yield (cf. Table 4.5). The content of

p65/RelA was tested by an anti p65/RelA antibody, scheduled for the subsequent immunoprecipitation (Figure 4.8).

The binding of the antibody is optimal in the extract derived from the so called white matter of the brain, whose name derives from the myelin of axons. This tissue is mechanically enriched by their major toughness. The high p65/RelA binding using this preparation could be a hint for a high degree of p65 transport. The p65/RelA level in whole cell extract, including the nucleus, is comparatively lower. It is only a hint, but no evidence, because no p65/RelA concentration is measured, but a ratio p65/RelA binding per 20 µg loaded total protein. Variation in local total protein concentration, especially in very small areas like the synaptosomes, does not permit to conclude concentration differences from p65/RelA mass ratio. This might be a reason for the low signal of p65/RelA in synaptosomal extracts, although it is known that p65 is transported from the synapse. However, it is not clearly understood how the synaptosomal p65/RelA is generated - maybe by anterograde transport or by translation in synaptosomal polyribosomes [200]. There is also less knowledge about the turn over. The more intense signal of p65/RelA observed using extract of frozen whole brain compared to fresh tissue may be related to an improved cell lysis including nuclei by freezing. This fits to the higher total protein concentration in frozen extracts. The murine extract only shows a weak response to the anti p65/RelA antibody, which could be related to different species. Overall, the axon enriched porcine brain extracts are the most promising. They show a high p65/RelA binding, deliver high yields, promise to preferentially provide interactors in transport and they are not frozen, which might destroy preformed transport complexes.

The use of porcine sample material brings a new problem with it. Because the pig genome has not been fully sequenced, the mass spectrometric data has to be aligned to a human data base. Although humans and pigs are phylogenetical closely related, the differences in human and porcine protein sequence lead to differences in peptide masses. The porcine peptides, whose mass differ from the corresponding human peptides, cannot be detected. This provokes the effect that very conserved proteins are easily detected and less conserved ones are not. The detected cytosolic heat shock protein 90kDa alpha, class A member 1, short transcript shows for example 99% similarity in the amino acid sequence between human (homo sapiens) and pig (sus scrofa). Additionally, most of the sequential differences are located in one small

region from AA 259 to 284. For the NF-κB subunit RelA, the similarity is only 94%. This might be a reason why the last protein, even though primary precipitated, could not be found. Nevertheless, the detection of proteins like the mentioned HSP90 with reliable high scores or the detection of the immunoglobulin light chain fragment of the anti p65/RelA capturing antibody suggests the trustiness of the method.

5.3 p65/RelA interactors are part of the endocytosis network

Three proteins which are detected by mass spectrometry, enlisted in Table 5.1: p65/RelA interactors detected by MS are involved in the endocytosis network. This proteins are clathrin, dynamin and the heat shock cognate 70 (HSC70 or HSPA8) [188]. Other components are related to the filament system like actin, tubulin and the abundant neurofilament light polypetide (NEFL). This leads to the question if there is a connection of endocytosis and signalling combined with retrograde transport of NF-κB. During clathrin dependent endocytosis cargo molecules are included into vesicles surrounded by a cage of the polymerized coat protein clathrin [47]. Clathrin is directed via the multimeric cargo adaptor protein AP1-4 [55, 54, 90, 167 180] or the neuron specific, monomeric assembly proteins auxillin and AP180 [2, 171]. The formation of clathrin coated vesicles (CCV) is dependent on dynamin [196]. CCV form during endocytosis, by the assembly of dynamin into helical structures at the neck of clathrin-coated buds [205]. The hydrolysis of GTP by the GTPase activity of dynamin triggers a conformational change and constricts and pinches off the bud neck membrane [203]. The chaperone and ATPase HSC70 is needed for uncoating the constricted CCV. Recruited by APs, it unhinges clathrin from the polymer coat under ATP hydrolysis [103]. HSC70 also binds to free clathrin to inhibit spontaneous polymerization [103]. Our mass spectrometry results suggest that each of this endocytosis network proteins and the NF-κB subunit RelA are arranged closely together to certain, but probably different time points. The benefit of such complexes is not yet explored.

A possible link between the endocytosis network and NF-κB is the fact, that both may be activated by the same stimulus. As previously described, the nerve growth factor (NGF) activates via binding on the p75 neurotrophin receptor ($p75^{NTR}$) NF-κB

in neurons [101]. For motor neurons, it has been observed, that the retrograde transport of the same receptor upon ligand binding depends on clathrin mediated endocytosis, in a way that only $p75^{NTR}$ from clathrin coated pits can be directed to retrograde transport [50]. Both signals, neurotrophin activated NF-κB transport and clathrin dependent $p75^{NTR}$ transport, could be part of a signal cascade which ensures a specific response by this combination. The observed arrangements could either take place during the activation initiation of both pathways or during transport. Microtubular transport is also reported for CCV [60, 174]. Furthermore recent publications suggest that endocytosis may be required for NF-κB signalling. It has been found out that the Toll like receptor signalling, employing the Rel homolog dorsal is dependent on endocytosis in drosophila. It is estimated that the receptor signaling takes place from endocytotic compartment rather than the plasma membrane [138]. Wherever NF-κB and endocytosis proteins are connected, there might be a powerful key position for the regulation of the signaling cascade.

Potential regulators could be the BAG (Bcl-2-associated athanogene) proteins. The best characterized protein is BAG-1, which functions as a nucleotide exchange factor for HSC70. It triggers substrate unloading from the chaperone. It contains an ubiquitin like domain and therefore is located next to the proteasome. BAG-1 interacts with the carboxyl terminus of HSC70 interacting protein (CHIP). The last protein can recruit ubiquitin ligase, so the complex is able to direct substrates to the proteasome, label them for degradation and release them from the chaperone [5]. Interestingly, another member of this family, BAG-4 equipped with a minimal Bag domain of two thirds of BAG-1 length modulates HSP70 and HSC70 chaperone activity, too [31, 198]. This protein is also known as silencer of death domain (SODD) released from the TNF-R during TNF induced NF-κB signalling [104] It is not known whether SODD is also associated to other receptors of the TNF-R super family, but at least for TNFR1, BAG4/SODD links the NF-κB activation to endocytosis by the opportunity to modulate the activity of HSC70 uncoating the endocytosed vesicle.

Table 5.1: p65/RelA interactors detected by MS

Protein	MALDI-MS	LC-ESI-MS/MS	Relation to p65/RelA or retrograde transport
beta 5-tubulin	√		microtubule subunit
beta actin	√		microtubule related filaments
clathrin, heavy polypeptide (Hc)	√		endocytosis network
dymanin 1	√	√	endocytosis network
heat shock 70kDa protein 8 (HSC70)	√	√	endocytosis network
hepatoma-derived growth factor, related protein 3	√		similar effects, retrogr. cargo
dihydropyrimidinase-related protein 2		√	transport regulator
HSP90 alpha (cytosolic), class A member 1		√	retrograde transport (e.g. GR)
HSP90 alpha (cytosolic), class B member 1		√	retrograde transport (e.g. GR)
immunoglobulin light chain (fragment)		√	anti p65/RelA fragment
NEFL; neurofilament, light polypeptide	√	√	microtubule related filaments
tubulin alpha 6	√	√	microtubules subunit

5.4 Heat shock proteins / chaperone based trafficking

Besides HSPA8 which could be related to the endocytosis network, the heat shock protein 90 kDa is found as an p65/RelA interactor in mass spectrometry (Figure 4.11). Heat shock proteins are the most frequent proteins in unstressed cells. For example, HSP90 constitutes 1-2% of cytoplasmic protein. Their function is not limited to housekeeping like the control of activity and turnover, but it has been known that they also interact and transport signal molecules as transcription factors or kinases [172]. There are five genes encoding different forms of HSP90. The heat shock protein 90kDa alpha (cytosolic), class A member 1 (HSP90AA1) was detected here.

Our expectations to observe NF-κB transport are confirmed by the finding of tubulin, which provides the essential tracks, and the associated neuro- [155] and actin filaments. Fortunately, HSP90 is known to play a role in the transport of transcription factors such as the glucocorticoid receptor (GR). The glucocorticoid receptor interacts with HSP90 [186]. The in vivo function of the receptor is dependent on HSP90, which was shown by induced expression [168], mutation [165], and pharmacological inhibition by Geldanamycin of HSP90 [214]. Besides the glucocorticoid receptor, it interacts with at least 20 other transcription factors [172],

among them sexual hormone receptors [105, 193] and the SV40 large T antigen [156]. So it seems plausible to assume that HSP90 also plays a role in the NF-κB transport.

There are some connections in GR and NF-κB signaling. They share interactors, namely HSP90 and a 70 kDa heat shock protein. Furthermore they show a physical association in IP and functional antagonism [176]. While NF-κB is related to immune and inflammatory responses in many cases, glucocorticoids are connected to anti inflammatory activities. It is reported that the activation of the GR with dexamethasone (ligand) reduces the activity of the interleukin 6 promoter driven by a RelA enhancer. Vice versa activation of the mouse mammary tumor virus promoter by a combination of dexamethasone and glucocorticoid receptor is inhibited by overexpression of p65 [176].

Therefore it might be useful to have a closer look on a model for GR transport invented by William B. Pratt et al. [172]. This model suggests that the assembly of the transport complex takes places in two major steps. In the first step, the GR forms a "primed" complex with the heat shock protein, ATPase HSP70 and the cochaperone HSP40 in an ATP dependent manner [159]. HSP40 as well as HSP70 with bond ATP can bind to GR alone [87, 116]. The order of assembly is unknown, but HSP70-ADP/GR must be stabilized by HSP40 [116]. The hydrolysis of ATP may be responsible for partially opening the GR binding cleft and priming the complex for the second step. In the second step, a HSP90 dimer bond to the HSP organizing protein (HOP) enters the complex. HOP preferentially binds to the ADP-bound form of HSP90 [106]. HOP mediates the interaction of HSP70 and HSP90 via two tetratricopeptide repeats (TPR) [43, 131], which is a protein-protein interaction module [25]. Dependent on ATP, the binding cleft of GR is opened for ligand binding [116]. The now ATP bond HSP90 releases HOP and binds to p23, an acidic 23-kDa protein [108], which only binds to the ATP-dependent conformation of HSP90 [202] and stabilizes receptor-HSP90 heterocomplexes after conversion to the steroid-binding state [59]. HSP70 may be also released by the mature complex and is not found in an stoichiometric manner. HSP90 of the mature complex is connected to the transport machinery via immunophilin (see Figure 5.1). The retrograde transport of GR is based on the motor protein dynein.

Transport of the Glucocorticoid receptor

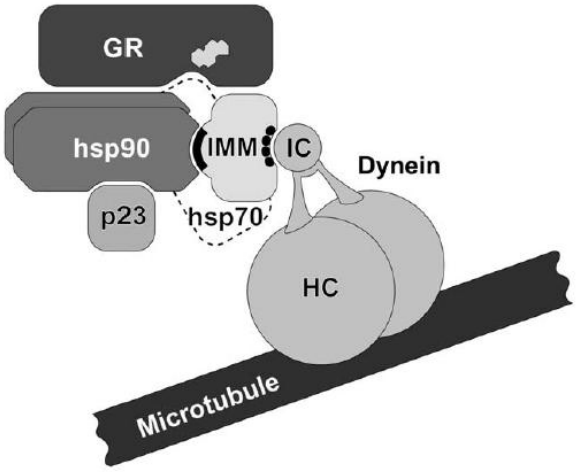

Figure 5.1: Transport of the GR

Pratt, W.B.; Galigniana, M.D.; Harrell, J.M.; DeFranco, D.B. (2004) Cellular Signalling 16:857–872 [173].

Microtubular transport of the ligand bond Glucocorticoid receptor (GR) HSP90 heterocomplex. The complex, also containing p23, is connected to the intermediate chain (IC) of the motor protein dynein by immunophilins (IMMs). The interaction to HSP90 is mediated by the IMMs TRP domain, while it links to dynein or more exact to the dynactin complex via its PPIase domain [83]. The dynein associated dynactin complex and the dynein light chains are not shown. Dynein transports its cargo via its two heavy chains (HC), which have the processive motor activity, along microtubules in a retrograde movement to the nucleus. The broken line around HSP70 indicates that it is not found in the transport complex in a stoichiometric manner.

Upon arrival at the nuclear pores, the receptor-HSP-immunophilin complex crosses the membrane by importin-dependent facilitated diffusion and mediates further receptor cycling [173]. An involvement of importin in the GR complex transport has not yet been researched and importin is not regarded in the model. Because the transport, not only the nuclear import, of NF-κB depend on its NLS [81, 82], the model must be expanded for NF-κB.

5.5 RelA interacts with CRMP2 and HDGFRP-3

In mass spectrometry, two other components were found: The hepatoma-derived growth factor, related protein 3 and dihydropyrimidinase-related protein 2 (DPYSL2), also known as collapsin response mediator protein 2 (CRMP2). Both proteins play important roles in brain development.

The family of hepatoma-derived growth factor contains six members. The hepatoma-derived growth factor related protein 3 is, in contrast to the other members, exclusively expressed in the nervous system, predominantly in neurons [66]. Due to its high regulation during brain development it is estimated that HDGFRP-3 has other functions besides its ability to steer mitogenic activity, as for example axon guidance or synapse formation [1]. Interestingly, similar effects are connected to NF-κB activity [111]. HDGFRP-3 underlies retrograde nuclear transport and it contains a bipartide basic NLS which consists of the basic motif, KRKNEKAGSKRKK (residues 136–148) [97]. This corresponds to the NLSs of a NF-κB dimer. For example, the RelA NLS complies to the consensus sequence K-(K/R)-X-(K/R) in which X is any amino acid with the sequence $K_{301}RKR_{304}$ [15, 134], while p50 has the sequence RKRQR [24]. It could be shown in mutation assays that HDGFRP-3 nuclear localization depends on its bipartide NLS [65]. So it quite probable that they use the same transport machinery including importin-α dependent nuclear import. As NF-κB and HDGFRP-3 activity are both related to brain development and synaptic plasticity, this transport system could be a natural target for developmental regulation.

The second interactor CRMP2 is also very important for neuronal development, especially neurite growth. CRMP2 promotes neurite growth by microtubule assembly [11, 74]. Furthermore, it regulates microtubular transport by a N-terminal Kinesin-1 and a dynein HC binding domain found in the opposite of the protein in a 3D model [9]. Via kinesin and a cargo binding capability, it may transport other proteins in positive direction [121, 12, 209]. The dynein binding domain also blocks the motility of the motor protein. Thereby it may promote transport to distal regions [9]. In addition, it has been found that a c-terminal truncated form of CRMP2 is transported to the nucleus. The truncation is generated by posttranslational processing and it is believed that it unmasks a short NLS, which is enclosed in the

full length protein. The nuclear localization of the processed CRMP2 results in the inhibition of neurite outgrowth [181]. The mechanism is yet unknown.

5.6 Co-immunoprecipitation suggests GR analog NF-κB transport complex

In our co-immunoprecipitations, a physical interaction of RelA/p65 and HSC70 alias HSPA8 has been verified using the cross linking agent DSP (cf. Figure 4.16: p65/RelA and HSP CoIP cross linked). DSP can only link proteins with lysin ore arginine residues in a close range of 12 Å or less. The constitutive Hsc70 and inducible Hsp70 are generally considered, with rare exceptions [8], to be equivalent proteins exhibiting functional similarities [36]. However, although the overall structures of these two chaperones are almost identical, they do differ in some specific areas [149]. Their carboxyl-terminal domains (amino acid 510–641) differ considerably in structure ("only" 69% amino acid identity). This domain may stabilize the peptide-binding pocket more efficiently in Hsp70 than in Hsc70 and therefore may regulate the access of substrates to the peptide-binding pocket differently.

Based on the similarities, both heat shock proteins may be exchangeable and our found HSC70/HSPA8 may be also participate in the assembly of a transport complex. Furthermore, it has been shown that a random mutation in the ATPase domain impedes the interaction with RelA/p65 (cf. Figure 4.17: Decrease of p65/RelA interaction by HSC70 Phe68→Cys mutant). This correlates with the GR transport model in which HSP70 may bind the cargo independently from the type of bound nucleotide (ADP or ATP), but the further assembly of the complex, which grants stable interaction, needs HSP70s ATPase activity. It is also observed that the presence of brain extracts has a stabilizing effect on the HSC70 RelA/p65 interaction. This effect is not strong enough to achieve an interaction without the use of cross linking agent, but qualitatively strengthens the cross linked interaction (cf. Figure 4.19: Neuronal proteins influence p65/RelA and HSC70 interaction). This may be related to co-factors similar to the co-chaperone HSP40 or rather HOP and HSP90 from the GR-transport model. It could be estimated that some of these proteins, excluding the abundant HSP90, are enriched in neuronal extractions. The

HEK293 FT cells used for the expression of the observed interactors will probably express these co-factors at a lower level than neurons or not even at all.

The interaction of HSP90 to RelA/p65 detected by mass spectrometry could not be verified by co-immunoprecipitation (cf. Figure 4.16: p65/RelA and HSP CoIP cross linked). Nonetheless, the negative result in co-IP also cannot falsify the prior result, because it is still possiblethat an interaction is just too weak to be detected in co-IP even if a cross linker is used. It is known that HSP90 is unable to bind biologic substrates such as steroid receptors on its own and that it requires the assistance of several other proteins [172]. Maybe the supply of this chaperones, co-chaperones, adaptor proteins and nucleotides is not sufficient for the interaction. It is also important to notice that in the GR transport model, the association of HSP90 to the transport complex is not the first, but the second step.

In Figure 4.21 it was analyzed what kind of influence the presence of ATP and the temperature has on the interaction of RelA/p65 and HSC70. The result was quite surprising: while the addition of ATP does not show distinct effects, the increase in incubation temperature during IP makes the use of cross linker obsolete. Interestingly, also the ATP dependent p23 binding to HSP90 during the formation of the GR transport complex is improved at higher temperatures (30°C) by supporting the exchange of ADP by ATP in an active process [202]. However in this model, the binding of p23 goes along with the release of HOP and a part of HSP70. So the mechanism in RelA/p65 complex association must be differing, because elevated temperature increases the binding of HSP70 analog HSC70. Maybe also the first step analog to HSP40 and HSP70 binding, which is also ATP dependent, can be improved by increasing the temperature.

The poor effect of ATP may be related to basal level of ATP sufficient for interaction. The removal of basal ATP with apyrase may increase differences in binding behavior. Only with 1 mM additional ATP, there seems to be an increase in interaction. The double bands visible in the sample with no additional ATP and with 1 mM additional ATP may be based on by different levels of phosphorylation. On the one hand, phosphate groups improve the motility in gel electrophoresis by their high negative charge, on the other hand they block the binding of the hydrophobic fatty acid residue of SDS and thereby also impede the protein motility. The overall effect depends on the location of the phosphorylation.

5.7 HSC70 alias HSPA8 promotes RelA/p65 nuclear localization

After it has been shown that the heat shock cognate 70 kDa protein is an RelA/p65 interactor, it suggests itself to examine the biologic relevance of this interaction. In addition, the hypothesis of the participation of HSC70 in RelA/p65 signaling needed confirmative data. Therefore two strategies were pursued: A luciferase promoter assay and a nuclear localization assay by immunofluorescence. The luciferase assay inquires the effect of HSC70 on NF-κB dependent gene transcription, while the nuclear localization assay explores HSC70 effects on the distribution of RelA/p65 between nucleus and cytoplasm.

The luciferase assay displays the NF-κB activity by the activity of the luciferase enzyme encoded by a reporter gene equipped with a NF-κB promoter. The assay has shown that HSC70 promotes NF-κB activity by the definitive positive slope in Figure 4.23 and the significant fold change in Figure 4.24, but only in presence of overexpressed RelA/p65. The effect of HSC70 overexpression seems to be low compared to RelA/p65 overexpression. The reason for this reduced effect is that we monitor overexpression based on an unknown basal level of expression. At our chosen zero reference point, only the overexpression is zero, not the overall expression. We can be sure that the basal expression of HSC70 is much higher than those of RelA/p65, because the first is an abundant heat shock protein and the last a strictly regulated transcription factor. The relative increase in HSC70 expression, relative to basal expression, is much smaller compared to RelA/p65. This is also the explanation for the fact that there is no effect of HSC70 overexpression without co transfection with RelA/p65. Without the last, there is an excess supply of HSC70 which is not able to find enough RelA/p65 for interaction. Only by overexpression of RelA/p65, the role of the limiting factor passes over to HSC70.

If increasing levels of overexpression are compared, the HSC70 level demonstrates a similar effect for NF-κB activity like the RelA/p65 expression. So four-fold overexpression of HSC70 increases the NF-κB activity by two fold (cf. Figure 4.23: HSC70 increases NF-κB activity, 100 ng and 400 ng HSC70) and a five-fold increase in p65 overexpression increases the NF-κB activity also by two-fold (column 3 & 4, Figure 4.22). This means that HSC70 decisively participates in NF-κB activation.

The HSC70 dependent increase in NF-κB activity should be reversible by addition of deoxyspergualin (DSG). DSG binds with high affinity to HSC70 and increases its ATPase activity, it also inhibits nuclear localization of HSP70 and is correlated with a decrease NF-κB activity [162]. The mechanism is not yet understood. Our data in Figure 4.24 shows no difference in NF-κB dependent transcription after DSG treatment independent from HSC70 expression level. Although unexpected, there are two plausible explanations: The assay is inappropriate due to the long expression period (24 h) during which DSG is degraded or DSG interferes in transport, but translocation is diffusion dependent in the chosen HEK293 cells.

After having proven that the overexpression of HSC70 stimulates the transcription of NF-κB target genes, it remains to clarify how this effect is generated. As described above, we assumed a participation of HSC70 in NF-κB transport and a nuclear localization comparable to the glucocorticoid receptor model. This model includes nuclear import and intra nuclear functions of the receptor-HSP complex [173]. That means that although our nuclear localization experiments is not suitable to prove participation of HSC70 in tubular transport - transport is diffusion dependent in non neuronal cell - involvement in nuclear localization would substantiate suspicion of its relevance for transport, because the ability to pass the nuclear membrane is a prerequisite for being part of a transport complex.

There are previous publications about the nuclear translocation of HSC70 in response to oxidative stress, during apoptosis [49] and heat shock [123], which are typically accompanied by NF-κB activation. It is assumed that HSC70 is retained in the nucleus by its substrates and associates with nucleolar proteins [123]. This assumption was affirmed by the characterization of three nuclear transport signals. The first is a typical basic nuclear localization signal with the sequence ^{246}KRKHKKDISENKRAVRR^{262}, located in the N-terminal ATPase domain [48]. The others are a nuclear localization related signal NLRS and a nuclear export signal. These last two sequences are both localized in the peptide binding domain and interact inhibitory by themselves or bound protein substrate. Thereby, NLRS bound molecules may impede nuclear export. NLS as well as NLRS are sufficient for mediating nuclear import, but both regions are necessary to mediate a nuclear accumulation of HSC70, as observed for example during heat shock [129, 210]. It is

also reported that the related HSP70 promotes NF-κB nuclear translocation by the expression of a HSP70-p50 fusion protein [72].

To validate the dependence of NF-κB nuclear localization on HSC70, we used to approaches: The localization of RelA/p65 and HSC70 as end point determination in permanent NF-κB active and repressed cells and an in vivo time course experiment after TNF-α treatment. The repression of NF-κB activity was achieved by IκBα overexpression in the first approach . The first approach delivered the result that in absence of IκBα, the nuclear localization of p65/RelA is slightly increased if HSC70 is contemporaneously overexpressed (Figure 4.25., column 1&2). If RelA/p65 is inhibited by IκBα, there is a drastic change to nuclear localization of HSC70. These two observations perfectly support our hypothesis of HSC70 dependent NF-κB translocation. The relative exiguity of the first effect depends again on a level of basal HSC70, which is nearly sufficient to mediate the transport, and on the characteristic of an end time point determination. This means that we cannot observe potential differences in the translocation kinetics corresponding to HSC70 expression level and therefore, one molecule of HSC70 may translocate some RelA/p65 molecules by and by. The last mechanism only plays a negligible role, through the retention of HSC70 by RelA/p65 as postulated in [123, 210] and observed in Figure 4.26, column 2&4. Only this retention of HSC70 makes it possible to observe an increase in RelA/p65 nuclear translocation corresponding to HSC70 expression level. Although in principle, time course experiments are more trustworthy than snap shot experiments, the HSC70 independent induction of NF-κB could only be achieved in the first experiment, in which the transport equilibrium is reached. In this first experiment, there was a strong nuclear localization of RelA/p65 in absence of IκBα and a strong cytoplasmic localization in presence of IκBα. This well known correlation must be shown by the assay. However, the in vivo time course experiment does not show a nuclear localization of RelA/p65 in response to the employed stimulus (TNF-α). The statistical results (Figure 4.29) only display a small insignificant increase in nuclear RelA/p65 between 10 and 40 min after stimulation. According to recent publications, the translocation in response to TNF-α takes between 10-30 min and is completed after 40 min after stimulation [197]. A reason for this is probably the slight co expression of IκBα. On the one hand, the expression level of IκBα could be too high so that the activation of NF-κB by TNF-α is

inhibited. On the other hand, IκBα is necessary to prevent a nuclear localization of RelA/p65 in unstimulated cells as shown in the snap shot experiment. The overexpression by the fluorescence tagged RelA/p65 strongly increases the NF-κB activity. Without IκBα, there would not be a detectable TNF-α effect either. This means that a careful titration up to the appropriate IκBα level is necessary. It is quite probable that this aim has been overshot. While this explains the absence of a TNFα effect, one effect of HSC70 on Rela/p65 distribution is still visible: The HSC70-GFP retains RelA/p65 in the cytoplasm compared to the GFP transfected control. This can be evaluated as a sign of interaction and or of shuttling of RelA/p65 from the nucleus. It seems probable that HSC70 mediates nuclear im- and export of NF-κB, but the regulation is performed by other players as for example directly by IκBs. Another explanation for the strong nuclear depletion of RelA/p65 by HSC70 may be a potential interaction to IκBs. If HSC70 can also translocate IκBs, the RelA/p65 will efficiently be exported in presence of IκBα as we observed it.

The in vivo time course experiment shows no significant differences in the localization of HSC70 compared to GFP, which can be also related to the poor induction. HSC70 and GFP seem to tend to more nuclear localization during the time course. This could be presumed , by reason of the slight reduction of cytoplasmic volume in response to stress.

Some of these observed effects can also be related to the ability of HSC70 to export the nuclear import receptors of the importin-β family [126], but the nuclear localization of HSC70 itself and the IP results suggest a direct interaction of HSC70 and RelA/p65 and a promotion of nuclear import. The nuclear interaction to the NF-κB subunit to the HSC70s NES stands to the reason for nuclear accumulation of HSC70.

5.8 HSC70 interacts with NF-κB in a transport model

We have proven that HSC70 interacts with RelA/p65, affects its nuclear translocation and modulates the activity of the transcription of NF-κB target genes. We also know about the dynein dependent axonal transport of NF-κB, which shows parallels to glucocorticoid receptor transport, but there are also more hand-tight

connections: As mentioned above the NF-κB and the GR show a functional antagonism and a physical association [176]. This physical association, detected by Although Ray A. et. al., could be misinterpreted as a direct interaction. It could be also an indirect one mediated by heat shock proteins. The interaction study was performed by co-IP of cell free, in vitro synthesized RelA/p65 and GR, but the translation system uses reticulocyte extract, which contains high amounts of heat shock proteins [172]. Species differences between HSPs from reticulocyte extract, usually rabbit, and human RelA/p65 and GR probably do not affect the interaction by reason of the high conservation of HSPs. So the association may be a sign of potential co-transport. At first view, a co-transport seems contradictory to the observed functional antagonism. A competition or inhibitory interaction is rather expected. However, if we assume a competition for binding capacities in transport, we have to consider that this transport cannot be limited to one molecule per transport complex (v.i.). Therefore in a competition between cargo like RelA/p65 and GR the loading ratio is shifted. A state of exclusive transport of only one compound, if it exists at all, must alternate with a state in which both cargos are carried in varying numbers.

Another reason to assume co-transport can be derived from the physical properties of the transport complex. The dynein motor protein can proceed in various step lengths from 8 to 32 nm. The motoric force is anti proportionally correlated to the step length and reaches gigantic peaks of up to 1.1 pN [141]. By this force, a few (1-4!) dynein units can move whole organelles [10] and are fast enough for axonal transport [143]. The cooperation of the four dynein heads is rather necessary to prevent dissociation and processive, fast movement than to generate extra force [144]. This motoric force is surely not limited to the transport of one GR. It can be assumed that the GR transport model shows only a part of a large transport complex. If this also included vesicle transport, it would efficiently exploit the capacity supplied by the dynein motor.

NF-κB as well as vesicle transport may be induced by the same stimulus like the binding of NGF [50, 101] or EGF [62, 225]. Besides the full use of capacity, the co-transport of cytoplasmic proteins as NF-κB and vesicles may benefit from synergistic effects. For example, the recruitment of the motor protein may promote both, NF-κB and the vesicle transport. The coupling of NF-κB signaling and

endocytosis [138] has the same benefits on a subsequent co-transport. The characteristics of axonal transport cause that the cargos share the same destination over a long distance at least to the cell body. There we believe that collective co-transport is the plausible, efficient way of neuronal transport.

The remaining question concerns the role of the cargo adaptors, which are necessary to contemporaneously bind different targets to one motor protein. Therefore it takes a complex of proteins that is capable of binding different cargos, supplying a connection to the motor protein and assembling to a docking scaffold. In the model presented by W. Pratt et al. [173], HSPs undertake the first two functions. The same applies to the dynactin complex. It directly binds to dynein and is the adaptor between dynein and HSP in an interaction chain (dynein - dynactin - immunophilin - HSPs - cargo) [83]. Dynactin also maintains further interactions with organelles via its Arp1 subunits and the protein spectrin [91, 161]. But although the dynactin complex is a large 1.1 MDa complex consisting of eleven subunits [119], there are no reports about additional oligomerization and therefore, the accessibility of the dynactin complex for cargo is limited. That means it cannot bind to a large number of cargo molecules directly or just by binary interactors. This function needs either a branched network of proteins which supports three or more interactions or a oligomer of proteins, maybe both. Figure 5.2 shows the confirmed part of the transport complex and illustrates the question for further cargo binding sides.

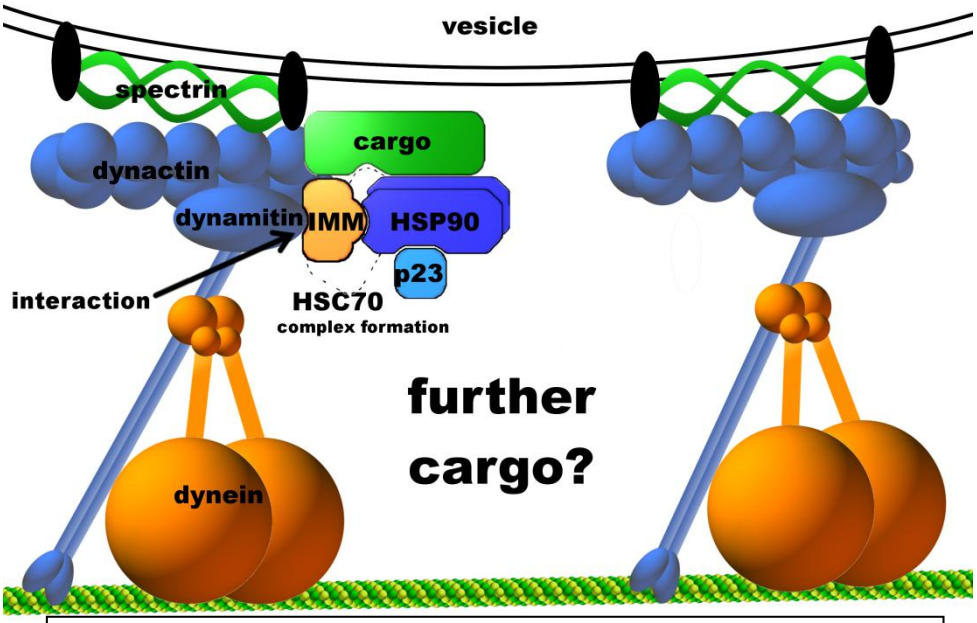

Figure 5.2: The dynein transport complex and the question for further cargo binding sides

HSP90 as well as HSC70 are reported to oligomerize. In both cases, oligomerization is dependent on ATP and is largely increased at an elevated temperature. But in contrast to HSP90 and HSP70 respectively, HSC70 forms oligomers at 37°C under in vitro conditions. Furthermore HSP90 multimers, dimers and oligomers, still show chaperone activity, while HSP70 and HSC70 lose their substrate binding capabilities upon oligomerizetion [8, 41]. A C-terminal domain of HSC70 is responsible of both self association or subtrate binding [69]. Beside this, the domain interacts with the ATPase domain and modulate its activity [20]. It has been proposed that the self association and oligomerization regulates the activity of the chaperone by constituting an inactive reserve. This stored HSC70 can be released by monomerization quickly. The equilibrium of monomeric and multimeric HSC70 is tightly controlled not only by substrate and ATP concentration, but also by protein co-factors [8]. Maybe the oligomerized HSC70 is not limited to its function as a reserve, but also as a scaffold protein in transport, while cargo interaction is mediated by HSP90. This hypothesis is substantiated by the fact that HSC70 forms aggregates with spectrin during translocation. This aggregates can be dissolved by addition of ATP [57]. Spectrin is known as the scaffold protein which mediates the interaction of dynactin and transported vesicles. The association of spectrin and HSC70 may provide a docking platform. At least it is a sign that HSC70 has function enduring transport and not only in transport complex formation.

All together HSC70 is a pivotal player in cellular transport. It participates in loading the cargo on HSP90, as seen for the GR, and it may mediate nuclear import by its NLS. HSC70 is involved in processing of endocytosed and transported clathrin coated vesicle, too. Furthermore, it may serve as a docking platform to grant a larger number of cargo molecules access to the transport machinery. Therefore it might interact with spectrin, oligomerize, associated with HSP90 to form transport complexes. It also may recognize cargo NLS [98] or interact with importins by its own NLS [48] and therefore ensure NLS specificity as detected in NF-κB transport [153]. This detected and potential functions make HSC70 an important target for regulation.

6 Summary

In this work, new NF-κB interaction partners were identified, among these the heat shock protein HSC70. For this protein, further interactions with the NF-κB signaling were explored and detected. The transcription factor NF-κB is an important regulatory element in a broad variety of cell processes. In addition to its well studied role in inflammation, in immune response, and in apoptosis it is known to steer the development of neuronal cells. In these cells with spacious signal pathways, active transport of NF-κB is indispensable. Mediators during this transport and subsequent nuclear import can be detected as NF-κB interaction partners. The identification of new interaction partner and therefore potential mediators in transport may help to improve and expand existing models.

New NF-κB interaction partners were detected by immunoprecipitation of porcine brain extracts with a anti RelA/p65 antibody and subsequent mass spectrometric analysis. The porcine origin lead to the preferential finding of conserved proteins. The detected proteins are part of the endocytosis network, are filament compounds or play a role in intracellular transport. This includes the endocytosis network proteins clathrin, dynamin and HSC70, the filaments actin, tubulin and NEFL and the components of transport complexes heat shock proteins HSC70 and HSP90, the transport regulators CRMP-2 and the cargo HDGFRP3. The physical associated proteins detected by mass spectrometry may interact with NF-κB during one or some processes as for example signalling, transport, nuclear import or transcription activation. A reasons for the finding of players in endocytosis may be a conjunction of endocytosis and NF-κB signalling [138] or co-transport of vesicles and NF-κB.

From the detected proteins the heat shock proteins are most promising candidates to be a cargo adaptor in NF-κB transport. The reason is that HSP are known to mediate the transport of other protein, especially the glucocorticoid receptor described by the group of W. Pratt [173] and they are capable of the binding of a broad variety of substrates. The interaction of RelA/p65 was tested in co-immunoprecipitation. While RelA/p65 interacts with HSC70 it does not with HSP90. The interaction is weak and only detectable in presence of a cross linking agent. The weak interaction of RelA/p65 and HSC70 can be increased by elevated temperatures (37°C) or the addition of brain extracts. We believe that the elevated temperature increases by

complex formation by the support the ATPase activity of HSC70. The beneficial effect of brain extract on the interaction indicates that some co factors or co-chaperones participates in the interaction which are preferentially expressed in neurons. The HEK293 cell line used for the expression of the interaction partners lack this co-factors because NF-κB is diffusion dependent in this cells. This is an evidence for the participation of HSC70 in NF-κB transport and not only for nuclear import or other purposes for interaction.

If the transport of NF-κB is comparable to GRs, HSP70 or HSC70 are employed in the transport complex formation while the "mature" complex contains two molecules HSP90 and only substoichiometric amounts of HSP70. If this is true, the absence of HSP90 in our IP complexes mean that we may monitor early, "immature" complexes.

Next to its role in transport HSC70 is also known to effect nuclear localization of many targets. So we also tested its effect on RelA/p65 localization. We could show that HSC70 promotes the nuclear localization of free, non inhibited RelA/p65 and RelA/p65 in return retains HSC70 in the nucleus. In a luciferase assay we could show that this HSC70 increased NF-κB nuclear localization leads to a boost of the transcription of NF-κB target genes. This ability to mediate nuclear localization also improves the function of HSC70 containing transport complexes if they are present intra and extra nuclear, as described for GR.

Finally we discuss the heat shock protein like HSC70 may be an important connector or regulator in a real in vivo transport complex, of which the proposed model of W. Pratt et. al. only describes a detail excerpt. So HSC70 is involved in many more processes than nuclear import and the loading of cargo onto small transport complexes. It is well known to mediated endocytosis, which connection to NF-κB is supported by our mass spectrometry data and which is a frequent starting point of transport processes. It may also be regulated by TNF-α stimulated NF-κB activation [31, 104, 198]. Furthermore HSC70 builds up aggregates with spectrin during translocation [57], which may serve as a docking platform in transport. This let us believe that HSC70 occupies a key role in transport processes, from plasma membrane to nucleus, which a broad variety of different functions. Therefore HSPs, especially HSC70, must be considered in future NF-κB transport models.

7 Outlook

The RelA/p65 interaction can be further characterized by IP experiments. It is likely that the chaperone activity of heat shock proteins plays a role in the complex formation in transport. Our results suggests that a depletion of basal ATP is necessary to achieve significant effects on interaction strength by ATP. Furthermore we could not verify an interaction of HSP90 and RelA/p65 in co IP. As explained above this does not contradict or falsify an association, because It could be the caused by a very weak interaction. Maybe an increase in temperature to 37°C (no heat shock conditions) strengthens the association by promotion of the ATPase activity so an interaction can be monitored. This would apply to the GR model in which HSP90 binds after HSP70 prepared by anterior steps of ATP hydrolysis. The next step in co IP would be the establishment of a minimal system of complex proteins starting from the GR complex with HSC70, HSP40, HSP90, HOP and p23.

Besides immunoprecipitation and western blotting new interaction complexes may be identified by mass spectrometry. Therefore complexes, containing RelA/p65, other cargos or potential mediators as HSPs, can be separated by native gel electrophoresis as for example blue native electrophoresis. The components of this purified complexes can be identified by liquid chromatography and tandem mass spectrometry. This would allow the research of HDGFRP-3 transport, which is believed to be co-transported with NF-κB in result of our mass spectrometric measurements. It would also be suitable to get more information about the character of CRMP2 / NF-κB interaction.

As described the use of porcine sample material complicates the identification of less conserved proteins using a human data base for the analysis. The expansion of porcine data bases will make this obsolete and will enable a faster and better analysis of the data.

Next to this, the participation of HSC70 in transport of NF-κB must be confirmed in vivo. In our workgroup, experiments are currently performed to verify NF-κB-HSP interaction or co-localization in neurons by "Duo Link". In this method antibodies coupled with nucleotide sequences are directed against the target proteins. Close proximity of the nucleotide sequences enables an amplification and a subsequent detection with fluorescence tagged oligonucleotides. The verification of in vivo

interactions could be achieved by labeling the interaction partners for FRET measurements, too. The best method to observe transport in neurons would be fluorescence recovery after photo bleaching (FRAP) in combination with the HSC70 inhibitor DSG.

Furthermore, it would be interesting to find out if NLS mutants of the GR undergo axonal transport or if this mutation inhibits it, because this has been shown for NF-κB, but has not been investigated for GR. If both transport systems obey the same regulations, an assumed co transport is more likely. In this case, an expansion of the model for GR transport [173] would also be necessary, in which maybe HSC70 plays a role for NLS recognition.

8 Literature index

[1] Abouzied, M.M.; Baader, S.L.; Dietz, F.; Kappler, J., Gieselmann, V.; Franken S. (2004):
Expression patterns and different subcellular localization of the growth factors HDGF (hepatoma-derived growth factor) and HRP-3 (HDGF-related protein-3) suggest functions in addition to their mitogenic activity.
Biochem. J., 378:169–176.

[2] Ahle, S.; Ungewickell, E. (1986):
Purification and properties of a new clathrin assembly protein.
EMBO J., 5(12):3143–3149.

[3] Akira, S.; Takeda, K. (2004):
Toll-like receptor signalling.
Nat Rev Immunol., 4(7):499-511.

[4] Albensi, B.C.; Mattson, M.P. (2000):
Evidence for the involvement of TNF and NF-kappaB in hippocampal synaptic plasticity.
Synapse, 35:151–159.

[5] Alberti, S.; Esser, C.; Hohfeld, J. (2003):
BAG-1-a nucleotide exchange factor of Hsc70 with multiple cellular functions.
Cell Stress & Chaperones, 8(3):225-231.

[6] Alkalay, I.; Yaron, A.; Hatzubai, A.; Orian, A.; Ciechanover, A.; Ben-Neriah, Y. (1995):
Stimulation dependent I kappa B alpha phosphorylation marks the NF-kappa B inhibitor for degradation via the ubiquitin-proteasome pathway.
Proc. Natl. Acad. Sci. U S A., 92(23):10599-10603.

[7] Amir, R.E.; Haecker, H.; Karin, M.; Ciechanover, A. (2004):
Mechanism of processing of the NF-kappa B2 p100 precursor: identification of the specific polyubiquitin chain-anchoring lysine residue and analysis of the role of NEDD8-modification on the SCF(beta-TrCP) ubiquitin ligase.
Oncogene., 23(14):2540-2547.

[8] Angelidis, C.E.; Lazaridis, I.; Pagoulatos, G.N. (1999):
Aggregation of hsp70 and hsc70 in vivo is distinct and temperature-dependent and their chaperone function is directly related to non-aggregated forms.
Eur. J. Biochem. 259(1-2):505-512.

[9] Arimura, N.; Hattori, A.; Kimura, T.; Nakamuta, S.; Funahashi, Y.; Hirotsune, S.; Furuta, K.; Urano, T.; Toyoshima, Y.Y.; Kaibuchi, K. (2009):
CRMP-2 directly binds to cytoplasmic dynein and interferes with its activity.
J. Neurochem., 111(2):380-390.

[10] Ashkin, A.; Schutze, K.; Dziedzic, J.M.; Euteneuer, U.; Schliwa, M. (1990):
Force Generation of Organelle Transport Measured In Vivo by an Infrared Laser Trap.
Nature; 348:346-348.

[11] Baas, P.W. (2002):
Neuronal polarity: microtubules strike back.
Natur Cell Biology, 4:E194-E195.

[12] Baas, P.W.; Deitch, J.S.; Black, M.M.; Banker, G.A. (1988):
Polarity orientation of microtubules in hippocampal neurons: uniformity in the axon and nonuniformity in the dendrite.
Proc. Natl. Acad. Sci. U S A, 85(21):8335–8339.

[13] Bachelerie, F.; Alcami, J.; Arenzana-Seisdedos, F.; Virelizier, J-L. (1991):
HIV enhancer activity perpetuated by NF-κB induction on infection of monocytes.
Nature, 350:709-712.

[14] Bachis, A.; Colangelo, A.M.; Vicini, S.; Doe, P.P.; De Bernardi, M.A.; Brooker, G.; Mocchetti, I. (2001):
Interleukin-10 prevents glutamate-mediated cerebellar granule cell death by blocking caspase-3-like activity.
J. Neurosci., 21:3104–3112.

[15] Baeuerle, P.A.; Baltimore, D. (1988):
I kappa B: a specific inhibitor of the NF-kappa B transcription factor.
Science, 242(4878):540-546.

[16] Bakalkin, G.; Yakovleva, T.; Terenius, L. (1993):
NF-kappa B-like factors in the murine brain. Developmentally-regulated and tissue-specific expression.
Brain Res. Mol. Brain Res., 20:137–146.

[17] Baldwin, A.S. Jr. (1996).
The NF-kappa B and I kappa B proteins: new discoveries and insights.
Annu. Rev. Immunol., 14:649-83.

[18] Barger, S.W.; Horster, D.; Furukawa, K.; Goodman, Y.; Krieglstein, J.; Mattson, M.P. (1995):
Tumor necrosis factors alpha and beta protect neurons against amyloid beta-peptide toxicity: evidence for involvement of a kappa B-binding factor and attenuation of peroxide and Ca^{2+} accumulation.
Proc. Natl. Acad. Sci. U. S. A., 92:9328–9332.

[19] Bauer, M.K.; Lieb, K.; Schulze-Osthoff, K.; Berger, M.; Gebicke-Haerter, P.J.; Bauer, J.; Fiebich, B.L. (1997):
Expression and regulation of cyclooxygenase-2 in rat microglia.
Eur. J. Biochem., 243:726–731.

[20] Benaroudj, N.; Fouchaq, B.; Ladjimi, M.M (1997):
The COOH-terminal Peptide Binding Domain Is Essential for Self-association of the Molecular Chaperone HSC70
J. Biol. Chem., 272(13):8744–8751.

[21] Bernard, O.; Cory, S.; Gerondakis, S.; Webb, E.; Adams, J.M. (1984):
Sequence of the murine and human cellular myc oncogenes and two modes of myc transcription resulting from chromosome translocation in B lymphoid tumours.
The EMBO journal, 2(12):2375-2383.

[22] Bianchi, K.; Meier, P. (2009):
A tangled web of ubiquitin chains: breaking news in TNFR1 signaling.
Mol. Cell., 36(5):736-742.

[23] Blair, W.S.; Bogerd, H.P.; Madore, S.J.; Cullen, B.R. (1994):
Mutational analysis of the transcription activation domain of RelA: identification of a highly synergistic minimal acidic activation module.
Mol. Cell. Biol., 14:7226-7234.

[24] Blank, V.; Kourilsky, P.; Israel, A. (1991):
Cytoplasmic retention, DNA binding and processing of the NF-xB p50 precursor are controlled by a small region in its C-terminus.
EMBO J., 10(13):4159-4167.

[25] Blatch, G.L.; Lässle, M. (1999):
The tetratricopeptide repeat: a structural motif mediating protein-protein interactions.
Bioassays. 21(11):932-939.

[26] Bonaiuto, C.; McDonald, P.P.; Rossi, F.; Cassatella, M.A. (1997):
Activation of nuclear factor-kappa B by beta-amyloid peptides and interferongamma in murine microglia.
J. Neuroimmunol., 77:51–56.

[27] Bonizzi, G.; Karin, M. (2004):
The two NF-kappaB activation pathways and their role in innate and adaptive immunity.
Trends Immunol., 25:280–288.

[28] Bours, V.; Franzoso, G.; Azarenko, V.; Park, S.; Kanno, T.; Brown, K.; Siebenlist, U. (1993):
The oncoprotein Bcl-3 directly transactivates through κ B motifs via association with DNA-binding p50B homodimers.
Cell, 72(5):729–39.

[29] Braun, S.; Liebetrau, W.; Berning, B.; Behl, C. (2000):
Dexamethasoneenhanced sensitivity of mouse hippocampal HT22 cells for oxidative stress is associated with the suppression of nuclear factor-kappaB.
Neurosci. Lett., 295:101–104.

[30] Breeden, L.; Nasmyth, K. (1987):
Similarity between cell-cycle genes of budding yeast and fission yeast and the Notch gene of Drosophila.
Nature, 329:651-654.

[31] Briknarová, K.; Takayama, S.; Homma, S.; Baker, K.; Cabezas, E.; Hoyt, D.W.; Li, Z.; Satterthwait, A.C.; Ely, K.R. (2002):
BAG4/SODD protein contains a short BAG domain.
J. *Biol. Chem.,* 277(34):31172-31178.

[32] Bruce, A.J.; Boling, W.; Kindy, M.S.; Peschon, J.; Kraemer, P.J.; Carpenter, M.K.; Holtsberg, F.W.; Mattson, M.P. (1996):
Altered neuronal and microglial responses to excitotoxic and ischemic brain injury in mice lacking TNF receptors.
Nat. Med., 2:788–794.

[33] Bull, P.; Morley, K.L.; Hoekstra, M.F.; Hunter, T.; Verma, I.M. (1990):
The mouse c-rel protein has an N-terminal regulatory domain and a C-terminal transcriptional transactivation domain.
Mol Cell Biol, 10:5473-5485.

[34] Burke, M.A.; Bothwell, M. (2003):
p75 neurotrophin receptor mediates neurotrophin activation of NF-kappa B and induction of iNOS expression in P19 neurons.
J. Neurobiol. 55:191–203.

[35] Caamaño, J.; Hunter, C. A. (2002):
NF-κB Family of Transcription Factors: Central Regulators of Innate and Adaptive Immune Functions.
Clinical Microbiology Reviews, July:414–429.

[36] Callahan, M.K.; Chaillot, D.; Jacquin, C.; Clark, P.R.; Me'noret, A. (2002):
Differential Acquisition of Antigenic Peptides by Hsp70 and Hsc70 under Oxidative Conditions.
J. Biol. Chem., 277(37):33604–33609.

[37] Campbell, E.M.; Hope, T.J. (2003):
Role of the cytoskeleton in nuclear import.
Adv. Drug Deliv. Rev., 55:761–771.

[38] Cantera, R.; Roos, E.; Engstrom, Y. (1999):
Dif and cactus are colocalized in the larval nervous system of Drosophila melanogaster.
J. Neurobiol. 38:16–26.

[39] Carter, B.D.; Kaltschmidt, C.; Kaltschmidt, B.; Offenhauser, N.; Bohm-Matthaei, R.; Baeuerle, P.A.; Barde Y.A. (1996):
Selective activation of NF-κB by nerve growth factor through the neurotrophin receptor p75.
Science, 272:542–545.

[40] Cauley, K.; Verma, I.M. (1994):
Kappa B enhancer-binding complexes that do not contain NF-kappa B are developmentally regulated in mammalian brain.
Proc. Natl. Acad. Sci. U. S. A. 91:390–394.

[41] Chadli, A.; Ladjimi, M.M.; Baulieu, E.E.; Catelli, M.G. (1999):
Heat-induced oligomerization of the molecular chaperone Hsp90. Inhibition by ATP and geldanamycin and activation by transition metal oxyanions.
Journal of Biological Chemistry, 274:4133-4139.

[42] Chen, B.; Piel, W.H.; Gui, L.; Bruford, E.; Monteiro, A. (2005):
The Hsp90 family of genes in the human genome: insights into their divergence and evolution.
Genomics, 86(6):627–637.

[43] Chen, S.; Prapapanich, V.; Rimerman, R.A.; Honoré, B.; Smith, D.F. (1996):
Interactions of p60, a mediator of progesterone receptor assembly, with heat shock proteins hsp90 and hsp70.
Mol. Endocrinol., 10:682–693.

[44] Chen, Z.J.; Sun, L.J. (2009):
Nonproteolytic functions of ubiquitin in cell signaling.
Mol. Cell., 33(3):275-286.

[45] Claudio, E.; Brown, K.; Park, S.; Wang, H.; Siebenlist, U. (2002):
BAFF-induced NEMOindependent processing of NF-kappa B2 in maturing B cells.
Nat Immunol., 3(10):958-965.

[46] Coope, H.J.; Atkinson, P.G.; Huhse, B.; Belich, M.; Janzen, J.; Holman, M.J.; Klaus, G.G.; Johnston, L.H.; Ley, S.C. (2002):
CD40 regulates the processing of NF-kappaB2 p100 to p52.
EMBO J., 21(20):5375-5385.

[47] Crowther, R.A.; Pearse, B.M. (1981):
Assembly and packing of clathrin into coats.
J. Cell Biol.,1981, 91:790-797.

[48] Dang, C.V.; Lee, W.M.F. (1989):
Nuclear and Nucleolar Targeting Sequences of c-erb-A, c-myb, N-myc, p53, HSP70, and HIV tat Proteins.
J. Biol. Chem., 264(30):18019-18023.

[49] Dastoor, Z.; Dreyer, J.(2000):
Nuclear translocation and aggregate formation of heat shock cognate protein 70 (Hsc70) in oxidative stress and apoptosis.
Journal of Cell Science, 113, 2845-2854.

[50] Deinhardt, K.; Reversi, A.; Berninghausen, O; Hopkins, C.R.; Schiavo1, G. (2007):
Neurotrophins Redirect p75NTR from a Clathrin-Independent to a Clathrin-Dependent Endocytic Pathway Coupled to Axonal Transport.
Traffic, 8:1736–1749.

[51] Dejardin, E. (2007):
The alternative NF-kappaB pathway from biochemistry to biology: pitfalls and promises for future drug development.
Biochem. Pharmacol., 72(9):1161-1179.

[52] Dejardin, E.; Droin, N.M.; Delhase, M.; Haas, E.; Cao, Y.; Makris, C.; Li, Z.W.; Karin, M.; Ware, C.F.; Green, D.R. (2002):
The lymphotoxin-beta receptor induces different patterns of gene expression via two NF-kappaB pathways.
Immunity., 17(4):525-535.

[53] Delhase, M.; Hayakawa, M., Chen, Y.; Karin, M. (1999):
Positive and negative regulation of IkappaB kinase activity through IKKbeta subunit phosphorylation.
Science, 284:309–313.

[54] Dell'Angelica, E.C.; Mullins, C.; Bonifacino, J.S. (1999):
AP-4, a novel protein complex related to clathrin adaptors.
J. Biol. Chem., 274:7278-7285.

[55] Dell'Angelica, E.C.; Ohno, H.; Ooi, C.E.; Rabinovich, E.; Roche, K.W.; Bonifacino, J.S. (1997):
AP-3: an adaptor-like protein complex with ubiquitous expression.
EMBO J., 16:917-928.

[56] Devin, A.; Cook, A.; Lin, Y.; Rodriguez, Y.; Kelliher, M.; Liu, Z. (2000):
T*he distinct roles of TRAF2 and RIP in IKK activation by TNF-R1: TRAF2 recruits IKK to TNF-R1 while RIP mediates IKK activation.*
Immunity., 12(4):419-429.

[57] Di, Y.P.; Repasky, E.; Laszlo, A.; Calderwood, S.; Subjeck, J. (1995):
Hsp70 translocates into a cytoplasmic aggregate during lymphocyte activation.
J. Cell Physiol., 165(2):228-38.

[58] DiDonato, J.; Mercurio, F.; Rosette, C.; Wu-Li, J.; Suyang, H.; Ghosh, S.; Karin, M. (1996):
Mapping of the inducible IkappaB phosphorylation sites that signal its ubiquitination and degradation.
Mol. Cell Biol., 16(4):1295-1304

[59] Dittmar, K.D.; Demady, D.R.; Stancato, L.F.; Krishna, P.; Pratt, W.B. (1997):
Folding of the glucocorticoid receptor by the heat shock protein (hsp) 90-based chaperone machinery. The role of p23 is to stabilize receptor/hsp90 heterocomplexes formed by hsp90/p60/hsp70.
J. Biol. Chem., 272:21213–21220.

[60] Doohan, M.E.; Palevitz, B.A. (1980):
Microtubules and coated vesicles in guard cell protoplasts of Allium cepa L.
Planta, 149:389-401.

[61] Drew, P.D.; Lonergan, M.; Goldstein, M.E.; Lampson, L.A.; Ozato, K.; McFarlin, D.E. (1993):
Regulation of MHC class I and beta 2-microglobulin gene expression in human neuronal cells. Factor binding to conserved cis-acting regulatory sequences correlates with expression of the genes.
J. Immunol., 150:3300– 3310.

[62] Driskell, O.J.; Mironov, A.; Allan, V.J.; Woodman P.G.(2007):
Dynein is required for receptor sorting and the morphogenesis of early endosomes.
Nature Cell Biology, **9:**113-120.

[63] Ducut Sigala, J.L.; Bottero, V.; Young, D.B.; Shevchenko, A.; Mercurio, F.; Verma, I.M. (2004):
Activation of transcription factor NF-kappaB requires ELKS, an IkappaB kinase regulatory subunit.
Science, 304:1963– 1967.

[64] Ehrlich, L.C.; Hu, S.; Peterson, P.K.; Chao, C.C. (1998):
IL-10 down-regulates human microglial IL-8 by inhibition of NF-kappaB activation.
NeuroReport, 9:1723–1726.

[65] El-Tahir, H.M.; Abouzied, M.M.; Gallitzendoerfer, R.; Gieselmann, V.; Franken, S. (2009):
Hepatoma-derived Growth Factor-related Protein-3 interacts with Microtubules and Promotes Neurite Outgrowth in Mouse Cortical Neurons.
J. Biol. Chem., 284(17):11637–11651.

[66] El-Tahir, H.M.; Dietz, F.; Dringen, R.; Schwabe, K.; Strenge, K.; Kelm, S.; Abouzied, M.M.; Gieselmann, V.; Franken, S. (2006):
Expression of Hepatoma-derived growth factor family members in the adult central nervous system.
BMC Neuroscience, 7(6) doi:10.1186/1471-2202-7-6.

[67] Fagerlund, R.; Kinnunen, L.; Kohler, M.; Julkunen, I.; Melen, K. (2005):
NFkappa B is transported into the nucleus by importin alpha 3 and importin alpha 4.
J. Biol. Chem., 280(16):15942–15951.

[68] Fernyhough, P.; Smith, D.R.; Schapansky, J.; Van Der Ploeg, R.; Gardiner, N.J.; Tweed, C.W.; Kontos, A.; Freeman, L.; Purves-Tyson, T.D.; Glazner, G.W. (2005):
Activation of nuclear factor-κB via endogenous tumor necrosis factor α regulates survival of axotomized adult sensory neurons.
J. Neurosci., 25:1682–1690.

[69] Fouchaq, B.; Benaroudj, N.; Ebel, C.; Ladjimi, M.M. (1999):
Oligomerization of the 17-kDa peptide-binding domain of the molecular chaperone HSC70.
Eur. J. Biochem., 259:379-384.

[70] Franzoso, G.; Bours, V.; Park, S.; Tomita-Yamaguchi, M.; Kelly, K.; Siebenlist, U. (1992):
The candidate oncoprotein Bcl-3 is an antagonist of p50/NF-κB-mediated inhibition.
Nature, 359(6393): 339–42.

[71] Fridmacher, V.; Kaltschmidt, B.; Goudeau, B.; Ndiaye, D.; Rossi, F.M.; Pfeiffer, J.; Kaltschmidt, C.; Israel, A.; Memet, S. (2003):
Forebrain-specific neuronal inhibition of nuclear factor-kappaB activity leads to loss of neuroprotection.
J. Neurosci., 23:9403–9408.

[72] Fujihara, S.M.; Nadler, S.G. (1999):
Intranuclear targeted delivery of functional NF-kB by 70 kDa heat shock protein.
The EMBO Journal, 18(2):411–419.

[73] Fujita, T.; Nolan, G.P.; Liou, H.C.; Scott, M.L.; Baltimore, D. (1993):
The candidate proto-oncogene bcl-3 encodes a transcriptional coactivator that activates through NF-κB p50 homodimers.
Genes Dev. 7(7B):1354–63.

[74] Fukata, Y.; Itoh, T.J.; Kimura, T.; Ménager, C.; Nishimura, T.; Shiromizu, T.; Watanabe, H.; Inagaki, N.; Iwamatsu, A.; Hotani, H.; Kaibuchi, K (2002):
CRMP-2 binds to tubulin heterodimers to promote microtubule assembly.
Natur Cell Biology, 4:583-591.

[75] Ghosh, S.; Karin, M. (2002):
Missing Pieces in the NF-κB Puzzle.
Cell, 109(2):81-96.

[76] **Ghosh, S.; May, M. J.; Kopp, E. B. (**1998):
NF-κB and Rel proteins: evolutionarily conserved mediators of immune responses.
Annu. Rev. Immunol., 16**:**225–259.

[77] **Ginis, I.; Hallenbeck, J.M.; Liu, J.; Spatz, M.; Jaiswal, R.; Shohami, E. (2000):**
Tumor necrosis factor and reactive oxygen species cooperative cytotoxicity is mediated via inhibition of NF-kappaB.
Mol. Med., 6:1028–1041.

[78] **Grilli, M.; Pizzi, M.; Memo, M.; Spano, P. (1996):**
Neuroprotection by Aspirin and Sodium Salicylate Through Blockade of NF-κB Activation.
Science, 274(5291):1383-1385.

[79] **Guerrini, L.; Blasi, F.; Denis, D.S. (1995):**
Synaptic activation of NF-κB by glutamate in cerebellar granule neurons in vitro.
Proc. Natl. Acad. Sci. U. S. A. 92:9077–9081.

[80] **Gundersen, G.G.; Cook, T.A. (1999):**
Microtubules and signal transduction.
Curr. Opin. Cell Biol., 11:81–94.

[81] **Hanz, S.; Fainzilber, M (2006):**
Retrograde signaling in injured nerve – the axon reaction revisited.
Journal of Neurochemistry, 2006, 99, 13–19.

[82] **Hanz, S; Perlson, E.; Willis, D.; Zheng, J.; Massarwa, R.; Huerta, J.J.; Koltzenburg, M.; Kohler, M.; van-Minnen, J.; Twiss, J.L.; Fainzilber, M. (2003):**
Axoplasmic Importins Enable Report Retrograde Injury Signaling in Lesioned Nerve.
Neuron, 40:1095–1104.

[83] **Harrell, J.M.; Murphy, P.J.M.; Morishima, Y.; Chen, H.; Mansfield, J.F.; Galigniana, M. D.; Pratt, W.B. (2004):**
Evidence for Glucocorticoid Receptor Transport on Microtubules by Dynein.
J.Biol. Chem., 279(52):54647–54654.

[84] Harrison, T.; Graham, F.; Williams, J. (1977):
Host-range mutants of adenovirus type 5 defective for growth in HeLa cells.
Virology, 77(1):319-329.

[85] Haskill, S.; Beg, A.A.; Tompkins, S.M.; Morris, J.S.; Yurochko, A.D.; Sampson-Johannes, A.; Mondal, K.; Ralph, P.; Baldwin, A.S. Jr. (1991):
Characterization of an immediate-early gene induced in adherent monocytes that encodes IkB-like activity.
Cell, 65:1281-1289.

[86] Hayakawa, M.; Miyashita, H.; Sakamoto, I.; Kitagawa, M.; Tanaka, H.; Yasuda, H.; Karin, M.; Kikugawa, K. (2003):
Evidence that reactive oxygen species do not mediate NF-kappaB activation.
EMBO J., 22:3356–3366.

[87] Hernandez, M.P.; Chadli, A.; Toft, D.O. (2002):
Hsp40 binding is the first step in the hsp90 chaperoning pathway for the progesterone receptor.
J. Biol. Chem., 277:11873–11881.

[88] Heusch, M.; Lin, L.; , Geleziunas, R.; Greene, W.C. (1999):
The generation of NF- κB 2 p52: mechanism and efficiency.
Oncogene,18: 6201-6208

[89] Heyninck, K.; Beyaert, R. (2005):
A20 inhibits NF-kappaB activation by dual ubiquitin-editing functions.
Trends Biochem. Sci., 30:1–4.

[90] Hirst, J.; Bright, N.A.; Rous, B.; Robinson, M.S. (1999):
Characterization of a fourth adaptor-related protein complex.
Mol. Biol. Cell, 10:2787-2802.

[91] Holleran, E.A.; Tokito, M.K.; Karki, S.; Holzbaur, E.L. (1996):
Centractin (ARP1) associates with spectrin revealing a potential mechanism to link dynactin to intracellular organelles.
J. Cell Biol., 135(6/2):1815-1829.

[92] Howe, C.L. (2005):
Modeling the signaling endosome hypothesis: why a drive to the nucleus is better than a (random) walk.
Theor. Biol. Med. Model., 2:43 et seqq.

[93] Hsu, H.; Shu, H.B.; Pan. M.G.; Goeddel, D.V. (1996):
TRADD-TRAF2 and TRADD-FADD interactions define two distinct TNF receptor 1 signal transduction pathways.
Cell, 84(2):299-308.

[94] Huang, J.; Brady, S.T.; Richards, B.W.; Stenoien, D.; Resau, J.H.; Copeland, N.G.; Jenkins, N.A. (1999):
Direct interaction of microtubule- and actin-based transport motors
Nature, 397:267-270.

[95] Huang, T.T.; Kudo, N.; Yoshida, M.; Miyamoto, S. (2000):
A nuclear export signal in the N-terminal regulatory domain of IκBα controls cytoplasmic localization of inactive NF-κB/IκBα complexes.
PNAS, 97(3):1014-1019.

[96] Huxford, T.; Huang, D.; Malek, S.; Ghosh, G. (1998):
The Crystal Structure of the IκBα/NF-κB Complex Reveals Mechanisms of NF-κB Inactivation.
Cell, 95(6):759-770.

[97] Ikegame, K.; Yamamoto, M.; Kishima, Y.; Enomoto, H.; Yoshida, K.; Suemura, M.; Kishimoto, T.; Nakamura, H. (1999):
A New Member of a Hepatoma-Derived Growth Factor Gene Family Can Translocate to the Nucleus.
Biochemical and Biophysical Research Communications, 266:81–87.

[98] Imamoto, N.; Matsuoka, Y.; Kurihara, T.; Kohno, K.; Miyagi, M.; Sakiyama, F.; Okada, Y.; Tsunasawa, S.; Yoneda, Y. (1992):
Antibodies against 70-kD heat shock cognate protein inhibit mediated nuclear import of karyophilic proteins.
J. Cell Biol., 119(5):1047-1061.

[99] Inoue, J.; Kerr, L.; Kakizuka, A.; Verma, I. (1992):
IkBγ, a 70 kd protein identical to the C-terminal half of p110 NF-kB: a new member of the IkB family.
Cell, 68:1109-1120.

[100] Invitrogen (2010):
Growth and Maintenance of the 293FT Cell Line.
http://tools.invitrogen.com/content/sfs/manuals/293ft_cells_man.pdf

[101] J.N. Wood (1995):
Regulation of NF-kappa B activity in rat dorsal root ganglia and PC12 cells by tumour necrosis factor and nerve growth factor.
Neurosci. Lett., 192:41–44.

[102] Jacobs, M.D.; Harrison, S.C. (1998):
Structure of an IkappaBalpha/NF-kappaB complex.
Cell, 95:749–758.

[103] Jiang, R.; Gao, B.; Prasadi, K.; Greene, L.E.; Eisenberg, E. (2000):
Hsc70 Chaperones Clathrin and Primes It to Interact with Vesicle Membranes.
J. Biol. Chem., 275(12):8439–8447.

[104] Jiang, Y.; Woronicz, J.D.; Liu, W.; Goeddel, D.V. (1999):
Prevention of Constitutive TNF Receptor 1 Signaling by Silencer of Death Domains.
Science, 283(5401):543-546.

[105] Joab, I.; Radanyi, C.; Renoir, M.; Buchou, T.; Catelli, M.G.; Binart, N.; Mester, J.; Baulieu, E.E. (1984):
Common nonhormone binding component in nontransformed chick oviduct receptors of four steroid hormones.
Nature, 308:850–853.

[106] Johnson, B.D.; Schumacher, R.J.; Ross, E.D.; Toft, D.O. (1998):
Hop modulates hsp70/hsp90 interactions in protein folding.
J. Biol. Chem., 273:3679–3686.

[107] Johnson, C.; Van Antwerp, D.; Hope, T.J. (1999):
An N-terminal nuclear export signal is required for the nucleocytoplasmic shuttling of IκBα.
EMBO J., **18:**6682-6693.

[108] Johnson, J.L.; Toft, D.O. (1994):
A novel chaperone complex for steroid receptors involving heat shock proteins, immunophilins, and p23.
J. Biol. Chem., 269:24989–24993.

[109] Kaltschmidt, B.; Uherek, M.; Volk, B.; Baeuerle, P.A.; Kaltschmidt, C.; (1997):
Transcription factor NF-κB is activated in primary neurons by amyloid β peptides and in neurons surrounding early plaques from patients with Alzheimer disease.
Proc. Natl. Acad. Sci. U. S. A. 94:2642– 2647.

[110] Kaltschmidt, B.; Uherek, M.; Wellmann, H.; Volk, B.; Kaltschmidt, C. (1999):
Inhibition of NF-kappaB potentiates amyloid beta-mediated neuronal apoptosis.
Proc. Natl. Acad. Sci. U. S. A.. 96:9409–9414.

[111] Kaltschmidt, B.; Widera, D.; Kaltschmidt, C. (2005):
Signaling via NF-κB in the nervous system.
Biochimica et Biophysica Acta, 1745:287–299.

[112] Kaltschmidt, C.; Kaltschmidt, B.; Baeuerle, P.A. (1993):
Brain synapses contain inducible forms of the transcription factor NF-κB.
Mech. Dev., 43:135–147.

[113] Kaltschmidt, C.; Kaltschmidt, B.; Baeuerle, P.A. (1995):
Stimulation of ionotropic glutamate receptors activates transcription factor NF-κB in primary neurons.
Proc. Natl. Acad. Sci. U. S. A. 92:9618–9622.

[114] Kaltschmidt, C.; Kaltschmidt, B.; Henkel, T.; Stockinger, H.; Baeuerle, P.A. (1995):
Selective recognition of the activated form of transcription factor NF-kappa B by a monoclonal antibody.
Biol. Chem. Hoppe Seyler 376:9–16.

[115] Kaltschmidt, C.; Kaltschmidt, B.; Neumann, H., Wekerle, H.; Baeuerle, P.A. (1994):
Constitutive NF-κB activity in neurons.
Mol. Cell. Biol. 14:3981–3992.

[116] Kanalakis, K.C.; Shewach, D.S.; Pratt, W.B. (2002):
Nucleotide binding states of hsp70 and hsp90 during sequential steps in the process of glucocor-ticoid receptor-hsp90 heterocomplex assembly.
J. Biol. Chem., 277:33698–33703.

[117] Kanayama, A.; Seth, R.B.; Sun, L.; Ea, C.K.; Hong, M.; Shaito, A.; Chiu, Y.H.; Deng, L.; Chen, Z.J. (2004):
TAB2 and TAB3 activate the NF-kappaB pathway through binding to polyubiquitin chains.
Mol Cell., 15(4):535-548.

[118] Kang, S.M.; Tran, A.C.; Grilli, M.; Lenardo, M.J. (1992):
NF-kB subunit regulation in nontransformed CD4+ T lymphocytes.
Science, 256:1452-1456.

[119] Karki, S.; Holzbaur, E.L., (1999):
Cytoplasmic dynein and dynactin in cell division and intracellular transport.
Curr. Opin. Cell Biol., 11:45–53.

[120] Kawai, T.; Akira, S. (2007):
Signaling to NF-kappaB by Toll-like receptors.
Trends Mol. Med., 13(11):460-469.

[121] Kawano, Y.; Yoshimura, T.; Tsuboi, D.; Kawabata, S.; Kaneko-Kawano, T.; Shirataki. H.; Takenawa, T.; Kaibuchi, K. (2005):
CRMP-2 is involved in Kinesin-1-dependent transport of the Sra-1/WAVE1 complex and axon formation.
Mol. Cell. Biol., 25:9920–9935.

[122] Kimura, T.; Arimura, N.; Fukata, Y.; Watanabe, H.; Iwamatsu, A.; Kaibuchi, K. (2005):
Tubulin and CRMP-2 complex is transported via Kinesin-1.
J. Neurochem., 93:1371–1382.

[123] Kodiha, M.; Chu, A.; Lazrak, O.; Stochaj, U. (2005):
Stress inhibits nucleocytoplasmic shuttling of heat shock protein hsc70.
Am. J. Physiol. Cell Physiol., 289:C1034-C1041.

[124] Koerner, M.; Rattner, A.; Mauxion, F.; Sen, R.; Citri, Y. (1989):
A brain-specific transcription activator.
Neuron 3:563–572.

[125] Kolesnick, R.; Golde, D.W. (1994):
The sphingomyelin pathway in tumor necrosis factor and interleukin-1 signaling.
Cell, 77:325–328.

[126] Kose, S.; Furuta, M.; Koike, M.; Yoneda, Y.; Imamoto, N. (2005):
The 70-kD heat shock cognate protein (hsc70) facilitates the nuclear export of the import receptors.
J. Cell Biology, 171(1):19–25.

[127] Kovalenko, A.; Chable-Bessia, C.; Cantarella, G.; Israel, A.; Wallach, D.; Courtois, G. (2003):
The tumour suppressor CYLD negatively regulates NF-kappaB signalling by deubiquitination.
Nature, 424:801–805.

[128] L. Graham, J. Smiley (1977):
Characteristics of a Human Cell Line Transformed by DNA from Human Adenovirus Type 5.
Journal of general virologyl 36:59-72.

[129] Lamian, V.; Small, G.M.; Feldherr, C.M. (1996):
Evidence for the Existence of a Novel Mechanism for the Nuclear Import of Hsc70.
Experimental Cell Research, 228(1):84-91.

[130] Langford, G.M. (2002):
Myosin-V, a versatile motor for short range vesicle transport.
Traffic, 3:859–865.

[131] Lassle, M.; Blatch, G.L.; Kundra, V.; Takatori, T.; Zetter, B.R. (1997):
Stressinducible, murine protein mSTI1. Characterization of binding domains for heat shock proteins and in vitro phosphorylation by different kinases.
J. Biol. Chem., 272:1876–1884.

[132] Lee, S.H.; Hannink, M. (2002):
Characterization of the nuclear import and export functions of Ikappa B(epsilon).
J. Biol. Chem., 277(26):23358-23366.

[133] Lee, S.J.; Zhou, T.; Choi, C.; Wang, Z.; Benveniste, E.N. (2000):
Differential regulation and function of Fas expression on glial cells.
J. Immunol., 164:1277–1285.

[134] Leung, S.W.; Harreman, M.T., Hodel, M.R.; Hodel, A.E.; Corbett, A.H. (2003):
Dissection of the karyopherin alpha nuclear localization signal (NLS)-binding groove–functional requirements for NLS binding.
J. Biol. Chem., 278:41947–41953.

[135] Lilienbaum, A.; Israel, A. (2003):
From calcium to NF-kappa B signaling pathways in neurons.
Mol. Cell. Biol., 23:2680– 2698.

[136] Lin, X.; Mu, Y.; Cunningham, E.T. Jr.; Marcu, K.B.; Geleziunas, R.; Greene, W.C. (1998):
Molecular determinants of NF-kappaB-inducing kinase action.
Mol Cell Biol. 18(10):5899-5907.

[137] Ling, L.; Cao, Z.; Goeddel, D.V. (1998):
NF-kappaB-inducing kinase activates IKK-alpha by phosphorylation of Ser-176.
Proc. Natl. Acad. Sci. U S A, 95(7):3792-3797.

[138] Lunda, V.K.; DeLottoa, Y.; DeLottoa, R. (2010):
Endocytosis is required for Toll signaling and shaping of the Dorsal/NF-κB morphogen gradient during Drosophila embryogenesis.
PNAS, 107(42):18028–18033.

[139] Malek, S.; Chen, Y.; Huxford, T.; Ghosh, G. (2001):
IκB-β, but Not IκB-α, Functions as a Classical Cytoplasmic Inhibitor of NF-κB Dimers by Masking Both NF-κB Nuclear Localization Sequences in Resting Cells.
J. Bio. Chem., 276(48):45225–45235.

[140] Malek, S.; Huxford, T.; Ghosh, G. (1998):
Ikappa Balpha functions through direct contacts with the nuclear localization signals and the DNA binding sequences of NF-kappaB.
J. Biol. Chem., 273:25427–25435.

[141] Mallik, R.; Carter, B.C.; Lex, S.A.; King, S.J.; Gross, S.P. (2004):
Cytoplasmic dynein functions as a gear in response to load.
Nature, 427(6975):649-652.

[142] Marchetti, L.; Klein, M.; Schlett, K.; Pfizenmaier, K.; Eisel, U.L. (2004):
Tumor necrosis factor (TNF)-mediated neuroprotection against glutamateinduced excitotoxicity is enhanced by N-methyl-d-aspartate receptor activation. Essential role of a TNF receptor 2-mediated phosphatidylinositol 3-kinase-dependent NF-kappa B pathway.
J. Biol. Chem., 279:32869–32881.

[143] Martin, M.; Iyadurai, S.J.; Gassman, A.; Gindhart, J.G.; Hays Jr., T.S.; Saxton, W.M. (1999):
Cytoplasmic dynein, the dynactincomplex, and kinesin are interdependent and essential for fast axonal transport.
Mol. Biol. Cell, 10:3717–3728.

[144] McGrath, J.L. (2005):
Dynein motility: four heads are better than two.
Curr. Biol., 15(23):R970-R972.

[145] Meberg, P.J.; Kinney, W.R.; Valcourt, E.G.; Routtenberg, A. (1996):
Gene expression of the transcription factor NF-κB in hippocampus: regulation by synaptic activity.
Mol. Brain Res., 38:179–190.

[146] Meffert, M.K.; Chang, J.M.; Wiltgen, B.J.; Fanselow, M.S.; Baltimore, D. (2003):
NF-kappaB functions in synaptic signaling and behavior.
Nat. Neurosci., 6(10):1072–1078.

[147] Meissner, P.; Pick, P.; Kulangara, A.; Chatellard, P.; Friedrich, K.; Wurm, F.M. (2001):
Transient Gene Expression: Recombinant Protein Production with Suspension-Adapted HEK293-EBNA Cells.
Biotechnology and Bioengineering, 75(2):197-203.

[148] Melkonian, K.A.; Maier, K.C.; Godfrey, J.E. Rodgers, M.; Schroer, T.A. (2007):
Mechanism of Dynamitin-mediated Disruption of Dynactin
J. Biol. Chem., 282(27):19355–19364.

[149] Menoret, A.; Chaillot, D.; Callahan, M.; Jacquin, C. (2002):
Hsp70, an immunological actor playing with the intracellular self under oxidative stress.
International Journal of Hyperthermia 18: 490–505.

[150] Mercurio, F.; DiDonato, J.A.; Rosette, C.; Karin, M. (1993):
p105 and p98 precursor proteins play an active role in NF-kB-mediated signal transduction.
Genes Dev., 7:705-718

[151] Micheau, O.; Tschopp, J. (2003):
Induction of TNF receptor I-mediated apoptosis via two sequential signaling complexes.
Cell, 114:181–190.

[152] Middleton, G.; Hamanoue, M.; Enokido, Y.; Wyatt, S.; Pennica, D.; Jaffray, E.; Hay, R.T.; Davies, A.M. (2000):
Cytokine-induced nuclear factor kappa B activation promotes the survival of developing neurons.
J. Cell Biol., 148:325–332.

[153] Mikenberg, I.; Widera, D.; Kaus, A.; Kaltschmidt, B.; Kaltschmidt, C. (2007):
Transcription Factor NF-kB Is Transported to the Nucleus via Cytoplasmic Dynein/Dynactin Motor Complex in Hippocampal Neurons.
PLoS ONE, 2(7):e589. doi:10.1371/journal.pone.0000589.

[154] Mikenberg, I.; Widera, D.; Kaus, A.; Kaltschmidt, B.; Kaltschmidt, C.(2006):
TNF-a mediated transport of NF-κB to the nucleus is independent of the cytoskeleton-based transport system in non-neuronal cells
European Journal of Cell Biology, 85:529–536.

[155] Minami, Y.; Sakai, H. (1985):
Dephosphorylation suppresses the activity of neurofilament to promote tubulin polymerization.
FEBS Lett., 185(2):239-242.

[156] Miyata, Y.; Yahara, I. (2000):
p53-Independent association between SV40 large T antigen and the major cytosolic heat shock protein, HSP90.
Oncogene, 19:1477–1484, 2000.

[157] Moerman, A.M.; Mao, X.; Lucas, M.M.; Barger, S.W. (1999):
Characterization of a neuronal kappaB-binding factor distinct from NF-kappaB.
Brain Res. Mol. Brain Res. 67:303– 315.

[158] Moorthy, A.K.; Savinova, O.V.; Ho, J.Q.; Wang, V.Y.; Vu, D.; Ghosh, G. (2006):
The 20S proteasome processes NF-κB1 p105 into p50 in a translation-independent manner
The EMBO Journal, 25:1945–1956

[159] Morishima, Y.; Kanelakis, K.C.; Murphy, P.J.M.; Schewach, D.S.; Pratt, W.B. (2001):
Evidence for iterative ratcheting of receptor-bound hsp70 between its ATP and ADP conformations during assembly of glucocorticoid receptor/hsp90 heterocomplexes.
Biochemistry, 40:1109–1116.

[160] Mosialos, G.; Hamer, P.; Capobianco, A.J.; Laursen, R.A.; Gilmore, T.D. (1992):
A protein kinase A recognition sequence is structurally linked to transformation by p59v-rel and cytoplasmic retention of p68c-rel.
Mol. Cell. Biol., 11:5867-5877.

[161] Muresan, V.; Stankewich, M.C; Steffen, W.; Morrow, J.S.; Holzbaur, E.L.F.; Schnapp, B.J. (2001):
Dynactin-Dependent, Dynein-Driven Vesicle Transport in the Absence of Membrane Proteins: A Role for Spectrin and Acidic Phospholipids.
Molecular Cell, 7:173–183.

[162] Nadler, S.G.; Eversole, A.C.; Tepper, M.A.; Cleaveland, J.S. (1995):
Elucidating the mechanism of action of the immunosuppressant 15-deoxyspergualin.
Ther. Drug. Monit., 17(6):700-703.

[163] Nakajima, K.; Kikuchi, Y.; Ikoma, E.; Honda, S.; Ishikawa, M.; Liu, Y.; Kohsaka, S. (1998):
Neurotrophins regulate the function of cultured microglia.
Glia 24:272–289.

[164] Naldini, L.; Blomer, U.; Gage, F. H.; Trono, D.; Verma, I. M. (1996):
Efficient Transfer, Integration, and Sustained Long-Term Expression of the Transgene in Adult Rat Brains Injected with a Lentiviral Vector.
Proc. Natl. Acad. Sci., USA 93:11382-11388.

[165] Nathan, D.F.; Lindquist, S. (1995):
Mutational analysis of hsp90 function: interactions with a steroid receptor and a protein kinase.
Mol. Cell. Biol., 15:3917–3925.

[166] ONeill, L.A.J.; Kaltschmidt, C. (1997):
NF-κB: a crucial transcription factor for glial and neuronal cell function.
Trends Neurosci., 20:252–258.

[167] Pearse, B.M.; Robinson, M.S. (1984):
Purification and properties of 100-kd proteins from coated vesicles and their reconstitution with clathrin.
EMBO J., 3:1951-1957.

[168] Picard, D.; Khursheed, B.; Garabedian, M.J.; Fortin, M.G.; Lindquist, S.; Yamamoto, K.R. (1990):
Reduced levels of hsp90 compromise steroid receptor action in vivo.
Nature, 348:166–168.

[169] Pistritto, G., Franzese, O.; Pozzoli, G.; Mancuso, C.; Tringali, G.; Preziosi, P.; Navarra, P. (1999):
Bacterial lipopolysaccharide increases prostaglandin production by rat astrocytes via inducible cyclo-oxygenase: evidence for the involvement of nuclear factor kappaB.
Biochem. Biophys. Res. Commun., 263:570–574.

[170] Pousset, F.; Dantzer, R.; Kelley, K.W.; Parnet, P. (2000):
Interleukin-1 signaling in mouse astrocytes involves Akt: a study with interleukin-4 and IL-10.
Eur. Cytokine Netw., 11:427–434.

[171] Prasad. K.; Lippoldt, R.E. (1988):
Molecular characterization of the AP180 coated vesicle assembly protein.
Biochemistry, 27(16):6098–6104.

[172] Pratt, W.B.; Toft, D.O. (2003):
Regulation of Signaling Protein Function and Trafficking by the hsp90/hsp70-Based Chaperone Machinery.
Exp. Biol. Med., 228(2):111-133.

[173] Pratt. W.B.; Galignianaa, M.D.; Harrella, J.M.; DeFranco, D.B. (2004):
Role of hsp90 and the hsp90-binding immunophilins
in signalling protein movement.
Cellular Signalling 16:857–872

[174] Rappoport, J.Z.; Taha, B.W.; Simon, S.M. (2003):
Movement of plasma-membrane-associated clathrin spots along the microtubule cytoskeleton.
Traffic, 4(7):460-467.

[175] Rattner, A.; Korner, M.; Walker, M.D.; Citri, Y. (1993):
NF-kappa B activates the HIV promoter in neurons.
EMBO J., 12:4261–4267.

[176] Ray, A.; Prefontaine, K.E. (1994):
Physical association and functional antagonism between the p65 subunit of transcription factor NF-κB and the glucocorticoid receptor
Proc. Natl. Acad. Sci. USA, 91:752-756.

[177] Ray, P.; Zhang, D.H.; Elias, J.A.; Ray, A. (1995):
Cloning of a differentially expressed IkB-related protein.
J. Biol. Chem., 270:10680-10685.

[178] Régnier, C.H.; Song, H.Y.; Gao, X.; Goeddel, D.V.; Cao, Z.; Rothe, M. (1997):
Identification and characterization of an IkappaB kinase.
Cell., 90(2):373-383.

[179] Rice, N.R.; MacKichan, M.L.; Israël, A. (1992):
The precursor of NF-kB p50 has IkB-like functions.
Cell, 71:243-253

[180] Robinson, M.S.; Bonifacino, J.S. (2001):
Adaptor-related proteins.
Curr. Opin. Cell Biol., 13:444-453.

[181] Rogemond, V.; Auger, C.; Giraudon, P.; Becchi, M.; Auvergnon, N.; Belin, M.; Honnorat, J.; Moradi-Amé, M. (2008):
Processing and Nuclear Localization of CRMP2 during Brain Development Induce Neurite Outgrowth Inhibition.
J. Biol. Chem., 283(21):14751–14761.

[182] Routtenberg, A. (2000):
It's about time.
in: Gold, P.E.; Greenough, W.T. (eds.)
Memory Consolidation, American Psychological Association, pp. 17–34.

[183] Ryseck, R-P.; Bull, P.; Takamiya, M.; Bours, V.; Siebenlist, U.; Dobrzanski, P.; Bravo, R. (1992):
RelB, a new Rel family transcription activator that can interact with p50-NF-kB.
Mol Cell Biol, 12:674-684.

[184] Saccani, S.; Marazzi, I.; Beg, A.A.; Natoli, G. (2004):
Degradation of promoter-bound p65/RelA is essential for the prompt termination of the nuclear factor kappaB response.
J. Exp. Med., 200.107– 113.

[185] Sachdev, S.; Hoffmann, A.; Hannink, M. (1998):
Nuclear Localization of IκBα Is Mediated by the Second Ankyrin Repeat: the IκBα Ankyrin Repeats Define a Novel Class of cis-Acting Nuclear Import Sequences.
Mol. Cell. Biol., 18(5):2524-2534.

[186] Sanchez, E.R.; Toft, D.O.; Schlesinger, M.J.; Pratt, W.B. (1985):
Evidence that the 90-kDa phosphoprotein associated with the untransformed L-cell glucocorticoid receptor is a murine heat-shock protein.
J. Biol. Chem., 260**:**12398–12401.

[187] Savinova, O.V.; Hoffmann, A.; Ghosh, G. (2009):
The NF-κB1 and NF-κB2 proteins p105 and p100 function as the core of high-molecular-weight heterogeneous complexes.
Mol Cell., 34(5):591-602.

[188] Schmid, E.M.; McMahon, H.T. (2007):
Integrating molecular and network biology to decode endocytosis.
Nature, 448:883-888.

[189] Schmitz, M.L.; Baeuerle, P.A. (1991):
The p65 subunit is responsible for the strong transcription activating potential of NF-kB.
EMBO J., 10:3805-3817.

[190] Schmitz, M.L.; Mattioli, I.; Buss, H.; Kracht, M. (2004):
NF-kappaB: a multifaceted transcription factor regulated at several levels.
Chem-BioChem., 5:1348–1358.

[191] Schmitz, M.L.; Stelzer, G.; Altmann, H.; Meisterernst, M.; Baeuerle, P.A. (1995):
Interaction of the COOH-terminal transactivation domain of p65 NF-kB with TATA-binding protein, transcription factor IIB, and coactivators.
J. Biol. Chem., 270:7219-7226

[192] Schmitz, M.L; dos Santos Silva, M.A.; Altmann, H.; Czisch, M.; Holak, T.A.; Baeuerle, P.A. (1994):
Structural and functional analysis of the NF-kB p65 C terminus. An acidic and modular transactivation domain with the potential to adopt an alphahelical conformation.
J. Biol. Chem., 269:25613-25620.

[193] Schuh, S.; Yonemoto, W.; Brugge, J.; Bauer, V.J.; Riehl, R.M.; Sullivan, W.P.; Toft, D.O. (1985):
A 90,000-dalton binding protein common to both steroid receptors and the Rous sarcoma virus transforming protein, pp60v-src.
J. Biol. Chem., 260:14292–14296.

[194] Sen, R.; Baltimore, D. (1986):
Multiple Nuclear Factors Interact with the lmmunoglobulin Enhancer Sequences.
Cell, Vol. 46, (70):5716 et seqq.

[195] Senftleben, U.; Cao, Y.; Xiao, G.; Greten, F.R.; Krähn, G.; Bonizzi, G.; Chen, Y.; Hu, Y.; Fong, A.; Sun, S.C.; Karin, M. (2001):
Activation by IKKalpha of a second, evolutionary conserved, NF-kappa B signaling pathway.
Science, 293(5534):1495-1499.

[196] Sever, S. (2002):
Dynamin and endocytosis.
Curr. Opin. Cell Biol., 14:463–467

[197] Shrum, C.K.; Defrancisco, D.; Meffert, M.K. (2009):
Stimulated nuclear translocation of NF-kappaB and shuttling differentially depend on dynein and the dynactin complex.
PNAS USA 106(8):2647-2652.

[198] Sondermann, H.; Scheufler, C.; Schneider, C.; Hohfeld, J.; Hartl, F.U.; Moarefi, I. (2001):
Structure of a Bag/Hsc70 complex: convergent functional evolution of Hsp70 nucleotide exchange factors.
Science, 291(5508):1553-1557.

[199] Sparacio, S.M.; Zhang, Y.; Vilcek, J.; Benveniste, E.N.(1992):
Cytokine regulation of interleukin-6 gene expression in astrocytes involves activation of an NF-kappa B-like nuclear protein.
J. Neuroimmunol., 39:231–242.

[200] Steward, O.; Reeves, T.M. (1988):
Protein-synthetic machinery beneath postsynaptic sites on CNS neurons: association between polyribosomes and other organelles at the synaptic site.
Journal of Neuroscience, 8:176-184.

[201] Stratagene (2005):
BL21-CodonPlus® Competent Cells INSTRUCTION MANUAL.
http://www.med.unc.edu/csb/PEP/manuals/codon_plus_manual.pdf

[202] Sullivan, W.;, Stensgard, B.; Caucutt, G.; Bartha, B.; McMahon, N.; Alnemri, E.S.; Litwack, G.; Toft, D. (1997):
Nucleotides and two functional states of hsp90.
J. Biol. Chem., 272:8007–8012.

[203] Sweitzer, S.M.; Hinshaw, J.E. (1998):
Dynamin undergoes a GTP-dependent confor-mational change causing vesiculation.
Cell, 93:1021–1029.

[204] Tada, K.; Okazaki, T.; Sakon, S.; Kobarai, T.; Kurosawa, K.; Yamaoka, S.; Hashimoto, H.; Mak, T.W.; Yagita, H.; Okumura, K.; Yeh, W.C.; Nakano, H. (2001):
Critical roles of TRAF2 and TRAF5 in tumor necrosis factor-induced NF-kappa B activation and protection from cell death.
J. Biol. Chem., 276(39):36530-36534.

[205] Takei, K.; McPherson, P.S.; Schmid, S.L.; De Camilli, P. (1995):
Tubular membrane invaginations coated by dynamin rings are induced by GTP-γS in nerve terminals.
Nature, 374:186–190.

[206] Tam, W.F.; Lee, L.H.; Davis, L.; Sen, R. (2000):
Cytoplasmic Sequestration of Rel Proteins by IκBα Requires CRM1-Dependent Nuclear Export.
Mol. Cell. Bio. 20(6):2269-2284.

[207] Ting, A.T.; Pimentel-Muiños, F.X.; Seed, B. (1996):
RIP mediates tumor necrosis factor receptor 1 activation of NF-kappaB but not Fas/APO-1-initiated apoptosis.
EMBO J., 15(22):6189-6196.

[208] Trompouki, E.; Hatzivassiliou, E.; Tsichritzis, T.; Farmer, H.; Ashworth, A.; Mosialos, G. (2003):
CYLD is a deubiquitinating enzyme that negatively regulates NF-kappaB activation by TNFR family members.
Nature, 424:793–796.

[209] Tsuboi, D.; Hikita, T.; Qadota, H.; Amano, M.; Kaibuchi, K. (2005):
Regulatory machinery of UNC-33 Ce-CRMP localization in neurites during neuronal development in Caenorhabditis elegans.
J. Neurochem., 95:1629–1641.

[210] Tsukahara, F.; Maru, Y. (2004):
Identification of Novel Nuclear Export and Nuclear Localization related Signals in Human Heat Shock Cognate Protein 70.
J. Biol. Chem., 279(10):8867–8872.

[211] Uhlik, M.; Good, L.; Xiao, G.; Harhaj, E.W.; Zandi, E.; Karin, M.; Sun, S.C. (1998):
NFkappaB-inducing kinase and IkappaB kinase participate in human T-cell leukemia virus I Tax-mediated NF-kappaB activation.
J. Biol. Chem., 273(33):21132-21136.

[212] Watt, R.; Stanton, L.W.; Marcu, K.B.; Gallo, R.C.; Croce, C.M.; Rovera, G. (1983):
Nucleotide sequence of cloned cDNA of human c-myc oncogene.
Nature, 303(5919):725-728.

[213] Wellmann, H.; Kaltschmidt, B.; Kaltschmidt, C. (2001):
Retrograde transport of transcription factor NF-κB in living neurons.
J. Biol. Chem., 276:11821–11829.

[214] Whitesell, L.; Cook, P. (1996):
Stable and specific binding of heat shock protein 90 by geldanamycin disrupts glucocorticoid receptor function in intact cells.
Mol. Endo., 10:705–712, 1996.

[215] Whiteside, S.T.; Israël, A. (1997):
I kappa B proteins: structure, function and regulation.
Semin. Cancer Biol., 8(2):75-82.

[216] www.**ncbi**.nlm.nih.gov:
Protein sequence of human heat shock cognate 71 kDa or Heat shock 70 kDa protein 8 (Accession number: P11142).
last update: Oct. 5, 2010.

[217] www.**ncbi**.nlm.nih.gov:
Homo sapiens v-myc myelocytomatosis viral oncogene homolog (avian) (MYC), mRNA (Accession number: NM_002467).
last update: Dec. 5, 2010.

[218] Xiao, G.; Fong, A.; Sun, S.C. (2004):
Induction of p100 processing by NF-kappaBinducing kinase involves docking IkappaB kinase alpha (IKKalpha) to p100 and IKKalpha-mediated phosphorylation.
J. Biol. Chem., 279(29):30099-30105.

[219] Yamamoto, M.; Sato, S.; Hemmi, H.; Hoshino, K.; Kaisho, T.; Sanjo, H.; Takeuchi, O.; Sugiyama, M.; Okabe, M.; Takeda, K.; Akira, S. (2003):
Role of adaptor TRIF in the MyD88-independent toll-like receptor signaling pathway.
Science, 301(5633):640-643.

[220] Yamazaki, S.; Muta, T.; Takeshige, K. (2001):
A novel IkappaB protein, IkappaB-zeta, induced by proinflammatory stimuli, negatively regulates nuclear factor-kappaB in the nuclei.
J. Biol. Chem., 276(29):27657-62.

[221] Yang, L.; Lindholm, K.; Konishi, Y.; Li, R.; Shen, Y. (2002):
Target depletion of distinct tumor necrosis factor receptor subtypes reveals hippocampal neuron death and survival through different signal transduction pathways.
J. Neurosci., 22:3025–3032.

[222] Yaron, A.; Hatzubai, A.; Davis, M.; Lavon, I.; Amit, S.; Manning, A.M.; Andersen, J.S.; Mann, M.; Mercurio, F.; Ben-Neriah, Y. (1998):
Identification of the receptor component of the IkappaBalpha-ubiquitin ligase.
Nature, 396:590–594.

[223] Yoon, S.O.; Casaccia-Bonnefil, P.; Carter, B.; Chao, M.V. (1998):
Competitive signaling between TrkA and p75 nerve growth factor receptors determines cell survival.
J. Neurosci. 18:3273–3281.

[224] Zabel,U.; Baeuerle, P.A. (1990):
Purified human IkB can rapidly dissociate the complex of the NF-kB transcription factor with its cognate DNA.
Cell, 61:255-265.

[225] Zelenaia, O.; Schlag, B.D.; Gochenauer, G.E.; Ganel, R.; Song, W.; Beesley, J.S.; Grinspan, J.B.; Rothstein, J.D.; Robinson, M.B. (2000):
Epidermal growth factor receptor agonists increase expression of glutamate transporter GLT-1 in astrocytes through pathways dependent on phosphatidylinositol 3-kinase and transcription factor NF-kappaB.
Mol. Pharmacol., 57:667–678.

[226] Zhong, H.; Voll, R.E.; Ghosh, S. (1998):
Phosphorylation of NF-kappa B p65 by PKA stimulates transcriptional activity by promoting a novel bivalent interaction with the coactivator CBP/p300.
Mol Cell., 5:661-671.

9 Appendix

9.1 List of figures

9.2 Index of tables

9.3 GST-p65/RelA sequence coverage in MS

```
coverage after mass spectrometry of GST-p65/RelA Sequence

001 mspilgywki kglvqptrll leyleekyee hlyerdegdk wrnkkfelgl efpnlpyyid
MS1
MS2
MS3
MS4
MS5
MS6
MS7
MS8

061 gdvkltqsma iiryiadkhn mlggcpkera eismlegavl dirygvsria yskdfetlkv
MS1
MS2
MS3
MS4
MS5
MS6
MS7
MS8

121 dflsklpeml kmfedrlchk tylngdhvth pdfmlydald vvlymdpmcl dafpklvcfk
MS1
MS2
MS3
MS4
MS5
MS6
MS7
MS8

181 krieaipqid kylksskyia wplqgwqatf gggdhppksd liegrgipde lfplifpaep
MS1
MS2
MS3
MS4
MS5
MS6
MS7
MS8                                                End of Data

241 aqasgpyvei ieqpkqRgmr frykcegrsa gsipgeRstd ttkthptiki ngytgpgtvr
MS1
MS2
MS3
MS4
MS5
MS6                                                End of Data
MS7                 End of Data

301 islvtkdpph Rphphelvgk dcRdgfyeae lcpdrcihsf qnlgiqcvkk Rdleqaisqr
MS1
MS2
MS3
MS4
MS5 End of Data
```

```
361 iqtnnnpfqv pIeeqrgdyd lnavRlcfqv tvRdpsgRpl rlppvlshpi fdnrapntae
MS1 ◀──────────────▶◀────────▶          ◀───────▶◀────────────▶
MS2 ◀──────────────▶◀────────▶          ◀───────▶◀────────────▶
MS3 ◀──────────────▶◀────────▶          ◀───────▶◀────────────▶
MS4 ◀──────────────▶                            ◀────────────▶

421 lkicrvnrns gsclggdeif Llcdkvqked ievyftgpgw eargsfsqad vhrqvaivfR
MS1                                             ◀─────────▶◀──────▶
MS2      ◀──────────▶◀──────────────────▶◀──────────▶◀──────────▶◀──────▶
MS3 End of Data
MS4 End of Data

481 tppyadpslq apvrvsmqlR RpsdRelsep mefqylpdtd drhRieekrk Rtyetfksim
MS1 ◀──────────────▶            ◀──────────────────▶  End of Data
MS2 ◀──────────────▶            ◀──────────────────▶  End of Data

541 kkspfsgptd pRopprriav psrssasvpk papqpypfts slstinydef ptmvfpsgqi

601 sqasalapap pqvlpqapap apapamvsal aqapapvpvL apgppqavap papkptqage

661 gtlseallql qfddedlgal lgnstdpavf tdlasvdnse fqqllnqgIp vaphttepml

721 meypeaItrL vtgaqRopdp apaplgapgl pngllsgded fssiadmdfs allsqiss
```

Description:

The measurements of the eight gel spots (see Figure 4.6) are named MS 1-8. The GST sequence is marked by a grey background. Aminoacids encoded by rare triplets (less than 1% of all codons for this AA) in E. coli are written white on black in bold capital letters. Smaller peptide fragments are marked with narrow bars. Longer, not completely digested fragments are marked with grey background. Very intense fragment signals are indicated by grey or black bars.

9.4 Sequence comparison of selected proteins between sus scrofa and homo sapiens

9.4.1 RelA/p65

Full name of human protein: v-rel reticuloendotheliosis viral oncogene homolog A (avian) (RELA), long transcript variant

Identities = 515/553 (94%), Positives = 526/553 (96%), Gaps = 2/553 (0%)

```
homo s.   1 MDELFPLIFPAEPAQASGPYVEIIEQPKQRGMRFRYKCEGRSAGSIPGERSTDTTKTHPT  60
            MD+LFPLIFP+EPA ASGPYVEIIEQPKQRGMRFRYKCEGRSAGSIPGERSTDTTKTHPT
sus s.    1 MDDLFPLIFPSEPAPASGPYVEIIEQPKQRGMRFRYKCEGRSAGSIPGERSTDTTKTHPT  60

homo s.  61 IKINGYTGPGTVRISLVTKDPPHRPHPHELVGKDCRDGFYEAELCPDRCIHSFQNLGIQC 120
            IKINGYTGPGTVRISLVTKDPPHRPHPHELVGKDCRDGFYEAELCPDRCIHSFQNLGIQC
sus s.   61 IKINGYTGPGTVRISLVTKDPPHRPHPHELVGKDCRDGFYEAELCPDRCIHSFQNLGIQC 120

homo s. 121 VKKRDLEQAISQRIQTNNNPFQVPIEEQRGDYDLNAVRLCFQVTVRDPSGRPLRLPPVLS 180
            VKKRDLEQAI+QRIQTNNNPFQVPIEEQRGDYDLNAVRLCFQVTVRDP+GRPLRLPPVLS
sus s.  121 VKKRDLEQAINQRIQTNNNPFQVPIEEQRGDYDLNAVRLCFQVTVRDPAGRPLRLPPVLS 180

homo s. 181 HPIFDNRAPNTAELKICRVNRNSGSCLGGDEIFLLCDKVQKEDIEVYFTGPGWEARGSFS 240
            HPIFDNRAPNTAELKICRVNRNSGSCLGGDEIFLLCDKVQKEDIEVYFTGPGWEARGSFS
sus s. 181  HPIFDNRAPNTAELKICRVNRNSGSCLGGDEIFLLCDKVQKEDIEVYFTGPGWEARGSFS 240

homo s. 241 QADVHRQVAIVFRTPPYADPSLQAPVRVSMQLRRPSDRELSEPMEFQYLPDTDDRHRIEE 300
            QADVHRQVAIVFRTPPYADPSLQAPVRVSMQLRRPSDRELSEPMEFQYLPDTDDRHRIEE
sus s.  241 QADVHRQVAIVFRTPPYADPSLQAPVRVSMQLRRPSDRELSEPMEFQYLPDTDDRHRIEE 300

homo s. 301 KRKRTYETFKSIMKKSPFSGPTDPRPPPRRIAVPSRSSASVPKPAPQPYPFTSSLSTINY 360
            KRKRTYETFKSIMKKSPF+GPTDPRP  RRIAVPSRSSASVPKPAPQPYPFT SLSTIN+
sus s.  301 KRKRTYETFKSIMKKSPFNGPTDPRPATRRIAVPSRSSASVPKPAPQPYPFTPSLSTINF 360

homo s. 361 DEFPTMVFPSGQI-SQASALAPAPPQVLPQAPAPAPAPAMVSALAQAPAPVPVLAPGPPQ 419
            DEF  M F SGQI  Q SALAPAP  VL QAPAPAPAPAM SALAQAPAPVPVLAPG  Q
sus s.  361 DEFTPMAFASGQIPGQTSALAPAPAPVLVQAPAPAPAPAMASALAQAPAPVPVLAPGLAQ 420

homo s. 420 AVAPPAPKPTQAGEGTLSEALLQLQFD-DEDLGALLGNSTDPAVFTDLASVDNSEFQQLL 478
            AVAPPAPK  QAGEGTL+EALLQLQFD DEDLGALLGN+TDP VFTDLASVDNSEFQQLL
sus s.  421 AVAPPAPKTNQAGEGTLTEALLQLQFDTDEDLGALLGNNTDPTVFTDLASVDNSEFQQLL 480

homo s. 479 NQGIPVAPHTTEPMLMEYPEAITRLVTGAQRPPDPAPAPLGAPGLPNGLLSGDEDFSSIA 538
            NQG+ + PHT EPMLMEYPEAITRLVTG+QRPPDPAP PLGA GL NGLLSGDEDFSSIA
sus s.  481 NQGVSMPPHTAEPMLMEYPEAITRLVTGSQRPPDPAPTPLGASGLTNGLLSGDEDFSSIA 540

homo s. 539 DMDFSALLSQISS  551
            DMDFSALLSQISS
sus s.  541 DMDFSALLSQISS  553
```

Legend:
NLS, + similar amino acid

9.4.2 HSP90AA1

Full name of human protein:
heat shock protein 90kDa alpha (cytosolic), class A member 1, short transcript

Identities = 722/733 (99%), Positives = 726/733 (99%), Gaps = 1/733 (0%)

```
homo s.   1 MPEETQTQDQPMEEEEVETFAFQAEIAQLMSLIINTFYSNKEIFLRELISNSSDALDKIR  60
            MPEETQTQDQPMEEEEVETFAFQAEIAQLMSLIINTFYSNKEIFLRELISNSSDALDKIR
sus s.    1 MPEETQTQDQPMEEEEVETFAFQAEIAQLMSLIINTFYSNKEIFLRELISNSSDALDKIR  60

homo s.  61 YESLTDPSKLDSGKELHINLIPNKQDRTLTIVDTGIGMTKADLINNLGTIAKSGTKAFME 120
            YESLTDPSKLDSGKELHINLIPNKQDRTLTIVDTGIGMTKADLINNLGTIAKSGTKAFME
sus s.   61 YESLTDPSKLDSGKELHINLIPNKQDRTLTIVDTGIGMTKADLINNLGTIAKSGTKAFME 120

homo s. 121 ALQAGADISMIGQFGVGFYSAYLVAEKVTVITKHNDDEQYAWESSAGGSFTVRTDTGEPM 180
            ALQAGADISMIGQFGVGFYSAYLVAEKVTVITKHNDDEQYAWESSAGGSFTVRTDTGEPM
sus s.  121 ALQAGADISMIGQFGVGFYSAYLVAEKVTVITKHNDDEQYAWESSAGGSFTVRTDTGEPM 180

homo s. 181 GRGTKVILHLKEDQTEYLEERRIKEIVKKHSQFIGYPITLFVEKERDKEVSDDEAEEKED 240
            GRGTKVILHLKEDQTEYLEERRIKEIVKKHSQFIGYPITLFVEKERDKEVSDDEAEEKED
sus s.  181 GRGTKVILHLKEDQTEYLEERRIKEIVKKHSQFIGYPITLFVEKERDKEVSDDEAEEKED 240

homo s. 241 KEEEKEKEEKESEDKPEIEDVGSDEEEEKKDGDKKKKKKIKEK-YIDQEELNKTKPIWTR 299
            KEEEKEKEEKESEDKPEIEDVGSDEEEE+K    KKKKK  ++ YIDQEELNKTKPIWTR
sus s.  241 KEEEKEKEEKESEDKPEIEDVGSDEEEEEKKDGDKKKKKKIKEKYIDQEELNKTKPIWTR 300

homo s. 300 NPDDITNEEYGEFYKSLTNDWEDHLAVKHFSVEGQLEFRALLFVPRRAPFDLFENRKKKN 359
            NPDDITNEEYGEFYKSLTNDWEDHLAVKHFSVEGQLEFRALLFVPRRAPFDLFENRKKKN
sus s.  301 NPDDITNEEYGEFYKSLTNDWEDHLAVKHFSVEGQLEFRALLFVPRRAPFDLFENRKKKN 360

homo s. 360 NIKLYVRRVFIMDNCEELIPEYLNFIRGVVDSEDLPLNISREMLQQSKILKVIRKNLVKK 419
            NIKLYVRRVFIMDNCEELIPEYLNFIRGVVDSEDLPLNISREMLQQSKILKVIRKNLVKK
sus s.  361 NIKLYVRRVFIMDNCEELIPEYLNFIRGVVDSEDLPLNISREMLQQSKILKVIRKNLVKK 420

homo s. 420 CLELFTELAEDKENYKKFYEQFSKNIKLGIHEDSQNRKKLSELLRYYTSASGDEMVSLKD 479
            CLELFTELAEDKENYKKFYEQFSKNIKLGIHEDSQNRKKLSELLRYYTSASGDEMVSLKD
sus s.  421 CLELFTELAEDKENYKKFYEQFSKNIKLGIHEDSQNRKKLSELLRYYTSASGDEMVSLKD 480

homo s. 480 YCTRMKENQKHIYYITGETKDQVANSAFVERLRKHGLEVIYMIEPIDEYCVQQLKEFEGK 539
            YCTRMKENQKHIYYITGETKDQVANSAFVERLRKHGLEVIYMIEPIDEYCVQQLKEFEGK
sus s.  481 YCTRMKENQKHIYYITGETKDQVANSAFVERLRKHGLEVIYMIEPIDEYCVQQLKEFEGK 540

homo s. 540 TLVSVTKEGLELPEDEEEKKKQEEKKTKFENLCKIMKDILEKKVEKVVVSNRLVTSPCCI 599
            TLVSVTKEGLELPEDEEEKKKQEEKKTKFENLCKIMKDILEKKVEKVVVSNRLVTSPCCI
sus s.  541 TLVSVTKEGLELPEDEEEKKKQEEKKTKFENLCKIMKDILEKKVEKVVVSNRLVTSPCCI 600

homo s. 600 VTSTYGWTANMERIMKAQALRDNSTMGYMAAKKHLEINPDHSIIETLRQKAEADKNDKSV 659
            VTSTYGWTANMERIMKAQALRDNSTMGYMAAKKHLEINPDHSIIETLRQKAEADKNDKSV
sus s.  601 VTSTYGWTANMERIMKAQALRDNSTMGYMAAKKHLEINPDHSIIETLRQKAEADKNDKSV 660

homo s. 660 KDLVILLYETALLSSGFSLEDPQTHANRIYRMIKLGLGIDEDDPTADDTSAAVTEEMPPL 719
            KDLVILLYETALLSSGFSLEDPQTHANRIYRMIKLGLGIDEDDPTADD+SAAVTEEMPPL
sus s.  661 KDLVILLYETALLSSGFSLEDPQTHANRIYRMIKLGLGIDEDDPTADDSSAAVTEEMPPL 720

homo s. 720 EGDDDTSRMEEVD  732
            EGDDDTSRMEEVD
sus s.  721 EGDDDTSRMEEVD  733
```

9.5 Vector maps

vector / construct sheet — Nr: 23

Name:	pGEX-5X-1	Date:	06.02.09	Concentration:	236 ng/µL
Deliv. by:	Prof. Dr. D. Staiger	Length:	4972 bp	Nr. of clycerol stock:	-
Institute:	Universität Bielefeld, Original DNA purchasable at GE Healthcare				

Vector

Name:	pGEX-5X-1	Length:	4972 bp	
Promoter:	tac promoter	Resistance	Prok.:	Ampicillin
Ori repl.:	unknown (low copy)		Euk.:	-
Signal peptide:	none			
Tag:	GST			

N-terminal	x	yes	MCS	x yes
C-terminal		yes	Recombination	yes
cleavage?		yes	other	yes
			not provided	yes

Insert

Name:	-	Organism:	-
Cloning sites:	-	Length:	-

Description:

-

Controls

Digestion			Sequencing	
	Enzyme(s):	XhoI, PstI		
	Fragment(s):	4004 bp, 968 bp		ok
	Result(s):	ok	x	not sequenced

Notes:
Induction inducible with 1-5 mM IPTG.

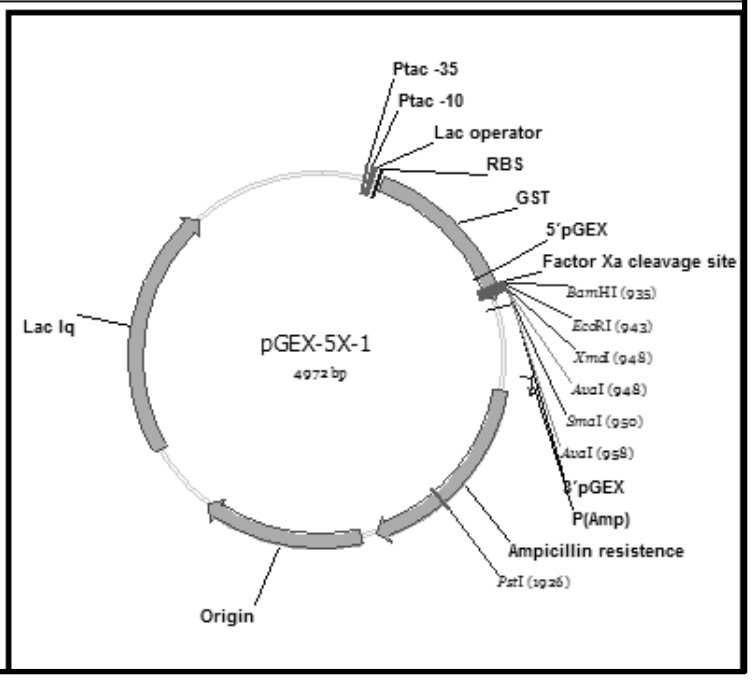

vector / construct sheet

Nr:	64

Name:	pGEX-5X-1 IkBa	Date:	24.03.09	Concentration:	200 ng/µL
Constr. by:	Kralemann / Engelen	Length:	5914	Nr. of clycerol stock:	-
Institute:	Universität Bielefeld, Biologie V				

Vector

Name:	pGEX-5X-1	Length:	4955		
Promoter:	tac	Resistance	Prok.:	Ampicillin	
Ori repl.:	unknown		Euk.:	-	
Signal peptide:	none	Cloning opportunities			
Tag:	GST	MCS	[x]	yes	
N-terminal	[x] yes	Recombination	[ ]	yes	
C-terminal	[ ] yes	other	[ ]	yes	
cleavage?	[ ] yes	not provided	[ ]	yes	

Insert

Name:	IkBa	Organism:	Human
Cloning sites:	BamHI / XbaI	Length:	959 bp

Description: Inhibitory subunit of transcription factor NFkappaB, other name: NFKBIA: nuclear factor of kappa light polypeptide gene enhancer in B-cells inhibitor, alpha

Controls

Digestion			Sequencing	
	Enzyme(s):	BglI		
	Fragment(s):	3271 bp, 2643 bp	[x]	ok
	Result(s):	OK	[ ]	not sequenced

Notes:
Induction inducible with 1-5 mM IPTG.

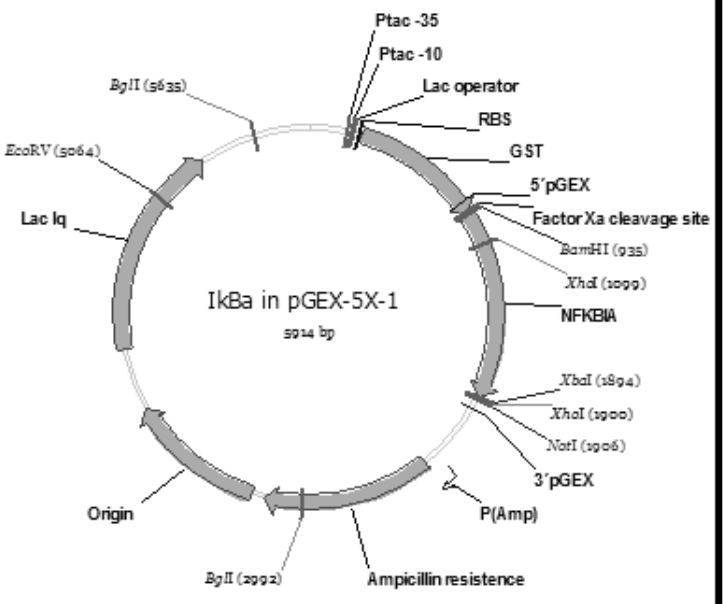

vector / construct sheet

Nr:	63

Name:	pGEX-5X-1 p65 WT	Date:	24.03.09	Concentration:	400 ng/µL
Constr. by:	Kralemann / Engelen	Length:	6616 bp	Nr. of clycerol stock:	
Institute:	Universität Bielefeld, Biologie V				

Vector

Name:	pGEX-5X-1	Length:	4949 bp
Promoter:	tac	Resistance Prok.:	Ampicillin
Ori repl.:	unknown	Euk.:	-
Signal peptide:	none		
Tag:	GST		

N-terminal	x	yes	MCS	x	yes
C-terminal		yes	Recombination		yes
cleavage?		yes	other		yes
			not provided		yes

Insert

Name:	p65 Wildtyp	Organism:	Human
Cloning sites:	BamHI / XhoI	Length:	1667 bp (p65: 1653 bp)

Description: Subunit of transcription factor NFkappaB, gene product of RelA, with transactivation and DNA binding domain
NCBI Accession NM_021975, Version NM_021975.3

Controls

Digestion			Sequencing	
	Enzyme(s):	BglI		
	Fragment(s):	2643 bp, 2459 bp, 1511 bp	x	ok*
	Result(s):	ok		not sequenced

Notes:
Induction inducible with 1-5 mM IPTG.

*partially sequencend derived from p65 pGEX-5X-1 79 bp Del.

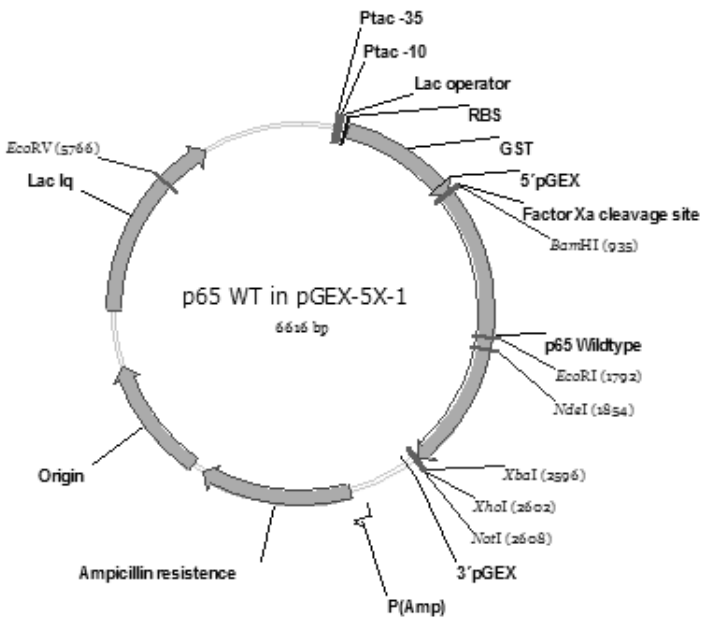

vector / construct sheet

Nr:	94

Name:	pEF FLAGpGKpuro B p65 WT	Date:	20.07.09	Concentration:	3,2 mg/mL
Constr. by:	Thomas Engelen	Length:	8,67 kb	Nr. of clycerol stock:	-
Institute:	Universität Bielefeld, Biologie V				

Vector

Name:	pEF FLAGpGKpuro B	Length:	7,01 kb	
Promoter:	EF-1α	Resistance	Prok.:	Ampicillin
Ori repl.:	f1		Euk.:	Puromycin
Signal peptide:	none			
Tag:	FLAG			

N-terminal	x	yes	MCS	x	yes
C-terminal		yes	Recombination		yes
cleavage?		yes	other		yes
			not provided		yes

Insert

Name:	p65 Wildtyp	Organism:	Human
Cloning sites:	BamHI/XbaI	Length:	1661 bp (p65: 1653 bp)

Description: Subunit of transcription factor NFkappaB, gene product of RelA, with transactivation and DNA binding domain
NCBI Accession NM_021975, Version NM_021975.3

Controls

Digestion			Sequencing	
	Enzyme(s):	EcoRI		
	Fragment(s):	~1500 bp, ~2600 bp, ~4500 bp		
	Result(s):	ok	x	not sequenced*

Notes:
*The MCS of pEF FLAG B was sequeced and p65 from pGEX-5X-1 was sequeced

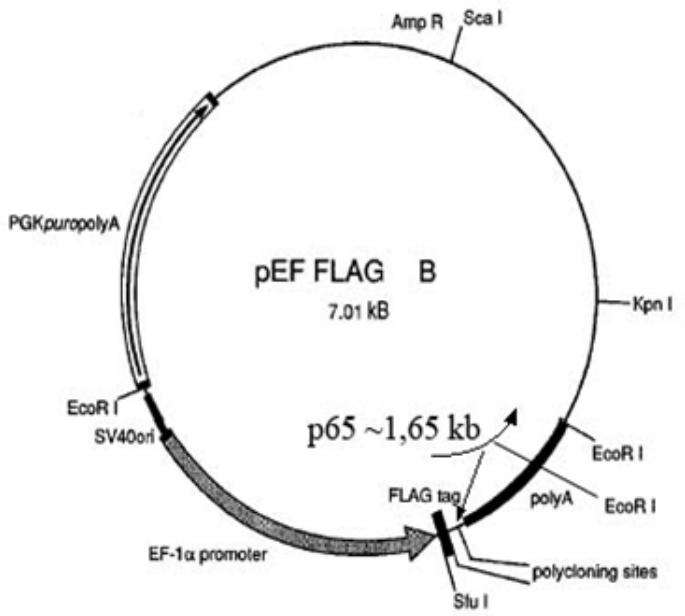

vector / construct sheet

Nr:	83 α

Name:	pcDNA3.1(+)c-Myc-HSPA8mut	Date:	16.07.09	Concentration:	1.4 g/L
Constr. by:	Thomas Engelen	Length:	7349 bp	Nr. of clycerol stock:	-
Institute:	Universität Bielefeld, Biologie V				

Vector

Name:	pcDNA3.1(+)c-Myc	Length:	5400 bp	
Promoter:	CMV	Resistance	Prok.:	Ampicillin
Ori repl.:	pUC		Euk.:	Neomycin
Signal peptide:	none			
Tag:	c-Myc			

N-terminal	x	yes	MCS	x	yes
C-terminal		yes	Recombination		yes
cleavage?		yes	other		yes
			not provided		yes

Insert

Name:	HSPA8	Organism:	Homo sapiens
Cloning sites:	BamHI/XbaI	Length:	1941 bp (ORF) + 8 bp

Description: Homo sapiens heat shock 70 kDa protein 8
Accession: BC016179; MGC: 17984; IMAGE: 3920744
Mutation: bp 203 TTT→TGT, Phe68→Cys (located in the ATPase domain)

Controls

Digestion			Sequencing	
	Enzyme(s):	KpnI / XbaI		
	Fragment(s):	1991 bp, 5358 bp	x	ok
	Result(s):	ok		not sequenced

Notes:
Derived from pcDNA3.1(+) c-Myc.
HSPA8 was inserted between BamHI and XbaI

Two AA added before BamHI for maintaining reading frame.

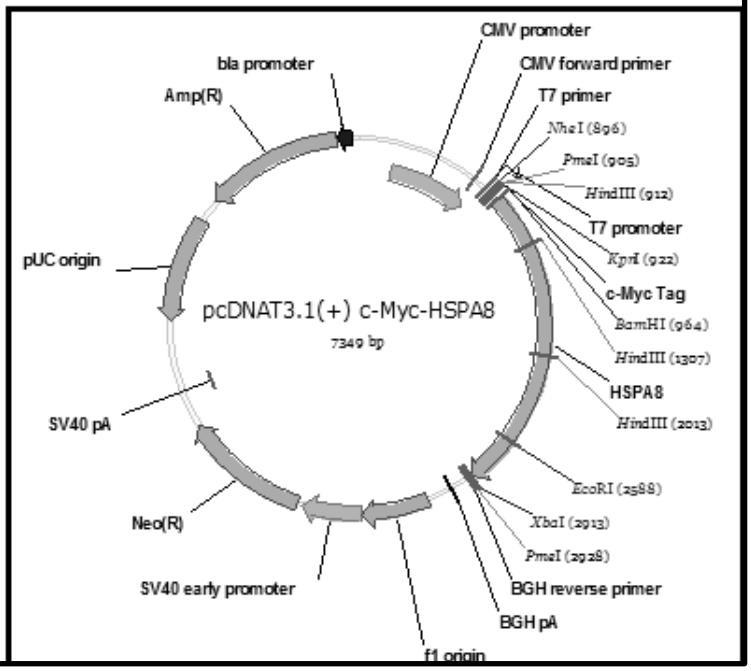

vector / construct sheet

Nr:	83

Name:	pcDNA3.1(+)c-Myc-HSPA8	Date:	16.07.09	Concentration:	3.1 g/L
Constr. by:	Thomas Engelen	Length:	7349 bp	Nr. of clycerol stock:	-
Institute:	Universität Bielefeld, Biologie V				

Vector

Name:	pcDNA3.1(+)c-Myc	Length:	5400 bp	
Promoter:	CMV	Resistance	Prok.:	Ampicillin
Ori repl.:	pUC		Euk.:	Neomycin
Signal peptide:	none			
Tag:	c-Myc			

N-terminal	x	yes	MCS	x	yes
C-terminal		yes	Recombination		yes
cleavage?		yes	other		yes
			not provided		yes

Insert

Name:	HSPA8	Organism:	Homo sapiens
Cloning sites:	BamHI/XbaI	Length:	1941 bp (ORF) + 8 bp

Description: Homo sapiens heat shock 70 kDa protein 8
Accession: BC016179; MGC: 17984; IMAGE: 3920744

Controls

Digestion			Sequencing	
	Enzyme(s):	KpnI / XbaI		
	Fragment(s):	1991 bp, 5358 bp	x	ok
	Result(s):	ok		not sequenced

Notes:
Derived from pcDNA3.1(+) c-Myc.
HSPA8 was inserted between BamHI and XbaI

Two AA added before BamHI for maintaining reading frame.

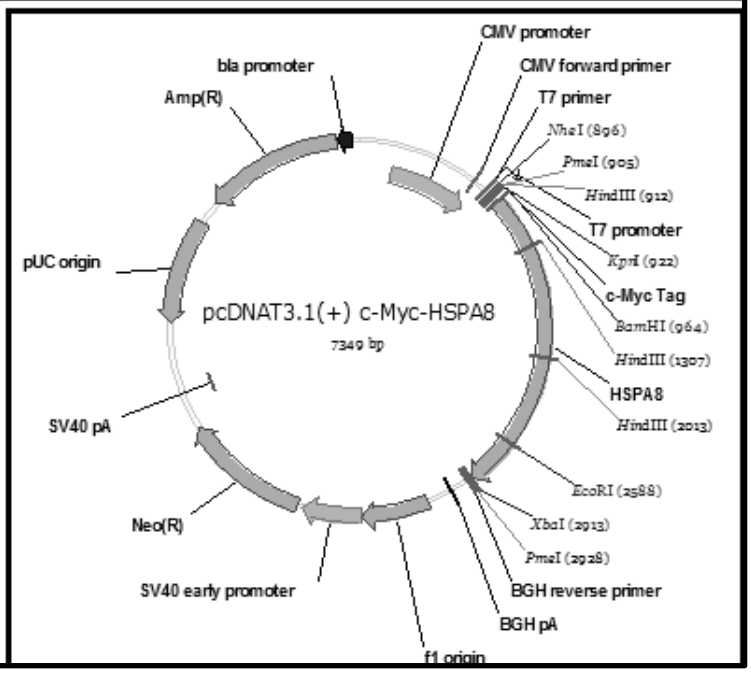

vector / construct sheet

Nr:	82

Name:	pcDNA3.1(+)c-Myc-HSP90AA1	Date:	15.07.09	Concentration:	2.7 g/L
Constr. by:	Thomas Engelen	Length:	7607 bp	Nr. of clycerol stock:	-
Institute:	Universität Bielefeld, Biologie V				

Vector

Name:	pcDNA3.1(+)c-Myc	Length:	5400 bp	
Promoter:	CMV	Resistance	Prok.:	Ampicillin
Ori repl.:	pUC		Euk.:	Neomycin
Signal peptide:	none			
Tag:	c-Myc			

N-terminal	x	yes	MCS	x	yes
C-terminal		yes	Recombination		yes
cleavage?		yes	other		yes
			not provided		yes

Insert

Name:	HSP90AA1	Organism:	Homo sapiens
Cloning sites:	BamHI/XbaI	Length:	2199 bp (ORF) + 8 bp

Description: Homo sapiens heat shock protein 90 kDa alpha (cytosolic), class A member 1; Accession: BC121062; MGC: 149801, IMAGE:40118488

Controls

Digestion			Sequencing	
	Enzyme(s):	KpnI / XbaI		
	Fragment(s):	2249 bp, 5358 bp	x	ok
	Result(s):	ok		not sequenced

Notes:
Derived from pcDNA3.1(+) c-Myc.
HSP90AA1 was inserted between BamHI and XbaI

Two AA added before BamHI for maintaining reading frame.

HSP90AA1 was amplified from pCR-BluntII TOPO HSP90

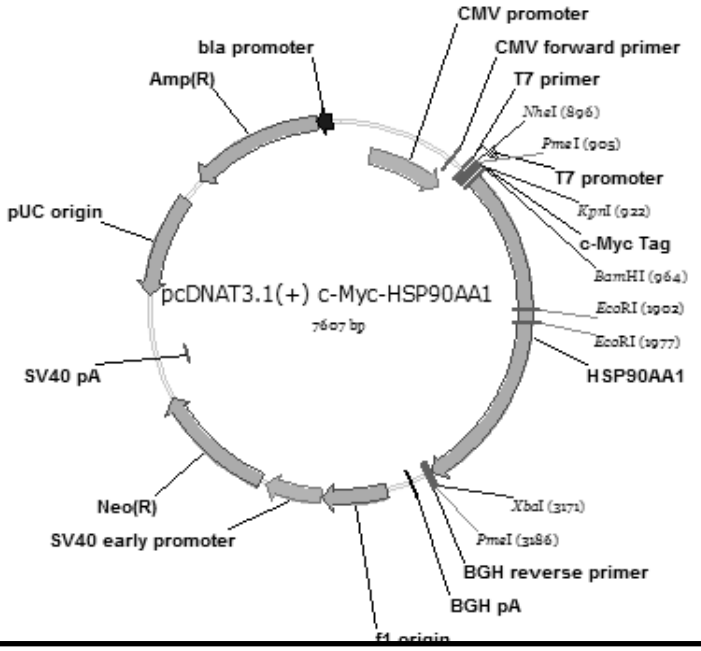

vector / construct sheet

Nr:	128

Name:	p65 Fpred	Date:	y: 2009	Concentration:	1 g/L
Constr. by:	Christin Zander	Length:	6.4 kb	Nr. of clycerol stock:	-

Vector

Name:	pEGFP-C1 (eGFP removed)	Length:	4,0 kb		
Promoter:	CMV IE	Resistance	Prok.:	Kanamycin*	
Ori Repl.:	pUCori		Euk.:	Neomycin*	
Signal peptide:	-	Cloning opportunities			
Tag:	FPred	MCS	[x]	yes	
N-terminal	[ ] yes	Recombination	[ ]	yes	
C-terminal	[x] yes	other	[ ]	yes	
cleavage?	[ ] yes	not provided	[ ]	yes	

Insert

Name:	p65 Fpred	Organism:	human / artificial
Cloning sites:	HindIII / NotI	Length:	1.65 + 0.8 kb

Description: Subunit of transcription factor NFkappaB, gene product of RelA (NCBI Accession NM_021975, Version NM_021975.2) c-terminal fused to the **F**luorescence **P**rotein **red** from pmaxFP-Red-C 613 bp -1419 bp (Lonza Cat.No. VDF-1031)

Controls

Digestion			Sequenzing**	
	Enzyme(s):	HindIII, AgeI, NotI		
	Fragment(s):	0.8 kb, 1.65 kB, 4.0 kb	[ ]	ok
	Result(s):	ok	[x]	not sequenced

Notes:
* bacterial and eukaryotic expression of Kanr/Neor

** verified by expression

vector / construct sheet

				Nr:	77
Name:	pcDNA3.1(+)-GFP	Date:		Concentration:	0.8 g/L
Constr. by:	Patrick Lüningschroer	Length:	6143 bp	Nr. of clycerol stock:	-
Institute:	Universität Bielefeld, Biologie V				

Vector

Name:	pcDNA3.1(+)	Length:	5428 bp	
Promoter:	CMV	Resistance	Prok.:	Ampicilin
Ori repl.:	pUC ori		Euk.:	Neomycin
Signal peptide:	-			
Tag:	-			

N-terminal	☐ yes	MCS	☒ yes
C-terminal	☐ yes	Recombination	☐ yes
cleavage?	☐ yes	other	☐ yes
		not provided	☐ yes

Insert

Name:	GFP	Organism:	Aequrea victoria*
Cloning sites:	NotI / XbaI	Length:	720 bp (+ 7 bp for restr. Sites)

Description: * mutated variant for optimized expression
enhanced green fluorescence protein (ORF of NCBI sequence Accession Nr. EU56363, Version EU56363.1)

Controls

Digestion		
	Enzyme(s):	PstI
	Fragment(s):	2071 bp, 4072 bp
	Result(s):	ok

Sequencing
☒ ok
☐ not sequenced

Notes:

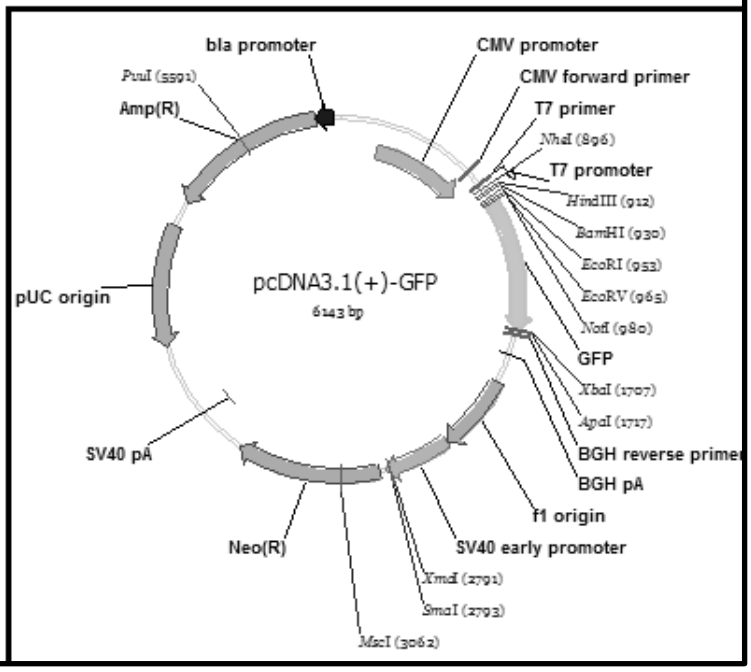

vector / construct sheet

Nr:	117

Name:	pcDNA3.1(+)-HSPA8-GFP	Date:	01.03.10	Concentration:	1.2 g/L
Constr. by:	Thomas Engelen	Length:	8042 bp	Nr. of clycerol stock:	-
Institute:	Universität Bielefeld, Biologie V				

Vector

Name:	pcDNA3.1(+)-GFP	Length:	6093 bp	
Promoter:	CMV	Resistance	Prok.:	Ampicilin
Ori repl.:	pUC ori		Euk.:	Neomycin
Signal peptide:	-			
Tag:	GPF			

N-terminal	[ ] yes	MCS	[x]	yes
C-terminal	[x] yes	Recombination	[ ]	yes
cleavage?	[ ] yes	other	[ ]	yes
		not provided	[ ]	yes

Insert

Name:	HSPA8	Organism:	human
Cloning sites:	BamHI / NotI	Length:	1938 bp (+ 11 bp for restr. Sites)

Description: HSPA8 alias HSC70, Homo sapiens heat shock 70 kDa protein 8
Accession: BC016179; MGC: 17984; IMAGE: 3920744

Controls

Digestion			Sequencing	
	Enzyme(s):	HindIII		
	Fragment(s):	6974 bp, 706 bp, 362 bp	[X]	ok
	Result(s):	ok	[ ]	not sequenced

Notes: -

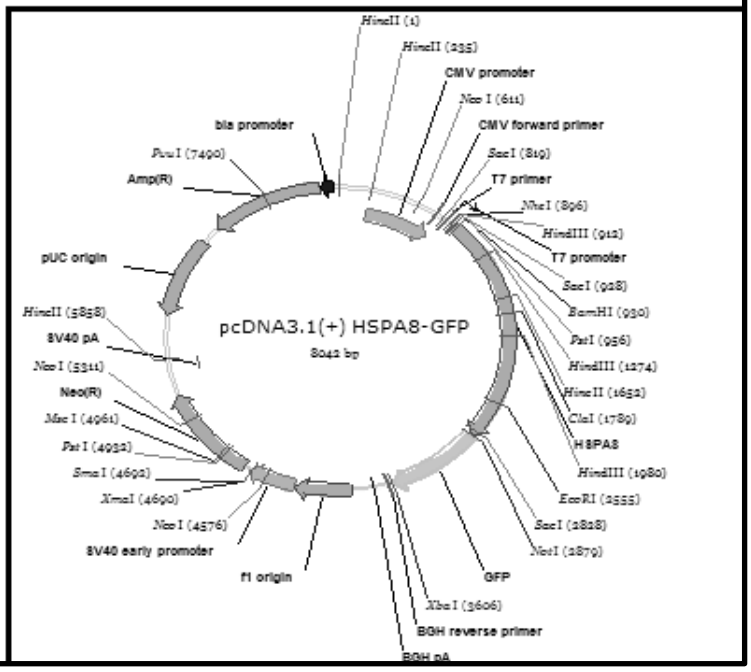

vector / construct sheet

Nr:	Bx 2, 7

Name:	CMV-MAD3	Date:	10.10.1991	Concentration:	1 g/L
Constr. by:	Thomas Henkel	Length:	6436 bp	Nr. of clycerol stock:	-

Vector

Name:	RcCMV	Length:	5446 bp		
Promoter:	CMV	Resistance	Prok.:	Ampicillin	
Ori Repl.:	f1 origin		Euk.:	Neomycin	
Signal peptide:	-	Cloning opportunities			
Tag:	-	MCS	[x]	yes	
N-terminal	[ ] yes	Recombination	[ ]	yes	
C-terminal	[ ] yes	other	[ ]	yes	
cleavage?	[ ] yes	not provided	[ ]	yes	

Insert

Name:	MAD3 (IκBα)	Organism:	human
Cloning sites:	Hind III / Xba I	Length:	990 bp

Description: nuclear factor of kappa light polypeptide gene enhancer in B-cells inhibitor alpha

Controls

Digestion			Sequenzing	
	Enzyme(s):	Hind III / Xba I		
	Fragment(s):	5446 bp, 990 bp	[x]	ok
	Result(s):	ok	[ ]	not sequenced

Notes:
Amplified by PCR from human uterus cDNA-Library subcloned into pCR1000 sequencend and verified by expression
cloned into Rc/CMV

References
Haskill et al. (1991), Cell 65:1281-1289
Henkel et al. (1992), Cell 68:1121-1133
Zabel et al. (1993), Embo J. 12:201-211